Cold Regions Research and Engineering Laboratory

US Army Corps of Engineers®
Engineer Research and
Development Center

Opportune Landing Site Program

Suitability Measurement and Analysis for El Centro Naval Air Facility OLS

Rosa T. Affleck, Charles C. Ryerson,
Lynette A. Barna, and Keran J. Claffey

October 2008

COVER: (center photo) Along the centerline of El Centro Opportune Landing Site, looking east at sunrise.

(outside photos) Personnel conducting soil measurements at El Centro OLS.

Suitability Measurement and Analysis for El Centro Naval Air Facility OLS

Rosa T. Affleck, Charles C. Ryerson, Lynette A. Barna, and Keran J. Claffey

US Army Engineer Research and Development Center
Cold Regions Research and Engineering Laboratory
72 Lyme Road
Hanover, New Hampshire 03755-1290

Abstract: The Army relies upon agility and speed, including the ability to conduct air transport operations where no runways exist, and where engineers cannot be pre-positioned. One of the most difficult problems is locating large, smooth, flat, and obstruction-free areas that are also sufficiently firm to support at least one aircraft operation, and preferably many. The Opportune Landing Site (OLS) program demonstrated the use of remote sensing technology and state-of-the-ground forecast tools to accelerate the process of selecting OLSs. To evaluate the quality of the selected OLSs, ground truth measurements were conducted at El Centro Naval Air Facility (NAF). Before conducting field measurements, several sites identified by OLS software were visually inspected to evaluate and select a suitable OLS for field testing. Evaluation procedures were based on Air Force Civil Engineer Support Agency (AFCESA) recommendations for evaluating airfield pavements. Soil strength and moisture measurements were made at several locations along the OLS, and overall quality was evaluated during three seasons. Assessment software was able to predict an OLS adequate for landing a C-130, but not capable for a C-17. This was true for all three field assessments at El Centro NAF.

Contents

Figures and Tables

Figures

Tables

Nomenclature

AFCESA	Air Force Civil Engineer Support Agency
AFRL-VA	Air Force Research Laboratory Air Vehicles Directorate
AGL	Allowable Gross Load
AMC	Air Mobility Command
ASTM	American Society for Testing Materials
ATT	Advanced Theater Transport
ATT SSTOL	Advanced Theater Transport Super Short Takeoff and Landing
BLM	Bureau of Land Management
BOLS	Boeing Opportune Landing Site
CBR	California Bearing Ratio
CIH	Clegg Impact Hammer
CIH_L	Light Clegg Impact Hammer (0.5-kg-mass hammer)
CIV	Clegg Impact Value
CIV\L	Clegg Impact Value for 0.5-kg-mass hammer
CONUS	Conterminous United States
CORS	Continuously Operated Reference Stations
CRREL	Cold Regions Research and Engineering Laboratory
DCP	Dynamic Cone Penetrometer
DoD	Department of Defense
ERDC	Engineer Research and Development Center

ETL   Engineering Technical Letter

FCS   Future Combat System

FOD   Foreign Object Damage

GIS   Geographic Information System

GPS   Global Positioning System

IOP   Intensive Operational Period

LZ   Landing Zone

NAF   Naval Air Facility

NRCS   Natural Resources Conservation Service

OLS   Opportune Landing Site

RAS   Runway Assessment Site

RMS   Root Mean Square

SAS   Soil Assessment Site

SSURGO   Soil Survey Geographic

TRANSCOM   US Transportation Command

USCS   Unified Soil Classification System

USDA   United States Department of Agriculture

UTM   Universal Transverse Mercator

WGS   World Geodetic System

Preface

1 Introduction

Effectiveness in modern warfare requires response to a wide variety of adversaries rapidly, lethally, and oftentimes stealthily. This requires, in part, the ability to conduct air transport operations to locations without existing runways, and where engineers cannot be pre-positioned because of time constraints and the need for surprise. One of the most difficult problems is locating large, smooth, flat, obstruction-free areas that are also sufficiently firm to support at least one aircraft operation, and preferably many. Today, locating adequate opportune landing sites requires skilled image analysts and days of work, augmented by site survey teams visiting candidate locations and assessing the proposed site or landing zone (LZ).

Several new approaches have been taken to improve the capability of rapidly locating OLSs from the use of satellite imagery (Manley 2001, Ryerson and McDowell 2007, Vincent and Jennings 2004). Using the approaches described by these authors, the OLS Program is demonstrating and improving upon the capability of current technology for locating satisfactory sites, with the future goal of landing airplanes without first placing "boots on the ground."

The OLS Program evolved from a capability developed by The Boeing Company to demonstrate that transport aircraft can operate out of many more locations than are available using prepared runways. That is, larger numbers of unimproved OLS sites should be available in any area than improved runways . Using software developed at Bowling Green State University (Vincent and Jennings 2004), The Boeing Company demonstrated that transports could be operated out of hundreds of austere runways.

Utilizing 30-m resolution LANDSAT imagery, Dr. Robert Vincent from BGSU developed techniques using five of the LANDSAT bands to exclude areas of dense, woody vegetation, freestanding water, sloping and undulating ground, and obstructions (Manley 2001, Vincent and Jennings 2004). LANDSAT pixels were provided with a score, the Boeing Landing Suitability Index, BLSI, which indicated the relative quality of a pixel for landing aircraft. Smaller BLSI numbers related to higher quality surfaces. When adjacent pixels of less than a threshold BLSI number equating to an acceptable surface were combined to form a contiguous surface of minimum

specified size and direction, an OLS was plotted on the LANDSAT image. Boeing and BGSU evaluated the OLS software at a number of field sites (Alvin 2000, Manley 2001, Vincent and Jennings 2004) in California, New Mexico, South Dakota, and Louisiana, and found that the software did locate sites with the attributes sought. Also, all sites were considered firm to support aircraft. Even though an explicit methodology was not created in the software to locate firm locations, OLSs located were, fortuitously, firm.

The OLS program is intended to demonstrate how existing technologies can rapidly accelerate the process of selecting OLSs using remote sensing technology and state-of-the-ground forecast tools (Ryerson and McDowell 2007). However, in the process of demonstration, techniques within the program are being improved and made more robust. The OLS program, started in mid-2004 and scheduled for completion in September 2007, consists of eight fundamental tasks. The Boeing Company will 1) provide software allowing the selection of OLS locations using satellite imagery, 2) provide a capability of predicting soil type, 3) provide a military utility study, and 4) integrate products from all partners into a coherent software package. The ERDC will 5) evaluate the capability of Boeing OLS software for reliably locating suitable OLSs and determine the ability of the software to locate smooth, flat, and obstruction-free landing sites seasonally, 6) provide the capability to predict soil moisture with depth, and 7) provide the capability of predicting soil strength. The capability of all partners will be evaluated in 8) a demonstration (blind test) during 2007. Though the end state in 2007 will not be a full operational capability, it will demonstrate the capabilities of current technology in a semi-integrated functional demonstration package.

This report primarily describes work addressing ERDC task 5 and portions of tasks 6 and 7. This was accomplished by conducting field work at CONUS locations selected by the Boeing OLS software according to criteria described in Section 2 of this report. Specifically, ERDC's goals were to establish whether OLSs selected by the software met criteria established by the AFCESA for contingency airfields, but modified by ERDC for OLS. The criteria modified for OLS to assess the surface conditions include vegetation (type and height), Foreign Object Damage (loose granular materials), flatness, roughness (undulations), mounds, standing water, surface debris and organic materials, surface drainage, and animals burrows. ERDC also examined the seasonal conditions of the OLS, including OLS loading capacity. The AFCESA criteria, created jointly by the Air Force and

the USACE, provide requirements for paved and unpaved runways regarding suitability for various types of aircraft, loadings, and number of operations (AFCESA 2002a, 2002b; UFC 3-260-02).

Ultimately, ERDC conducted field work at four locations: El Centro Naval Air Facility in southern California (Affleck et al. 2008), at Fort Bliss in New Mexico (this report), and at two locations in southern Indiana (Barna et al. 2008). This report describes field work conducted at Fort Bliss, and provides a seasonal assessment of the suitability of the software-selected OLS to be used as a viable landing site.

2   Background

A runway assessment site (RAS) consists of entire OLS runways as predicted by Boeing's software. The main objective of RAS is to evaluate the quality of OLSs selected by the Boeing software and to develop a knowledge base about OLS software indicators for "greenness" and "flatness" coefficients used to select the runways. The RAS also will be used to evaluate soil properties and the software's capabilities to select OLSs in any season.

The Air Force uses the following considerations when selecting permanent airfields: topography, vegetative cover, existing construction, weather elements, wind direction, soil conditions, flood hazard, natural and man-made obstructions, adjacent land use, availability of usable airspace, accessibility of roads and utilities, and potential for expansion capability. The potential for encroachment and effects of noise on the local community also must be considered (AFCESA 2004). In addition to several criteria mentioned above, AFCESA Engineering Technical Letter (ETL) 04-7 provides dimensional, marking, and lighting criteria and guidance for planning, design, construction, and evaluation of landing zones used for aircrew training and contingency operations of C-130 and C-17 aircraft. Other factors that would affect runway dimensions—such as altitude and temperature (it requires more takeoff distance in hot desert or high mountain locations because air is less dense)—must be considered. Runway dimensions are typically selected by the flyers and are never selected by the civil engineer. The OLS software is not designed to consider all criteria desired by the Air Force for permanent airfields. It is designed to select candidate locations for contingency operations, specifically areas that are smooth, flat, level, and free of obstructions and woody vegetation that would harm aircraft. It does not consider wind direction and speed, flood hazard, accessibility to roads and utilities, noise, or the potential for expansion, nor does it consider approach and departure corridor clearances. Therefore, the RAS characteristics were evaluated based only on what the software can be expected to predict. OLS dimensions were based on a minimum requirement of 20 by 914 m (60 by 3000 ft) and 30 by 1067 m (90 by 3500 ft) for C-130 and C-17 assault landing zones, respectively, for semi-prepared runways (ETL 04-7). However, wider and longer (i.e., 80 by 1200 m) runway dimensions also were examined to account for clear-

ance and overrun. These dimensions are for the study, and actual dimensions will vary on location, mission, and aircraft.

2.1 OLS Software

The Boeing OLS software uses the method developed by Dr. Robert Vincent, in which each pixel on a LANDSAT image is assigned with a BLSI value relating to the pixel's quality. A pixel with small BLSI number corresponds to a high-quality surface. An OLS is composed of adjacent pixels with BLSI number below a threshold value forming a continuous area of specified length and width. The recent version of Boeing OLS software (OLS-MS) version 7, the version of the software used for selecting the OLS for the fieldwork, requires vegetation and flatness (gradient) indices. These thresholds for vegetation and gradient are based on the selected pixels from areas in the four field sites that Dr. Robert Vincent and team identified as good based on their field observation and verification. The selected pixels fell within the bounds of vegetation value of 1.8 and gradient of 0.02 and found excellent correlation with the regions identified as acceptable landing sites by Dr. Robert Vincent and team (Blake, personal communication). The software requires input for OLS dimensions (length and width), but the OLS results can sometimes have longer lengths than the minimum length specified.

For El Centro, the software was run on LANDSAT imagery (frame 039_037) for 3 May 2000 with systematic georectification. The software was run using OLS-MS version 7 with a flatness index of 0.02 and a vegetation index of 1.8 for 30 by 900 m (90 by 3000 ft) and 80 by 1200 m (270 by 4000 ft) runway dimensions as shown in Figure 1. OLSs were used during an initial visual evaluation at El Centro in June 2005 but not all the OLSs in El Centro were visually evaluated, limiting access in some areas (Appendix A). Another OLS-MS version 7 run was conducted using 9 May 2005 imagery (frame 039_037). This imagery was run for 60- by 914-m (200- by 3000-ft) runway dimensions with the same flatness index and vegetation index (Fig. 2). The OLSs were mapped on an Orthophotograph for used in site selection and fieldwork.
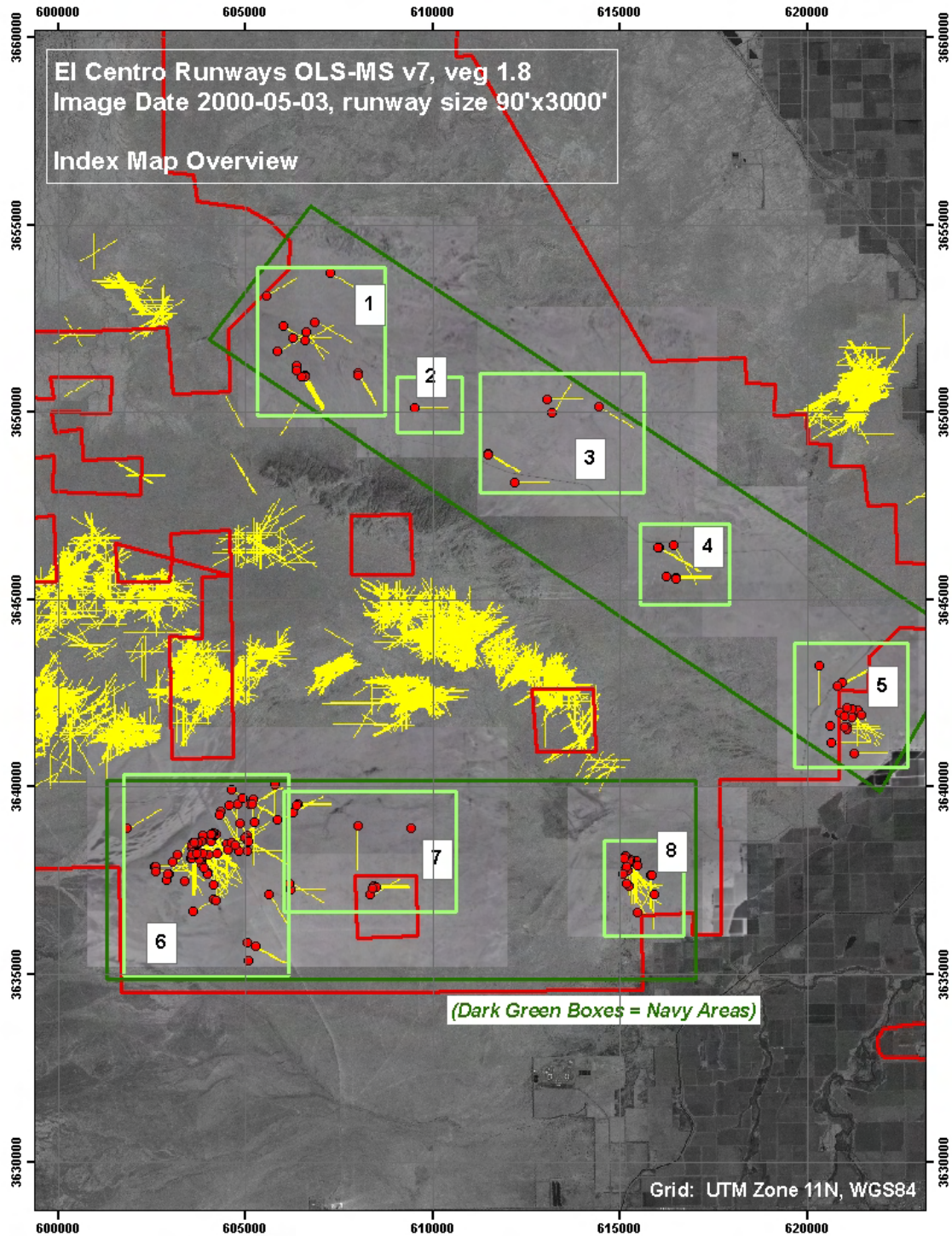
a. OLSs with 30-m by 914-m (90-ft by 3000-ft) runway dimension.

Figure 1. Red dots identify OLSs that were evaluated for potential field work during our initial visit in June 2005. Areas enclosed in dark green boxes belong to El Centro NAF (Areas 1 through 8) and adjacent areas are managed by Bureau of Land Management (BLM).
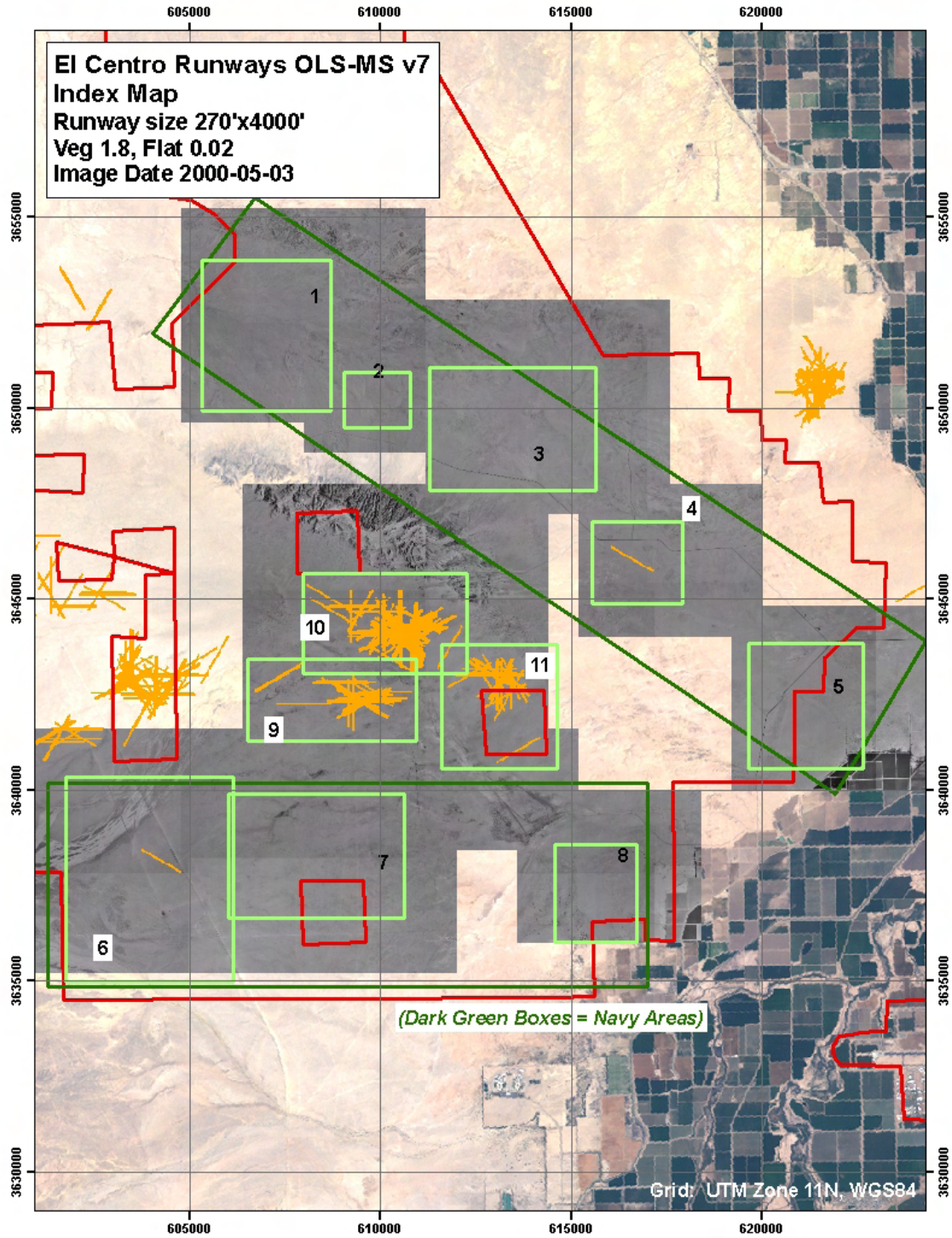
Figure 1b. OLSs with 80-m by 1200-m (270-ft by 3000-ft) runway dimension.

Figure 1 (cont'd).
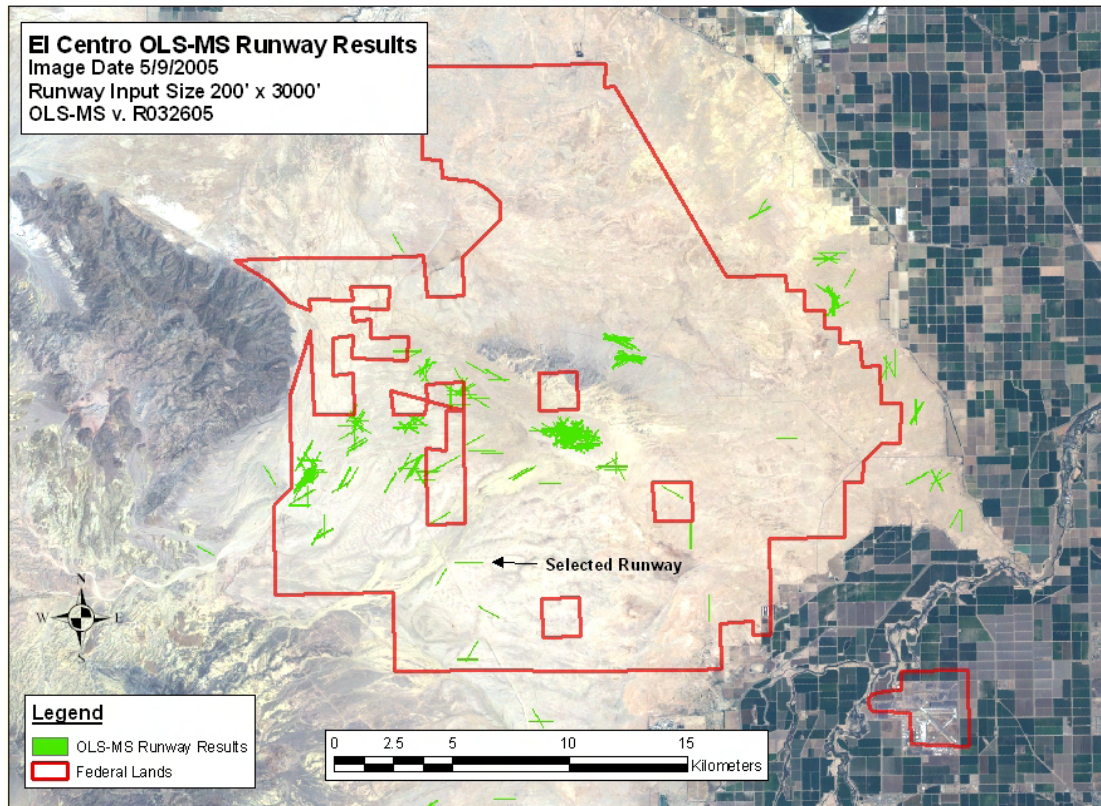
Figure 2. OLSs identified by Boeing software for 60-m by 914-m (200-ft by 3000-ft) runway dimensions.

After the fieldwork was completed, we discovered that the LANDSAT imagery used to locate OLSs was georeferencing only at systematic or basic level. Apparently a LANDSAT imagery is georeferenced at various degrees of geoprocessing precision (Ryerson et. al. in prep.). One level of georeferencing a LANDSAT imagery is at systematic or basic. Another degree of georeferencing a LANDSAT imagery is based on precision-corrected level using an orthophoto. The level of geoprocessing in the LANDSAT imagery resulted in the misplacement of the RAS location with an offset of 172 m to the east and 291 m to the north. A detailed discussion on the georeferencing of the imagery including the offset determination is reported in Section 7.2. The runway assessment site (RAS) describing the OLS using the systematic imagery is referred to in this report as SI-RAS and the OLS using precision-corrected imagery is assigned as PCI-RAS.

2.2 Site Selection

The RAS is located on US Naval Reservation land on the El Centro Naval Air Facility (NAF) located in the southwest desert of the Imperial Valley in

southern California. The valley consists of relatively flat desert terrain. It is almost bordered by mountains to the north, west, and southwest. Sand hills and dunes are located 45 miles to the east. To the southeast lies the Yuma Desert of Arizona and the Gran Desierto of Sonora, Mexico. The climate of the Imperial Valley area is arid, with hot summers and mild winters. The transition periods between summer and winter seasons are very short. Normally there is a little more than a week or two of a rapid transition to the dominant seasons of summer and winter (USDA Soil Survey 1981). Spring and autumn show few, if any, of the seasonal characteristics normal to other areas of the United States.

Evaluation of several OLSs was made during the initial site visit at El Centro NAF in June 2005 (see Appendix A for trip reports). The purpose of the visits was to visually evaluate OLSs identified by the Boeing software and to select an OLS suitable for extensive field testing. Some of these OLSs were also located on adjacent areas that belong to Bureau of Land Management (BLM), as shown in Figures 1 and 2. Initial contact from the agencies was conducted before the visual evaluation visit and permission from these agencies had to be obtained prior to the start of field testing. The general vicinity of the OLS that ERDC-CRREL selected is located approximately 20 km west of El Centro NAF headquarters and about 5 km north of Plaster City, California (Fig. 3). The land is on a Naval Reservation where air maneuver and air target live-fire training occur daily. Usage of this location was allowed by the range master. The primary considerations for selecting the OLS at El Centro NAF were favorable logistic conditions for field work activities and safety of the field personnel conducting the field work, as it is a military training area near targets.

From our initial site visit in June 2005, we highly considered the enclosed Area 6 (Fig. 1), specifically east of the railroad track. West of the railroad track is in the heavily restricted bombing practice area. In enclosed Area 6, the Boeing software detected only one 80-m by 1200-m (270-ft by 4000-ft) OLS in this area, which is west of the railroad track. However, the software found 30-m by 914-m (90-ft by 3000-ft) OLSs east of the railroad track. It was of particular importance to stay east of the railroad track (mainly for field personnel safety) and to be near a fenced tower to house our weather monitoring instruments. The same imagery was run for an OLS of 60-m by 914-m (200-ft by 3000-ft) runway dimensions as shown in Figure 2. The OLS selected for the fieldwork is near an access road, critical for logistics efficiency, including hauling instruments, and safety

during field work. Because the area is near an active bombing range, per-
mission was obtained prior to each field visit.

Figure 3. "El Centro OLS" identifies the general location of the RAS at El Centro NAF.

3   Runway Assessment Site (RAS) Analysis Criteria

3.1 Introduction

The purpose of the field work at El Centro was to determine whether the OLS software identified suitable landing sites that met both the geometric and strength requirements to land an aircraft. This field program, therefore, provided a "ground truth" assessment of the adequacy of the OLS software. Currently, there is no standard method of evaluating an OLS, and for this reason, a prime component of the field techniques used are based on existing Air Force procedures published in ETL 2002-19, *Airfield Pavement Evaluation Standards and Procedure* (AFCESA 2002a). Other sources drawn on to provide field measurements that would assist in evaluating an OLS came from vehicle mobility, pavement engineering, and ASTM standards. Figure 4 was modified from the Air Force pavement evaluation method to describe the process used to determine whether the software located a suitable landing site. Each step of the process is described in more detail.

3.1.1 Geometric Evaluation of RAS (Smooth, Level, Flat, Obstruction)

The first step of the field evaluation was to locate and mark the center end points using the coordinates of the OLS with the aid of a GPS. By locating the runway end points, sampling locations then can be marked or flagged for specific intervals (stationing) along the OLS. ETL 2002-19 (AFCESA 2002a, 2002b) guidelines for determining sampling locations for semi-prepared runways can be used for prioritizing to assess the runway's critical locations. For the RAS, we adopted similar procedure. However, the sampling layout was established to allow sampling of the entire RAS using a regular grid spacing (Fig. 5). Field teams performed as many tests as time permitted, and prioritized test locations by focusing on the weak soil areas first and covering each feature or aspect of the runway.

OLS Suitability Field Evaluation Procedures

Runway Geometric Properties

Locate center end points
Mark testing locations
Evaluate features:
  Smooth
  Flatness
  Level
  Obstruction-free (power lines, etc.)
  Hydrologic features (streams, ditch)

Aircraft Operational Requirements

Aircraft type
Number of passes
Type of mission

Estimate AGLs / Passes

Based on 15th percentile of Minimum CBR
  Compute allowable loads and passes (using charts)
  Use PCASE Evaluation Module

Compile Data & Analyze

Identifying strong and weak areas
Select representative profiles
Compile physical property data (PPD)

Perform Field Tests

Test pits
  Soil horizons
  Soil classification
  Soil moisture
  Density
DCP
Clegg hammer
Surface soil color
Vegetation cover – type & cover
Topography

Assess Surface Characteristics

Visual assessment of terrain features and surface condition:
  Potholes, FOD (loose granular materials), rut depth, mounds, debris and organic materials, vegetation type and height, surface drainage or swale
Determine obvious weaknesses or potential near-surface obstacles:
  Animal borrow or holes, standing water

Overall OLS Rating

Using Pass, Caution & Fail

MODIFIED FROM ETL 02-19, Figure 1

Figure 4. Procedures for determining suitability of an OLS, modified from practice established by AFCESA in ETL 2002-19 (AFCESA 2002a).

The smoothness and flatness of the runway were noted and defined in terms of undulation, gradient, or slope. Undulation and slope were measured typically using a level instrument. Vertical obstructions, such as power lines and power poles near the OLS, dense vegetation and vegetation greater than 1 m (3 ft) in height, were noted. If they exist in the area, the runway is not suitable. Although hydrologic features such as standing water, ditches, and streams may not be present on an OLS during the initial visit, they may occur at another time because of the climatic effects of the area. These features, if present, should be noted in terms of the length and width of any standing water areas.

Runway slope should follow guidelines for runway design. Table 1 provides the landing zones criteria and requirements in terms of dimensions and slope gradients for transverse and longitudinal directions from ETL 04-7. The criterion for the longitudinal grade is 3% maximum slope for landing zones. Minimum distance between grade changes is 61 m (200 ft). Grade changes cannot exceed 1.5% measured at 61-m (200-ft) intervals. ETL 04-7 also states that grade changes should be held to a minimum and should

be gradual. The required transverse grade is 1.5 to 5.0%. For specification of the longitudinal and transverse grades, we developed "Green" and "Red" ratings for the OLS evaluation. A rating of Green is assigned for longitudinal grades of less than 3% and for transverse grade of less than 5%. Red is assigned for greater than 3% and 5% for longitudinal grade and transverse grades, respectively. Abrupt grade change of greater than 1.5% with less than 61 m is considered red.
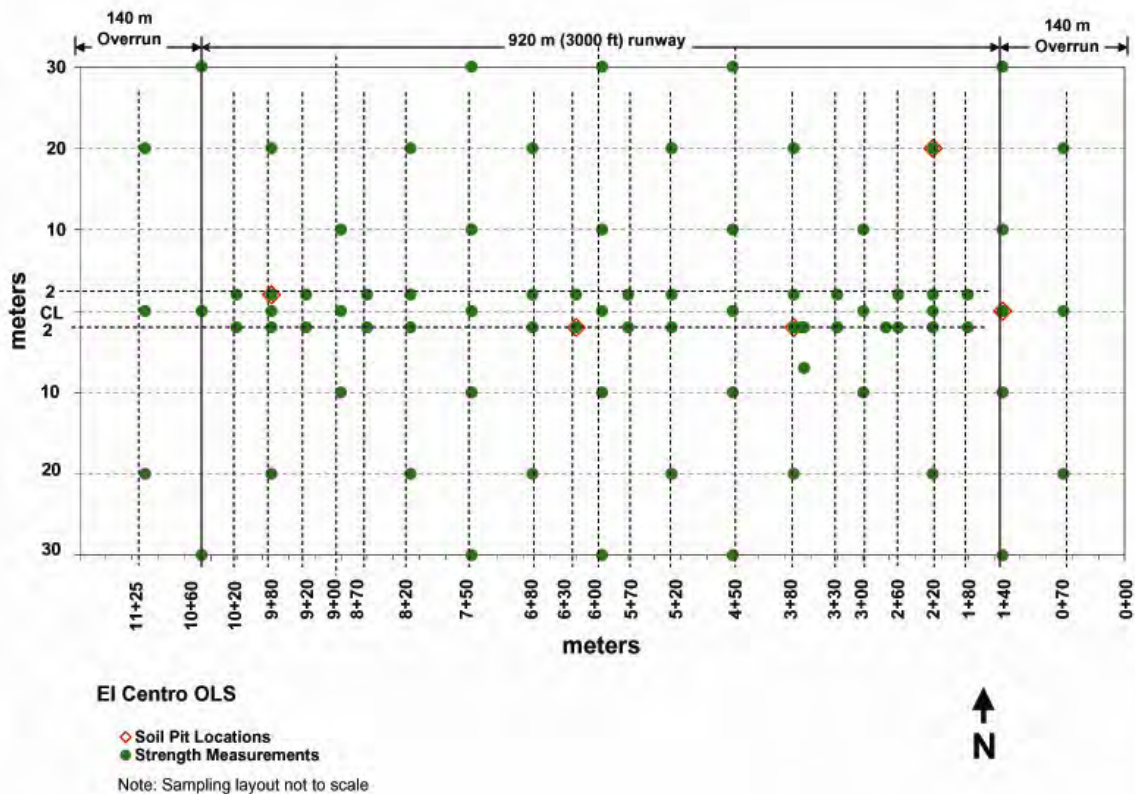
Figure 5. Sampling grid used to evaluate the RAS at El Centro NAF OLS. (Not drawn to scale.)

Table 2 summarizes the criteria used to evaluate the RAS in terms of its smoothness, flatness, obstruction, and hydrologic features.

Table 1. Runways for landing zone guidelines developed for C-130 and C-17 (adopted from AFCESA 2004).

Item No.	Item Description	Paved		Semi-Prepared		Remarks
		C-130	C-17	C-130	C-17	
1	Length	As required	As required	As required	As required	
2	Width	As required	As required	As required	As required	
3	Width of Shoulders	Min. 3 m (10 ft)				Remove all tree stumps and loose rocks in shoulder areas. Shoulders for paved LZs shall be paved. Shoulders for semi-prepared LZs should be stabilized to prevent erosion by jet blast. Where adequate sod cover cannot be established, the shoulders should be chemically stabilized.
4	Longitudinal Grades of Runway and Shoulders	Max. 3%				Hold to minimum practicable. Grades may be both positive and negative but must not exceed the limit specified.
5	Longitudinal Runway Grade Change	Max. 1.5% per 61 m (200 ft)				Grade changes should be held to a minimum and should be gradual. Minimum distance between grade changes is 61 m (200 ft). Grade changes cannot exceed 1.5% measured at 61 m (200 ft) intervals.
6	Transverse Grade of Runway	0.5% Min. 3.0% Max.				Transverse grades should slope down from the runway centerline. The intent of the transverse grade limit is to provide adequate cross slope to facilitate drainage without adversely affecting aircraft operations
7	Transverse Grade of Runway Shoulders	1.5% Min. 5.0% Max.				Transverse grades should slope down from the runway edge. The intent of the transverse grade limit is to facilitate drainage.
8	Width of Graded Area	10.5 m (35 ft)				Cut trees flush with the ground and remove rocks larger than 100 mm (4 in.) in diameter. Remove vegetation (excluding grass) to within 150 mm (6 in.) of ground. Jet blast may cause erosion of the graded area. For paved LZs where adequate vegetation cannot be established to prevent erosion, the graded area can be covered with a thin 38-mm to 51-mm (1.5-in. to 2.0-in.) asphalt layer.
9	Transverse Grade of Graded Area	2.0% Min. 5.0% Max.				Grades may slope up or down to provide drainage, but may not penetrate the primary surface.

Table 1 (cont'd). Runways for landing zone guidelines developed for C-130 and C-17 (adopted from AFCESA 2004).

Item No.	Item Description	Paved		Semi-Prepared		Remarks
		C-130	C-17	C-130	C-17	
10	Width of Maintained Area	18.5 m (60 ft)	21.5 m (70 ft)	18.5 m (60 ft)	21.5 m (70 ft)	Remove obstructions: cut trees flush with ground. Remove rocks that project more than 150 mm (6 in.) above grade. Remove vegetation (excluding grass) to within 150 mm (6 in.) of the ground.
11	Maintained Area: Transverse Grade	Maximum range: +10.0% to –20.0%				Grades may slope up or down provided drainage, but may not exceed +10.0% nor –20.0% slope.

Table 2. OLS geometric evaluation rating used on the RAS.

Geometric Criteria	Ratings	
	Green	Red
Flatness	Slope: <3% for longitudinal direction <5% for transverse direction	Slope: >3% for longitudinal direction >5% for transverse direction
Smoothness	Undulation (grade change, wavelength): <1.5% in ≥ less 61-m distance	Undulation (grade change, wavelength): >1.5% in < less 61-m distance
Obstacles	No power lines in the vicinity, no trees or vegetation < 1 m (3 ft)	Power line 200 m near the OLS, trees or vegetation >1 m (3 ft)
Hydrologic features	None	If present

3.1.2 Field Test Overview

Using the sampling layout (Fig. 5), several soil pits were excavated to determine the stratigraphy of the soil horizons, soil texture, soil density, and soil moisture profiles. Soil texture was determined by collecting samples for laboratory analysis to determine the soil classification. Surface soil color was determined using the Munsell color chart and not used in the analysis, but was intended to be used for another task under the OLS program. Soil density was measured primarily using a nuclear density gage, and drive cylinders which proved to be unsuitable for granular soils. Soil moisture content was measured at various depths using several methods. Soil strength was measured for surface and subsurface layers using several instruments. Soil strength profiles were collected using the Dynamic Cone Penetrometer (DCP). The DCP is the standard instrument and AFCESA's recommended tool to assess the soil strength profile of a runway. Because of lack of confinement in soil near the surface, the actual strength of the surface layer using the DCP is at some depth depending on the soil type (Webster et al. 1994). Surface soil strength was measured using the Clegg Impact Hammer (CIH), the Static Cone Penetrometer, and a Drop cone. Both the DCP and CIH are commonly used for assessment of strength on mechanically compacted soils for roads and airfields. The Static Cone Penetrometer is used to assess soil strength for vehicle mobility applications on cross-country terrain (i.e., natural soils) or trails. The Drop cone is used to assess soil compaction, and was designed for agricultural soils. Because the OLSs are on natural soil (not mechanically constructed soils), both the Static Cone Penetrometer and the Drop cone would provide useful information to complement the DCP and CIH. The Static Cone Penetrometer didn't work well at Fort Bliss and El Centro OLSs because of caliche or granular materials present in the soil.

Vegetation type was identified by collecting samples and taking photos along the RAS. Photos also were taken to estimate the amount of vegetation cover as described in Section 6.1.

Runway topography was determined from survey elevations at each marked location on the sampling map, as described in Section 4. Lateral and longitudinal profiles of the runway were derived from the survey data to examine runway flatness and smoothness. A more detailed laser-level profile of the runway centerline also was measured, information that also can be used to determine surface roughness or undulation.

3.1.3 Aircraft Operational Requirements

Knowledge of the aircraft type, gross loads, and traffic volume are necessary when evaluating an OLS and its potential capacity, because the capability of the structure will dictate allowable gross weight of the aircraft and overall number of operations that may be conducted. In this investigation, the RAS was evaluated as an unsurfaced runway suitable for C-130 and C-17 aircraft.

3.1.4 Data Compilation

All of the data collected to characterize the RAS were compiled and analyzed to help identify stronger or weaker areas and any other limitations. The RAS then was separated into representative areas based on thickness and types of soil layers, soil strength, and surface characteristics. The representative soil strength profile was then used to estimate the aircraft allowable gross load and/or the number of aircraft passes using the standard methodology briefly discussed below.

3.1.5 Estimates of Allowable Gross Loads/Allowable Passes

All of the information obtained to characterize the RAS was used in conjunction with the evaluation curves established in ETL 2002-19 (AFCESA 2002a) primarily to determine the allowable gross load (AGL) and allowable number of passes for the C-130 and C-17. For a semi-prepared airfield, there are two steps required to manually evaluate the runway: first, evaluate for the strength of the surface layer; second, evaluate for the thickness of the surface layer and the strengths and thicknesses of underlying layers. AFCESA developed the strength charts for specific aircraft as shown in Figure 6. Using the chart, the maximum number of passes can be determined by projecting horizontally the measured CBR value (y-axis) for the soil layer to intersect with the appropriate aircraft weight, and then project vertically to determine the number of passes (Fig. 7). This process is repeated for all subsurface soil layers and the layer that produces the lowest allowable number of passes is the controlling layer for the evaluation. Normally in airfield design, the number of passes are translated to loading type (i.e., channelized traffic for unsurfaced runway) to determine the runway coverage (e.g., a bell-shaped distribution of passes along the runway as a function traffic tapes). However, the loading type or runway coverage of the RAS is not included in this analysis.
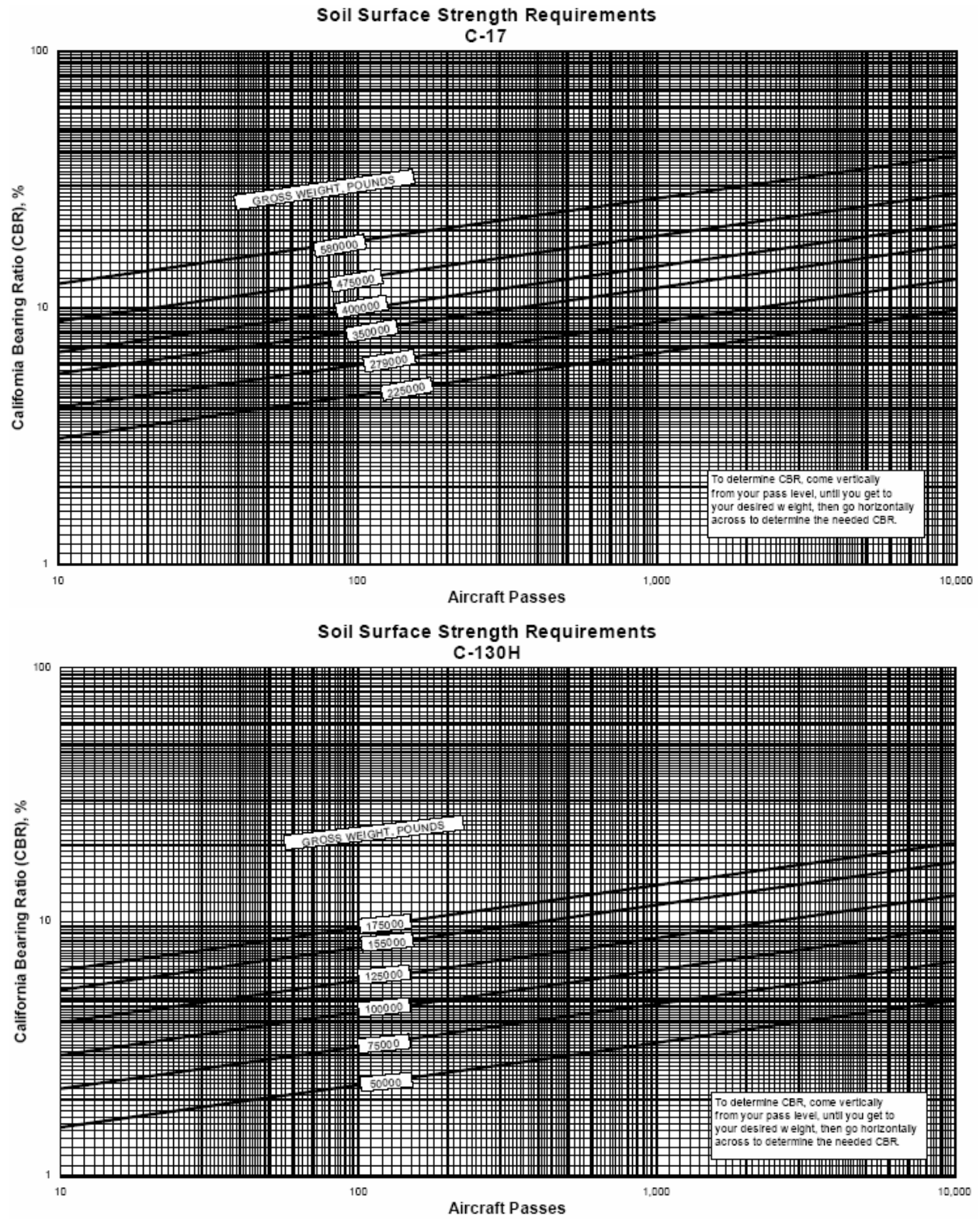
Figure 6. Soil strength on semi-prepared airfield for the C-17 and the C-130H.
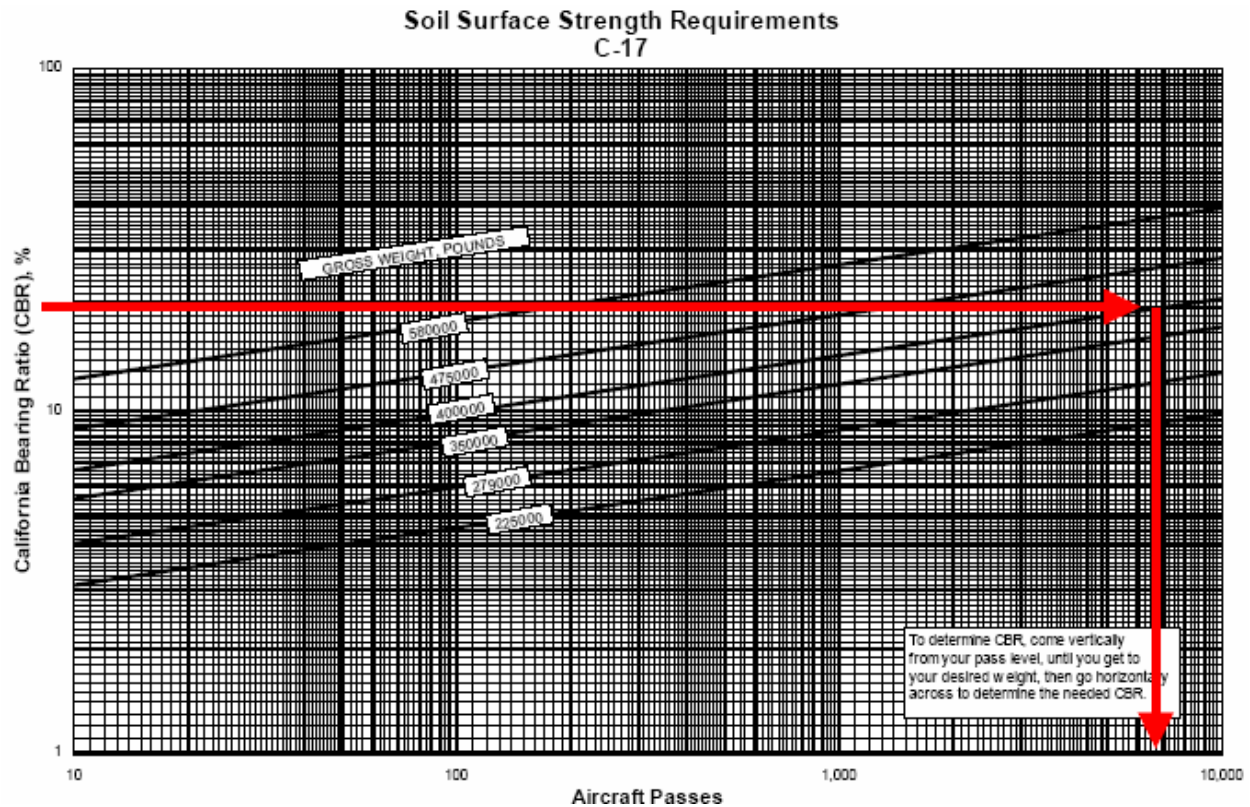
Figure 7. Example evaluation of surface strength on semi-prepared airfield for C-17 operations.

The structural capacity (aircraft load and number of passes) of the OLS was determined in layers of 0.15-m (6-in.) increments from the surface down to 1 m (3 ft). For airfield design, CBR value for the specific soil tested should be selected near the lower part of the range (UFC 3-260-02). Because of the scatter in CBR values where soil conditions vary substantially, take the representative CBR profile collected in test area by obtaining the 85th percentile of the maximum (or 15th percentile of the minimum) CBR values based on airfield design for subgrade soils. The scatter that can be expected with normal control procedures will vary with the soil type. The CBR profile used to determine maximum number of passes is based on the 15th percentile of the minimum CBR values collected on the OLS for each layer in 0.15-m (6-in.) increments.

PCASE (Pavement Design and Evaluation Software) is another source of evaluating the suitability of OLS for aircraft loading capacity (www.pcase.com). The software and documents can be downloaded through the Web site. The OLS loading capacity can be analyzed using PCASE evaluation module for unsurfaced runways. The module contains unsurfaced layer, subgrade, and unbound material types, which are appropriate for natural soil condi-

tions. The thickness of the layers and the corresponding CBR values can be imported into the module. The software is run for specific aircraft and will determine the aircraft load and number of passes.

3.1.6 Surface Characteristics

Assessment of terrain characteristics involved a visual survey of the surface characteristics of the RAS to record the near-surface terrain conditions in greater detail and to identify hazard areas to aircraft operations. This step identifies inhomogeneity within the RAS by evaluating it either for areas where the structure is potentially too weak (such as areas of ponding surface water) to support aircraft operations without resulting in excessive damage to the surface of the landing zone, or areas where aircraft operations may result in the OLS structure causing damage to the aircraft (an example is small, loose surface material being ingested into aircraft engines). Potentially weak areas would lessen either the number of landing and takeoff operations, or the allowable gross weight of the aircraft that the structure will support. The near-surface is considered to be within approximately 12 inches above or below (such as in the case of a drainage ditch) the horizontal plane of the natural terrain.

Procedures for evaluating and rating either semi-prepared or unsurfaced pavements are described in ETL 2002-19 (AFCESA 2002a) and provided the basis for characterizing RAS surface characteristics. Existing rating system for classifying the distress level on semi-prepared airfields for C-17 Contingency and Training Operations (ETL 97-9) consists of seven distress levels (potholes, loose aggregate, ruts, rolling resistance material [RRM], dust, jet blast erosion, and stabilized failure). These distress levels are coded as Green, Amber, and Red. Green means low risk to aircraft operations, Amber indicates a medium risk, and red designates high-risk operations and identifies areas that should be repaired before subsequent aircraft operations. ETL 97-9 rating system was used and amended to generate a list of criteria for assessing the condition of the RAS. Table 3 contains the criteria based on the impact of surface distresses for the C-17 (ETL 97-9), along with other features particular to aircraft operations on OLS.

Table 3. Surface characteristics used to evaluate the OLS.

	Surface Categories	Green	Amber	Red

1	Potholes
	   depth
	   diameter
		< 100 mm (4 in.) and/or
		< 380 mm (15 in.)
			100–230 mm (4–9 in.) and
			> 380 mm (15 in.)
				>230 mm (9 in.) and
				> 380 mm (15 in.)

2	Loose aggregate, coverage	< 10%	10 to 50%	> 50%
3	Rut depths	< 100 mm (4 in.)	100–230 mm (4–9 in.)	> 230 mm (9 in.)
4	Rolling resistance material, depth	< 90 mm (3.5 in.)	90–195 mm (3.5 –7.75 in.)	> 195 mm (7.75 in.)
5	Dust	Does not obstruct visibility	Partially obstructs visibility, appr. 400 m (¼ mile)	Thick; obstructs visibility
6	Jet blast erosion, depth	< 25 mm (1 in.)	25 to 75 mm (1 to 3 in.)	> 75 mm (3 in.)
7	Stabilized layer, depth	< 25 mm (1 in.)	25 to 50 mm (1 to 2 in.)	> 50 mm (2 in.)
8	Animal burrows* Number of holes Average hole diameter Area coverage and spacing	< 3 with < 25 m (1 in.) and 10 by 10 m area for every 200 m	3 to 6 with 25 m (1 in.) and 10 by 10 m area, at every 100 m.	>6 with > 25 m (1 in.) and 10 by 10 m area or bigger, at every 100 m or less.
9	Mounds* Height Base diameter	< 100 mm (4 in.) and/or < 380 mm (15 in.)	100 to 230 mm (4 to 9 in.) and > 380 mm (15 in.)	>230 mm (9 in.) > 380 mm (15 in.)
10	Vegetation* Height Stem or branch diameter	< 0.5 m (1.5 ft) no branches or bushes and tall grass	< 0.5 m (1.5 ft) < 1 in. diameter	> 0.5 m (1.5 ft) > 1 in.
11	Standing water* Depth Diameter	zero	0.25 mm (1 in.) and > 380 mm (15 in.)	> 50 mm (2 in.) and > 380 mm (15 in.)
12	Surface drainage paths,* depth	< 100 mm (4 in.)	100 to 230 mm (4 to 9 in.)	> 230 mm (9 in.)
13	Surface debris and organ- ics materials* Amount of organics Diameter logs or debris	<5% and < 50 mm (2 in.)	5 to 20% and > 50 – 100 mm (2 to 4 in.)	>20% and > 100 mm
14	Snow depths*	zero	25 to 50 mm (1 to 2 in.)	> 50 mm (2 in.)

* Additional evaluation features added specifically to evaluate RASs using similar approach to that for C-17 semi-prepared run-ways. These additional distress types are rated subjectively and further.

The features of the RAS were documented during a walk-through conducted during three visits in summer, fall, and spring. This entails examining the entire area of the RAS and documenting the physical characteristics. Each of the features was quantified in order to determine the rating representing the entire RAS (Table 3). The types of OLS features documented and evaluated included but were not limited to the following:

1. Potholes or depressions. Typically well-defined bowl-shaped depressions in the airfield surface. The number, location, and depth of potholes can be critical to aircraft operations.

2. Loose aggregate. Rock outcrop and loose aggregates (Fig. 8) including small stones on the surface 6 mm (0.25 in.) or larger can create problems such as FOD (Foreign Object Damage) and ingestion that could damage the engine and other parts of the aircraft. (FOD varies with plane and engine type.) Loose aggregate on the OLS surface can cause roughness of slippery conditions when wet. AFCESA recommended that rocks over 100 mm (4 in.) in diameter must be removed from the operational surface.

Loose Aggregate, Amber Severity

Figure 8. Picture from ETL 97-9 for severity rating of localized loose aggregate.

3. Rut depths. Surface depressions of 12 inches or less made from mechanical equipment, such as farm equipment or motorized vehicles, particularly within or across the aircraft wheel path area.

4. Rolling resistance material. Loose fine-grained surface material, such as from tilling, that increases drag (friction) upon takeoff, requiring a longer takeoff distance for the aircraft.

5. Dust. Loose material that becomes airborne when disturbed. The natural material on unsurfaced airfields and the multiple passes of the aircraft cause these fine materials to separate from the soil binder and become a significant problem for personnel, trailing aircraft, and the environment. ETL 97-9 suggests measuring dust by having a vehicle drive at 60 miles per hour down the runway and watching the dust cloud; if you cannot see the vehicle then the rating is Red. This method was not performed on the OLS, but was noted on nearby trails.

6. Jet blast erosion. Areas where soil is blown, stripped away by engine blast. Jet blast erosion is uncommon on the OLS unless the area was previously used as a landing zone.

7. Stabilized layer failure. Failure of a stabilized surface layer occurs. Desert areas can have a naturally stabilized layer such as duricrust and desert deposits. The desert forms evaporite deposits: as water with minerals evaporates the minerals are left behind to cement soil and aggregate particles together. These are often called duricrusts or pedecretes. Often termed by constituent: calcium carbonate deposits become caliche or calcrete, dolomite becomes dolocrete, gypsum becomes gypcrete, silica becomes silicrete, etc. Duricrusts can be weakly cemented or strongly cemented, can be discontinuous or massive. Desert pavement, on the other hand, is a process of ablation. A desert pavement has boulders and cobbles/aggregates and soil has the sand and fines progressively removed by wind. As sand and fines are removed, rocks accumulate on the surface until they form an almost continuous layer of rock and only scattered rock in a sandy soil matrix is typically found below the layer.

8. Animal burrows. Animal holes, surface scouring, and surface irregularities caused by wildlife or farm animals are signs that the soil structure has been disrupted and would weaken soil support for aircraft operations. Some of the burrows are connected in a series of subsurface small tunnels, creating pockets or voids in the soil strata. A measurement consisted of the size and number of holes;

the extent of the area with holes is critical because soil will collapse when subjected to loading.

9. Mounds. Soil accumulation typically around the lower part of bushes. Mounds are measured based on their surface profile (height and base diameter of the mounds). Mounds can be translated as inverted potholes. The size of the mounds were characterized similarly to the severity used for potholes.

10. Vegetation. Type and area of coverage of plant material found on the RAS. Vegetation of certain types, such as bushes or a field of corn, may impede aircraft operations.

11. Standing water/wet areas. Ponding of surface water indicates poorly draining soils resulting in weak areas. Areas are noted and characterized by depth and approximate diameter.

12. Surface drainage paths. Patterns of flow from runoff that cause surface roughness, including natural and man-made ditches.

13. Surface debris and organic materials. Loose materials present on the surface that can damage the aircraft, including logs, tree branches, organic litter from agricultural plants, and natural vegetation. The bulkiness and amount should be examined and quantified, because these materials could puncture the aircraft's tires or be ingested into the engine.

14. Snow depth. In areas of seasonal change, the presence of a snow layer is noted.

3.2 Overall OLS Rating

The overall rating of the entire OLS is determined based on approximation from the total analysis of the surface characteristics based on Table 3, the geometry properties (smoothness, flatness) using Table 2 and the soil strength for calculating the loading capacity of the natural soil structure. Table 4 is the culmination of all the ratings for each category representing the entire OLS from the evaluation information and analysis. An "excellent" OLS must have greater than or equal to 80% (11 out of 14) Green, 20% (3 out of 14) Amber ratings, and zero Red ratings for all surface categories for surface characteristics; it has 100% for geometric properties;

and the aircraft (C-130H or C-17) should have loading capacity between minimum and maximum gross load at 10 passes. A "marginal" OLS should exhibit 50% Green, 50% Amber, and no Red ratings for surface character-istics; 100% for geometric properties; and the aircraft (C-130H or C-17) should have assigned allowable loads between minimum and maximum weights of the aircrafts with between three and 10 passes. An "unaccept-able" or a "fail" rating will contain greater than 50% Red rating of surface characteristics and fewer than two passes at minimum aircraft load or less.

Table 4. Estimation for the overall rating of the entire OLS for C-17 and C-130.

Categories	Excellent or Pass	Marginal or Caution	Unacceptable or Fail
Surface characteristics	Green: ≥ 80% (11 out of 14), Amber: ≤ 20% (3 out of 14), Red: zero	Green: 50% Amber: ≥ 50% Red: zero	Green: zero Amber: ≤ 50% Red: ≥ 50%
Geometric properties	Green: 100%	Green: 100%	Green: <100%
Aircrafts loading capacity Using charts or PCASE: Allow. gross load	Between min. & max. weight	Between min. & max. weight	Minimum weight or less
Number of passes	≥5 and ≤10	≥3 and <5	<2
Or using average CBR Catego-ries:			
C-17 CBR @ min. weight @ max. weight	>6 <10	>2 & ≤6 >4 & ≤10	≤2 ≤4
C-130 CBR @ min. weight @ max. weight	>4 <12	>2 & ≤4 >6 & ≤12	≤2 ≤6
C17: minimum weight = 126.6 metric ton (279,000 lb), maximum weight = 265 metric ton (585,000 lb) C130: minimum weight = 31 metric ton (69,000 lb), maximum weight = 79 metric ton (175,000 lb)			

4   Runway Assessment Site (RAS) Evaluation

4.1 Evaluation Procedure, Measurement Technique, and Methodology

4.1.1 Weather Monitoring Instrumentation

The fenced tower area south of the RAS was used to house the weather observation station. The weather station included instrumentation to measure air temperature, relative humidity, wind speed/direction, rainfall, soil temperature, and soil moisture. The soil temperature probe consists of seven thermistors spaced 10 cm apart, was placed into the ground with the top thermistor just under the soil surface, and the bottom thermistor located at 60 cm below the surface. The soil moisture probe had sensors located 5 cm, 15 cm, 25 cm, 35, cm, 55 cm, and 95 cm below the soil surface. Data gathered from all the instrumentation will be used in the soil strength model, which is another task under the OLS program and is not part of this report.

4.2 Non-Seasonal Impacts

4.2.1 Surface Profile (Topography, Flatness, and Smoothness Measurements)

During the first field visit, the runway ends and sampling points were marked along the RAS using a total station surveying instrument with a Trimble GPS (Global Positioning System) Pathfinder. The GPS system is designated as "map grade," providing a positional accuracy to within 0.5 m (1.6 feet) when coupled with the Continuously Operated Reference Stations (CORS). The vertical datum was set using Delorme Topo USA digital map software (version 4.0) to determine the elevation of the sampling stations.

To capture the micro relief or undulation and surface roughness along the centerline of the RAS, a laser profile was collected every 1 m in areas that are noticeably rough and every 5 m in areas that are relatively smooth. The spacing for measuring the profile was solely on the perception of the data gatherer (i.e., 1-m profile readings for areas with mounds, depressions, or swales). A surface roughness value along the center line of the RAS is calculated from the elevation data taken by laser level using the Root Mean Square (RMS), as follows:

$$RMS = \sqrt{\frac{1}{n}\left(\sum f_i x_i^2\right)}$$
(1)

where, n = number of data

$$f_i x_i = \left(x_i - \bar{x} \right)$$

$\bar{x}$ = the mean of the data.

A profilometer also was used to illustrate roughness and flatness of the surface. This instrument consists of rods spaced 2 cm apart, and each rod is vertically marked at 1-cm intervals. Photos were taken to detect the undulation of the ground.

4.2.2 Soil Characterization (Surface Soil Color, Soil Type, Density, Organics)

The physical properties of the RAS soils were characterized using several techniques to assess runway suitability and to help implement the OLS moisture and soil strength algorithms. Assessment of the ability of the RAS to support aircraft operations required soil strength measurements to a depth of 1 m. The RAS field site also provided an opportunity to gather information that supported the ERDC OLS program for soil moisture and soil strength prediction tasks. Soil moisture with depth and soil physical characteristics such as texture, density, and plasticity were measured to support this work. Also, Boeing was tasked to identify soil type at OLS sites using satellite imagery and other terrain-related information. Therefore, surface soil color was identified with a Munsell chart, and surface soil samples were collected to assess mineralogy and organic matter content for Boeing hyperspectral analyses. All surface samples were taken and the organic matter analyses were completed. However, mineralogical analyses were not conducted because Boeing was forced to abandon the hyperspectral approach when the Hyperion satellite became unavailable.

Particle size distribution provides information about soil texture, which is one of the key properties for classifying soil type. The soil classification is directly related to the bearing capacity or strength of the soil. The process for determining soil classification on the RAS and characterizing soil profile is described below.

For the OLS project, soil density measurements at the RAS are valuable in understanding density values in natural soils and impact the soil strength. Frequently, "as-built" density values of engineered soils are reported in airfield studies. However, there is very limited information published for soil density values in natural soils, such as might be found at OLS sites. The measurements taken during the OLS project will add to the body of knowledge currently available. Another use for the density measurements, specifically the dry density, is that it is needed to convert the moisture content on a dry weight basis to a volumetric measurement. Using measured values provides a higher confidence for a model that uses inferred soil density values or values from the literature that may not fully represent the actual field conditions. From a practical standpoint, taking the measurements at the field site required equipment that is portable and easy to use (although some logistics are required for transportation of specialized equipment such as the nuclear density gage).

A density test with nuclear gage consists of a radioactive source at the end of the rod and the detector at the rear of the machine housing. The source rod is extended at 50-mm (2-in.) increments into the soil to take the density readings at each depth and the source rod can be extended down to 305 mm (12 in.). The density measured is the average density along a line between the source at depth and the sensor at the surface (i.e., reading at 305 mm [12 in.] is not the density at 305 mm [12 in.] but rather is the average density from 305 mm [12 in.] to the surface). Unlike assessing the density of constructed or mechanically compacted soils, deploying the nuclear gage to measure the soil density on natural, dry, granular soils such as this site was troublesome. In these dry, granular soils, when the template rod was pulled out of the soil, the hole partly filled, allowing only a shallow depth for the source rod to penetrate. As a result, in most cases density measurements were achieved with readings at maximum depths shallower than 305 mm (12 in.) or until the source rod resisted further extension. Also, some error in the readings could have been caused by soil disturbance during digging and the process of setting up the gage. To compensate for these errors, eliminating the top 100-mm readings was recommended because the longer the source rod is extended into the hole the more soil is included in the measurement, and the more reliable are the results. Therefore, the density readings reported here are the average densities at depths from 150 mm (6 in.) to the surface, and below.

The section below describes soil field characteristics measured at the El Centro RAS that are anticipated to be unaffected by seasonal change: soil texture, soil color identification, and soil density. Samples collected from the soil pits at varying depths were used to determine the soil texture with depth. The soil samples were sent back and analyzed for grain size, Atteberg limits, and specific gravity tests at the CRREL soil laboratory.

4.2.2.1 Field Soil Sampling and Testing

Soil pits were dug at selected locations (see Fig. 5) to collect soil samples at various depths to characterize the soil profile. Before digging and disturbing the ground, photos were taken a full 360° around the flagged location of the ground surface. In most instances, the color of the soil on the surface was identified using the Munsell soil color chart (Munsell 2000). Surface soil samples were collected before digging the pits. The pits were large, approximately 2 by 2 m (6 by 6 ft), because of soil slumping back into the hole. The objective depth of soil pits was 1 m. Photos were taken of the soil profile, and distinct soil layers were noted. Soil samples were taken at various depths and were sent back to CRREL for laboratory analysis of grain size distribution, Atteberg limits, organic content, moisture, and specific gravity.

Concurrent with digging each soil pit, soil density measurements were made to determine the density profile using the Troxler Model 3440 surface moisture-density nuclear gage. The nuclear gage is widely used in the USAF since at least 1976 and is routine in almost all military construction (on mechanically compacted soils during construction projects). The procedures used for the equipment comply with the ASTM D-2922 and ASTM D-3017. ASTM D-2922 states that acceptable precision using the nuclear gage for wet density readings are standard deviations of 5.4, 4.3, and 7.4 kg/m^3 (0.34, 0.27, and 0.46 lb/ft^3) for clay, poorly graded sand, and silt soils, respectively (for a single operator and direct transmission mode). The primary measurements from the gage are wet density (total density in units of grams per cubic centimeter or pounds per cubic foot) and soil moisture (M in units of grams or pounds of water per cubic centimeter or foot of dry soil). The nuclear gage also displays the dry density value calculated from the difference between the wet density and M.

When the nuclear gage is positioned in a soil pit, density measurements can be made at 50-mm (2-in.) intervals from the base of the probe to a depth of 305 mm (12 in.) below the base. This is accomplished by driving a

template rod into the soil from the surface, creating a hole into which a rod with a nuclear source is inserted. For measurements deeper than 305 mm (12 in.) from the base of the instrument, the soil pit was excavated down another 305 mm (12 in.) where the bottom of the pit was leveled to provide good contact and a base for the instrument. This process was repeated to the required depth. Density readings were attempted to a depth of 915 mm (36 in.). However, problems were encountered because of soil slumping, and hard and granular soil.

During the first IOP on 11–15 July 2005, four pits were dug on the OLS. The pits were located at 1+40 CL, 3+80 2S, 6+30 2S and 9+80 2N. The four pits were dug at various depths of 0.56, 0.61, 0.61, and 0.81 m (22, 24, 24, and 32 in.), respectively, and dependent on the difficulty of digging and soil slumping. Additional soil samples were taken during the second IOP on 17–21 October 2005, and two of these locations were sampled 1 m away from the prior pits (normally taken on the other side of sampling location). These soils were obtained at locations 6+30 2S, 7+50 30S, 9+80 2N, and 10+60 CL. No additional soil samples were collected during the third IOP.

4.2.2.2 Laboratory Testing

Samples were analyzed in the laboratory using ASTM standards D 421-85, D 422-63, D 4318-00, D 854-02, and D 2487-00 (both textural and plasticity characteristics [Atterberg limits] and specific gravity test). The resulting soil classification is reported per the Unified Soil Classification System (USCS) (ASTM 2003).

Surface soil samples were tested for organic content by weight following ASTM 2974. Test method A was conducted to determine moisture content; method C, an accepted method for geotechnical purposes, used a muffle furnace to determine ash content. Although ASTM 2974 is for peat-type soils to determine whether a soil is organic or not (i.e., classifying the soil with an O [organic] to be either OL [organic silt] or OH [organic clay]) based on the ratio of the liquid limit run with and without oven drying, this method was used for RAS soils in order to calculate the organic content in the soil. Samples were tested in groups of ten. Replicates of tests were performed on samples taken at each location to examine the variation in results using each test method.

4.3 Seasonal Impacts

Seasonal effects can influence the suitability of an OLS by producing changes in moisture, snow, soil frost, and thaw, including changes in ground animal activity and vegetation cover with resulting impact in soil strength. Seasonal impacts on the El Centro RAS were assessed by seasonal examination of the surface conditions, recording the types and height of vegetation and measuring the soil moisture and soil strength profiles.

4.3.1 Surface Conditions

The surface conditions were examined to discern weak areas, obstructions, and drainage. For example, a mound with animal holes is a sign that the soil will collapse when a load is applied. Vegetation cover, greenness, species, and height were examined. The vegetation cover was captured using photographs, and the types of vegetation species were identified by a CRREL botanist from the photographs.

4.3.2 Vegetation

4.3.2.1 Vegetation Type and Height

Vegetation identification was accomplished for dominant species by collecting samples and placing them in clear plastic bags. The vegetation samples and corresponding photos were then identified by botanist Robert Lichvar at CRREL. Minor species may have been missed. The representation vegetation height was noted for each plant.

4.3.2.2 Vegetation Cover and Greenness

Quantification of vegetation cover on the RAS is approximated using photos of the landscape taken from directly overhead and obliquely at several sampling locations. Because overhead photos are taken over an approximately 1-m area, they do not always capture the tall vegetation, such as the *Larria Tridentata* (Creosote bush) and *Grayia* (dune species). Photos of the landscape along the RAS were used to estimate the number of bushes within the RAS and approximate size of the crown of the bushes. Vegetation cover from the overhead photos are quantified by determining the total area covered by various plants. From the 3072- by 2304-pixel photos, the total area of the photo was calculated using the number of pixels (e.g., area = 7077888 pixel square). Each photo was analyzed using ArcMap

software (ArcGIS) by digitizing the polygons surrounding the plants, and the software calculated the total area of plant cover. Percent vegetation cover was calculated using the ratio of plant cover to total area multiplied by 100. This method of quantifying the vegetation cover is an approximation and does not include vegetation litter or organics such as dead grass or branches that were present on the surface. Also, extrapolation of the small photograph sample areas to the area of the RAS is also approximate. However, the photos are chosen to be representative of vegetation patterns observed. At six of these sampling locations, the vegetation cover was calculated from two oblique photos for the low-height plant species, then an average value was taken to represent the percent vegetation cover.

4.3.3 Soil Moisture

Soil moisture was measured with depth during every IOP. Several methods were used, including the Dynamax sensors (ML2 and PR2 probes) and gravimetric methods using the spoon and drive-cylinder samples (ASTM D 2216-98, ASTM D 2937-04). Dynamax sensors provide moisture content in percent volume, whereas oven-dried samples are reported in percent by weight. The volumetric soil moisture content of the soil was measured using the Dynamax Theta probe ML2 sensors and the Dynamax Profile Probe, PR2. Volumetric soil moisture content is the ratio between the volume of water present and the total volume of the sample, and is expressed in %Vol. It is important to note that desert soils often have minerals such as calcium sulfate, which can be anhydrate, hemihydrate, or hydrate depending on the amount of water bound in the mineral. The minerals can cause chaos with the moisture sensors used in the nuclear gage and for those dielectric constant moisture sensors as estimator for moisture content (Rollings 2007, personal communication). This water in the mineral is not available to affect soil behavior but gets picked up by the sensors.

The ML2 is a soil impedance-based measurement that contains electronics array of four sharpened stainless steel rods, or tines. The impedance is dependent almost solely on the soil apparent dielectric constant. The dielectric constant of soil is function of its water content (see http://www.dynamax.com/ or ftp://ftp.dynamax.com/Manuals/ml2x.pdf). To measure the soil moisture profile, the tines are inserted into the soil. ML2 readings were conducted on the surface and at various depths in the soil pits during IOP #1, by shoveling narrow holes during IOP #2, and only measuring at the surface during IOP #3.

The PR2 probe consists of a sealed polycarbonate rod, roughly 25 mm in diameter with electronic sensors (pairs of stainless steel rings) arranged at fixed intervals along its length. The signal is applied to the pairs of stainless steel rings and an electromagnetic field is transmitted, extending about 100 mm into the soil. The electromagnetic field is a function of the soil permittivity, which changes with water content in the soil (see PR2 User Manuals). PR2 sensors were installed during IOP #2; however, measurements were taken only during IOP #3.

The gravimetric soil moisture contents were obtained following standard procedures (ASTM D 2216–05) from specimens collected via spoon and drive-cylinder samples. For the spoon samples, soil specimens of 500 grams or more were collected, placed in airtight plastic bags, and weighed. Soil density measurements were made using the drive-cylinder method, and soil moisture contents were taken from these samples. The gravimetric soil moisture contents, w, were derived from the oven-dried samples taken in the RAS using

$$w = \frac{M_w}{M_s} 100(\%)$$

(2)

where M_w = mass of water, and

M_s = mass of soil solids (dry soil).

4.3.4 Soil Strength

Soil strength is one of the critical parameters determining whether soil bearing capacity is sufficient for landing an aircraft, or if the OLS is suitable for multiple passes. Seasonal differences in surface and subsurface soil strength were measured at selected locations on the sampling grid (Fig. 5) during each IOP (Table 6). In-situ soil strength measurements on the RAS were estimated and obtained using the Dynamic Cone Penetrometer, the Clegg Impact Hammer, and the Drop cone.

4.3.4.1 Dynamic Cone Penetrometer (DCP)

The Dynamic Cone Penetrometer (DCP) was used for measuring the soil strength profile for pavement and airfield applications (ASTM 2003 D 6951-03; FM 5-430-00-2), including expedient assessment of airfield conditions in terms of evaluating the field soil strength. Information from the

device is used to quantify the bearing capacity of the soil, and is translated into soil strength in terms of California Bearing Ratio (CBR) values ranging from 1 to 100% (where the 100% value is representative of the CBR or crushed limestone gravel). The DCP was used to a maximum depth of 1 m, the full depth capability of the instrument as configured for the OLS field work. Both manual and Digital Acquisition System (Vertek) methods were used to record the DCP values of cumulative penetration and number of blows.

The DCP consists of a steel rod with a 1.6-cm-diameter shaft and a 60° cone, which can be disposable. It can be fitted with either a 4.5- or 7.7-kg (10- or 17.1-lb) hammer. As the whole device is held vertically, the cone is tapped into the soil by the drop of the hammer from a set distance. The number of hammer blows is counted, and penetration depth is measured for each set of hammer blows. CBR values are calculated using a relationship (eq. 3) developed for use in pavement design or evaluation (Webster et al. 1992)

$$CBR\% = \frac{292}{DCPindex^{1.12}}$$
(3)

where CBR = soil strength

$DCPindex$ = average penetration caused by one hammer blow.

Because of lack of confinement on the soil surface, the DCP can measure strengths of thin layers below the surface for fine-grained plaster materials but requires thicker surface for the non-plastic coarse-grained materials. For silty sand (SM) soil, the average penetration depth required is 13 cm (5 in.) (Webster et al. 1994). One DCP profile was conducted at each sampling location on the RAS unless additional verification was needed or an incident occurred where the rod deviated from vertical.

4.3.4.2 Clegg Impact Hammer

Surface soil strength was measured using the Clegg Impact Hammer (CIH). The CIH is a nondestructive testing device for design and evaluation of pavements. The device consists of a cylindrical mass hammer (4.5-kg mass) that is dropped within a guide tube from a set height. The hammer is dropped four times at each location and the readings are recorded for each drop. The hammer is equipped with an accelerometer that meas-

ures the peak deceleration on impact. The readings are displayed as Clegg Impact Value (CIV) and the fourth reading is converted to CBR (ASTM 2003 D 5874; Clegg 1980). The CIH was tried on the RAS and it was found that the instrument readings were out of range for the type of soil conditions encountered. Therefore a light CIH (CIH$_L$), with a 0.5-kg (1.1-lb) mass and 50-mm- (1.97-in.-) diameter hammer, which was developed for testing softer materials, was used to assess RAS surface soil strength.

Similar to the CIH (standard 4.5-kg CIH), the CIH$_L$ consists of a hammer, guide tube, and a read-out unit. The hammer is equipped with an accelerometer and the instrument reads the peak deceleration on impact, which is the Clegg impact value (CIV) expressed in units of tenths of gravities (g). At a stationary location the hammer is dropped four times, noting the CIV for each drop, and this corresponds to one dataset. The mechanism in soils may be described as compaction immediately under the impact area (increasing with blows), and penetration of this compacted zone into the body of the material with consequent lateral and vertical deformations. At higher blow numbers the resistance to deformation resulting from the confinement may be seen as reflecting the overall stiffness of the surrounding material (Clegg 1978). On mechanically constructed soils, the CIV readings generally increase for each subsequent drop. However, it is not always the case for natural soils. The recommended practice is to use the fourth blow reading to calculate the CBR. The CIH$_L$ hammer is free-falling at 0.3 m (12 in.) inside the guide tube, and the instrument displays a Clegg impact value (CIV/L) that can be converted to soil strength.

A correlation of CIV/L$_4$ (fourth Clegg Impact Value for the 0.5-kg hammer) with CBR was developed by Millar (1977). This correlation was developed from few data points. Additional tests were conducted to expand the range of data and further refine the existing algorithm from CIV/L$_4$ to CBR (Affleck et al. in prep.), as

$$CBR = 0.0121\left(\text{CIV/L}_4\right)^2 + 0.1005\left(\text{CIV/L}_4\right) \qquad (4)$$

where CBR = soil strength measured using a CBR test (ASTM 2003)

(CIV/L$_4$) = the fourth drop Clegg impact value for 0.5-kg mass hammer.

Replicate CIV/L datasets were taken at each sampling location. Equation 3 was applied to each dataset, and then an average was taken at each sampling location to represent the surface CBR value.

4.3.4.3 Other Tools

Surface strength was measured using the Drop cone. The Drop cone, also called a Surface Damage Cone, was designed for measuring surface penetration resistance and soil compaction potential from vehicle traffic for agricultural applications (Godwin et al. 1991). The dynamic measurements taken by the Drop cone are based on work (kinetic energy) imparted to the soil and are reported as a force.

The Drop cone consists of a large 30° cone screwed to a rod weighing 2 kg, which is dropped from 1 m through a PVC guide tube. The combined weight of the rod and the cone is 4.5 kg. Penetration is measured for only a single drop and is generally taken for three measurements per location. Strength of the soil can be determined by calculating the force exerted by the cone needed to penetrate into the ground. Analyses using similar type of cones have been done by Abele (1990) and Vaz and Hopmans (2001), and other equations exist (Herrick and Jones 2002, Stolf et al., 2005). The force applied is the work done on the soil divided by the penetration distance using the equation,

$$R = \frac{Whn}{x} + W + Q \qquad (5)$$

where W = weight of drop hammer (kg)

h = height of drop (cm)

n = number of hammer blows

x = difference in depth between blow sets (cm)

Q = weight of tool (w/o hammer) (kg)

R = force (kg$_f$).

4.4 Site Description of Systematic Imagery Runway Assessment Site (SI-RAS)

4.4.1 Location

The OLS selected for the field work is 1197 m (3927 ft) long and 60 m (200 ft) wide. This OLS was a result of using the 9 May 2005 LANDSAT imagery for 200-ft by 3000-ft runway dimensions (Fig. 2). Its orientation is exactly east–west and 772 m north of the microwave tower near Target 103, as shown in green in Figure 9. The western end of the OLS is near a railroad track that runs in a northwest and southeast direction. West of the railroad track is an active bombing practice area of restricted use. There is an access road along the east side of the railroad track and another access road that runs northeast, about 500 m east of the OLS. Because the Naval reservation land is bounded by BLM lands, people can use the land for camping and vehicular recreation, including all-terrain vehicle use east of the railroad track. This was evident on the RAS location.
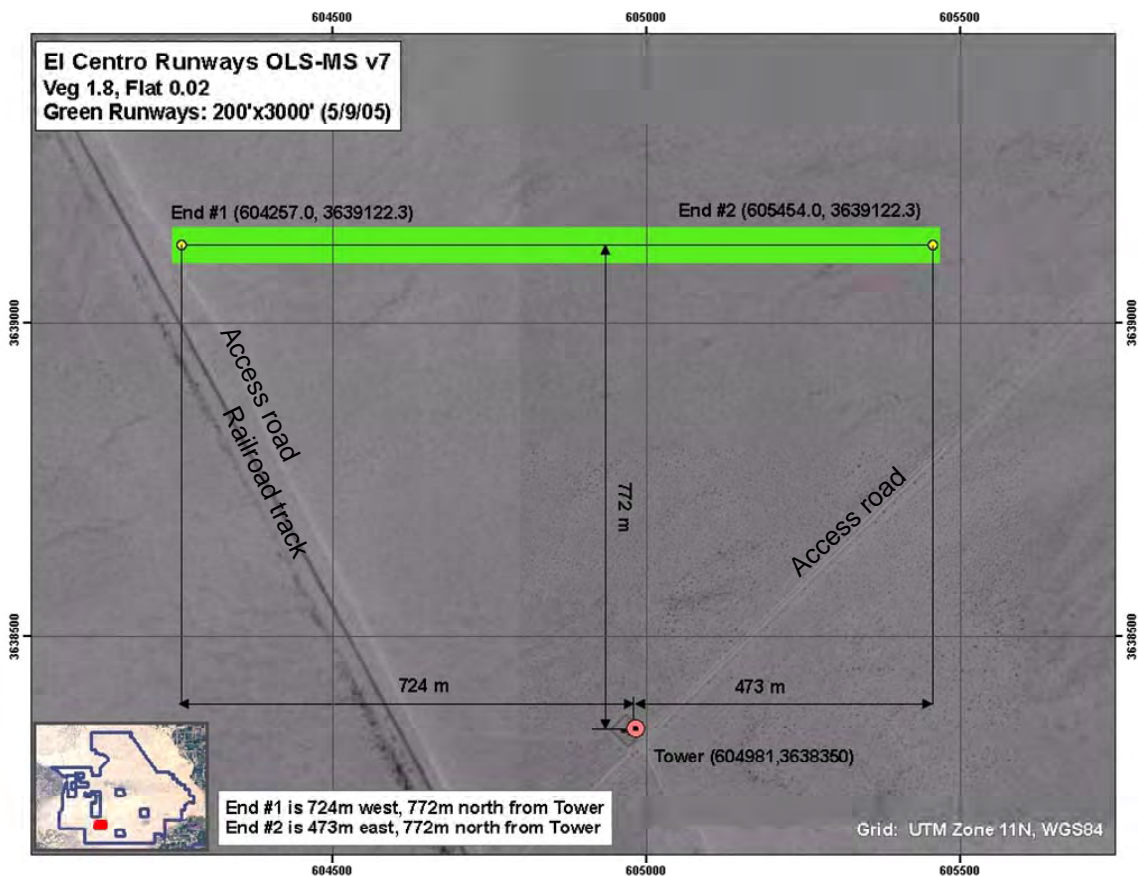
Figure 9. Coordinates of the center end locations of OLS and distances to microwave tower near Target 103.

4.4.2 Field Visits and Sampling at Systematic Imagery Runway Assessment Site (SI-RAS)

To capture seasonal effects, field visits or intensive operational periods (IOPs) were conducted for three seasons, listed in Table 5. The field visits were conducted during summer (IOP #1), fall (IOP #2), and spring (IOP #3) conditions. Field work was not conducted during the winter at El Centro. Surveys of surface and subsurface conditions were conducted for each IOP to examine the seasonal conditions, including terrain and vegetation features and measurement of soil properties.

Prior to IOP #1, a sampling grid was created for the EL Centro OLS. The beginning point of the runway starts at the east end with station 0+00 (End #2 in Fig. 9) with the coordinates of 605454 m east and 3639122 m north, UTM Zone 11N projection, WGS1984 datum. At station 0+00, grid points that are offset from the center line are denoted by the station along the centerline and whether they are located north or south of the centerline. For example, station 1+70 means it is located at 170 m (560 ft) from the runway start point, CL stands for the centerline, 10N means 10 m (33 ft) offset north of the centerline, 30S indicates 30 m (98 ft) offset south of the centerline. The sampling grid was developed to sample the entire RAS and used to denote locations for measuring surface and subsurface data including vegetation type and cover, soil pits for soil type, density, soil strength, and moisture (Fig. 5). The green dots in Figure 5 identify all sampling locations from all IOPs where at least one measurement was taken and also identify the locations where soil pits were excavated for profiles of soil type, moisture, and density (symbolized by the red diamond). A complete summary of all measurements recorded during each IOP and at each sampling station is given in Table 6.

Table 5. Intensive operational periods (IOPs) in El Centro NAF.

	Seasons	Field Visit Dates
IOP #1	Summer	11–15 July 2005
IOP #2	Fall	17–21 October 2005
IOP #3	Spring	23–24 April 2006

4.4.3 Weather Information

As expected, the El Centro site was a year-round warm, dry environment, with warmer temperatures in summer and cooler temperatures in winter.

Air temperature from July 2005 to April 2006 is shown in Figure 10a. The high temperatures approached 50 °C (122 °F) in July, around the time-frame during IOP #1 (Fig. 10b). Even with nighttime radiational cooling, no temperatures below freezing were recorded. Cooling occurred around 16 October, days before IOP #2 (Fig. 10c). Air temperature hovered around 20 °C (70 °F) during mid-day in the spring (IOP #3, Fig. 10d).

Table 6. Field measurements taken at El Centro Runway Assessment Site during each field visit.

DCP = Dynamic Cone Penetrometer (Strength Profile)   x indicates that a measurement was taken
Clegg = Clegg Hammer (Surface Strength)
Army Cone = Cone Index (Strength Profile)
Dor Cone (Surface Strength)
Dynamax = Soil Moisture (Surface and/or with depth)
S = Soil sample(s) taken for Grain size analysis, Surface organic content
D = Density (Density using Troxler and/or Density using drive cylinder)
V = Vegetation Cover (images)

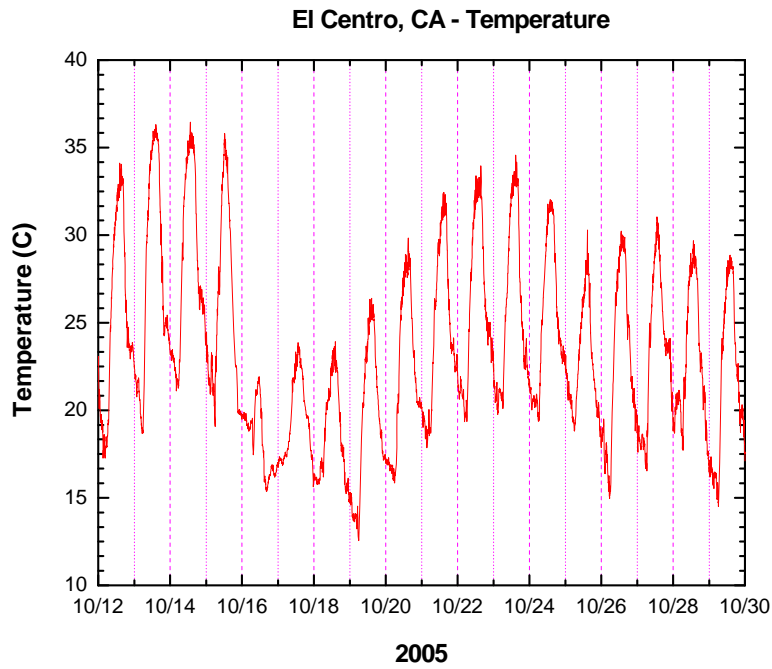| Sampling points	SUMMER (July 11-15, 2005)								FALL (October 17-21, 2005)								SPRING (April 23-24, 2006)							
	DCP	Clegg	Army Cone	Dor Cone	Dynamax	S	D	V	DCP	Clegg	Army Cone	Dor Cone	Dynamax	S	D	V	DCP	Clegg	Army Cone	Dor Cone	Dynamax	S	D	V
0+70 30S												x												
0+70 20S	x	x			x				x	x		x	x				x	x		x	x			
0+70 CL	x	x			x			x	x	x		x	x			x	x	x		x	x			x
0+70 20N	x	x			x				x	x		x	x				x	x		x	x			
1+40 30N	x	x			x				x	x		x	x				x	x		x	x			
1+40 10N	x	x			x				x	x		x	x				x	x		x	x			
1+40 CL	x	x	x	x	x	x	x	x	x	x		x	x		x	x	x	x		x	x			x
1+40 10S	x	x			x				x	x		x	x				x	x		x	x			
1+40 30S	x	x			x				x	x		x	x							x	x			
1+80 2S	x	x			x				x	x		x	x				x	x		x	x			
1+80 CL								x																x
1+80 2N	x	x			x				x	x		x	x				x	x		x	x			
2+20 20N	x	x			x			x	x	x		x	x	x	x		x	x		x	x			
2+20 2N	x	x			x				x	x		x	x				x	x		x	x			
2+20 CL	x	x			x			x	x	x		x	x				x	x		x	x			x
2+20 2S	x	x			x				x	x		x	x				x	x		x	x			
2+20 20S	x	x			x			x	x	x		x	x							x	x			
2+60 2S	x	x			x				x	x		x	x				x	x		x	x			
2+60 CL								x																x
2+60 2N	x	x			x				x	x		x	x				x	x		x	x			
3+00 10N	x	x			x				x	x		x	x				x	x		x	x			
3+00 CL	x	x			x			x	x	x		x	x				x	x		x	x			x
3+00 10S	x	x			x				x	x		x	x							x	x			
3+30 2S	x	x			x				x	x		x	x				x	x		x	x			
3+30 CL								x																x
3+30 2N	x	x			x				x	x		x	x				x	x		x	x			
3+68 2S	x																							
3+68 7S	x																							
3+72 2S	x																							
3+74 2S	x																							
3+80 20N	x	x			x				x	x		x	x				x	x		x	x			
3+80 2N	x	x			x				x	x		x	x				x	x		x	x			
3+80 CL								x																x
3+80 2S	x	x	x	x	x	x	x	x	x	x		x	x		x		x	x		x	x			
3+80 20S	x	x			x				x	x		x	x				x	x		x	x			
4+50 30S	x	x			x				x	x		x	x				x	x		x	x			
4+50 10S	x	x			x			x	x	x		x	x				x	x		x	x			
4+50 CL	x	x			x			x	x	x		x	x				x	x		x	x			x
4+50 10N	x	x			x				x	x		x	x				x	x		x	x			
4+50 30N	x	x			x				x	x		x	x				x	x		x	x			
5+20 20N	x	x			x			x	x	x		x	x				x	x		x	x			
5+20 2N	x	x			x				x	x		x	x				x	x		x	x			
5+20 CL								x																x
5+20 2S	x	x			x			x	x	x		x	x				x	x		x	x			
5+20 20S	x	x			x			x	x			x	x				x	x		x				
5+70 2S	x	x			x				x	x		x	x				x	x		x	x			
5+70 CL								x																x
5+70 2N	x	x			x				x	x		x	x				x	x		x	x			
6+00 30N	x	x			x			x	x	x		x	x				x	x		x	x			
6+00 10N	x	x			x			x	x	x		x	x				x	x		x	x			
6+00 CL	x	x			x			x	x	x		x	x				x	x		x	x			x
6+00 10S	x	x			x			x	x	x		x	x				x	x		x	x			
6+00 30S	x	x			x			x	x	x		x	x				x	x		x				
6+30 2S	x	x	x	x	x	x	x	x	x	x		x	x	x	x		x	x		x	x			
6+30 CL								x																x
6+30 2N	x	x			x							x	x				x	x		x	x			
6+80 20N	x	x			x				x	x		x	x				x	x		x	x			
6+80 2N	x	x			x							x	x				x	x		x	x			
6+80 CL								x																x
6+80 2S	x	x			x							x	x				x	x		x	x			
6+80 20S	x	x			x			x	x	x		x	x				x	x		x	x			
7+50 30S	x	x			x			x	x	x		x	x	x			x	x		x	x			
7+50 10S	x	x			x			x	x	x		x	x				x	x		x	x			
7+50 CL	x	x			x			x	x	x		x	x				x	x		x	x			x
7+50 10N	x	x			x			x	x	x		x	x				x	x		x	x			
7+50 30N	x	x			x			x	x	x		x	x				x	x		x	x			
8+20 20N	x	x			x			x	x	x		x	x				x	x		x	x			
8+20 2N	x	x			x				x	x		x	x				x	x		x	x			
8+20 CL								x																x
8+20 2S	x	x			x				x	x		x	x				x	x		x	x			
8+20 20S	x	x			x			x	x	x		x	x				x	x		x	x			
8+70 2S	x	x			x				x	x		x	x				x	x		x	x			
8+70 CL								x																x
8+70 2N	x	x			x				x	x		x	x				x	x		x	x			
9+00 10N	x	x			x			x	x	x		x	x				x	x		x	x			
9+00 CL	x	x			x			x	x	x		x	x				x	x		x	x			x
9+00 10S	x	x			x			x	x	x		x	x				x	x		x	x			
9+20 2S	x	x			x				x	x		x	x				x	x		x	x			
9+20 CL								x																x
9+20 2N	x	x			x				x	x		x	x				x	x		x	x			
9+80 20N	x	x			x				x	x		x	x				x	x		x	x			
9+80 2N	x	x	x	x	x	x	x	x	x	x		x	x	x	x		x	x		x	x			
9+80 CL	x	x			x			x	x	x		x	x				x	x		x	x			x
9+80 2S	x	x			x				x	x		x	x				x	x		x	x			
9+80 20S	x	x			x							x	x				x	x		x	x			
10+20 2S	x	x			x				x	x		x	x				x	x		x	x			
10+20 CL								x																x
10+20 2N	x	x			x				x	x		x	x				x	x		x	x			
10+60 30N	x	x			x			x	x	x		x	x				x	x		x	x			
10+60 CL	x	x			x			x	x	x		x	x	x			x	x		x	x			x
10+60 30S	x	x			x			x	x	x		x	x				x	x		x	x			
11+25 20S	x	x			x				x	x		x	x				x	x		x	x			
11+25 CL	x	x			x			x	x	x		x	x				x	x		x	x			x
11+25 20N	x	x			x			x	x	x		x	x				x	x		x	x			

El Centro, CA - Temperature

a. Air temperature near the RAS taken at the weather observation station.

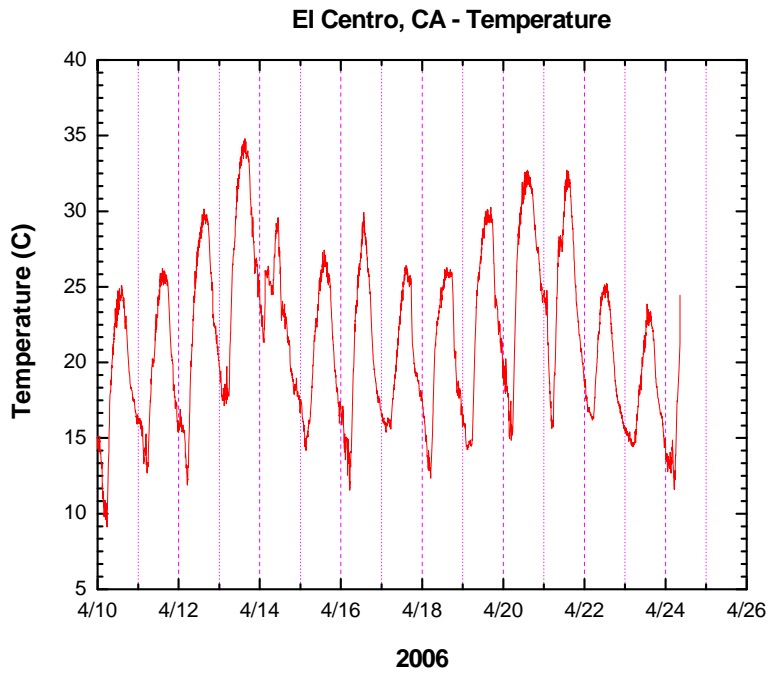### El Centro, CA - Temperature

b. First intensive operational period (IOP #1) timeframe (July 11–15, 2005).

Figure 10. Air temperature data taken at El Centro showing (a) continuous observation and (b) IOP #1, (c) IOP #2 and (d) IOP #3.

c. Second intensive operational period (IOP #2) timeframe (October 17–21, 2005).

d. Third intensive operational period (IOP #3) timeframe (April 23–24, 2005).

Figure 10 (cont'd). Air temperature data taken at El Centro showing (a) continuous observation and (b) IOP #1, (c) IOP #2 and (d) IOP #3.

A small amount of rain (47 mm) was recorded during the nine months of weather observation. The record showed that there were long periods of time between each recorded rainfall (Fig. 11a). Most interesting was the reaction of the soil moisture to the rainfall. Even during a relatively intense October rainfall event (which recorded 26 mm of rain over two days, and according to locals was the most intense amount of rainfall that had been seen in a long time) only the 5-cm and 15-cm sensors on the soil moisture probe recorded an increase in soil moisture, so water from the rain never penetrated the dry soil below the 15-cm level. A total of 29 mm of rain fell over a period of five days (Fig. 11b). Another, less intense, rainstorm (8 mm of rain) occurred in mid-March.

The wind speed data was sampled every 10 seconds and the output was averaged over a 5-minute period (Fig. 12). The wind speed data indicate that light wind is common in the area. Wind speeds of 12 m/sec (27 mph) or higher were occasionally observed, as displayed in Figure 12. Wind generally increased mid-day. The wind is normally blowing from the west and northwest. High wind speeds can cause dust storms in semi-arid environments with dry soils. On the other hand, a light breeze can improve visibility when dry soil becomes airborne after disturbance from vehicular or aircraft traffic.
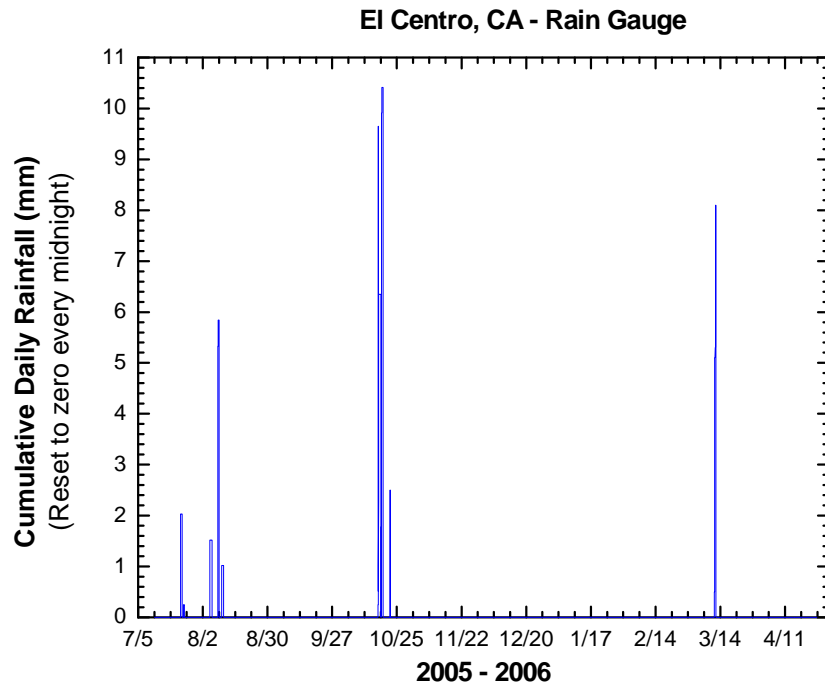
a. Monitored rain events during nine months of observation.
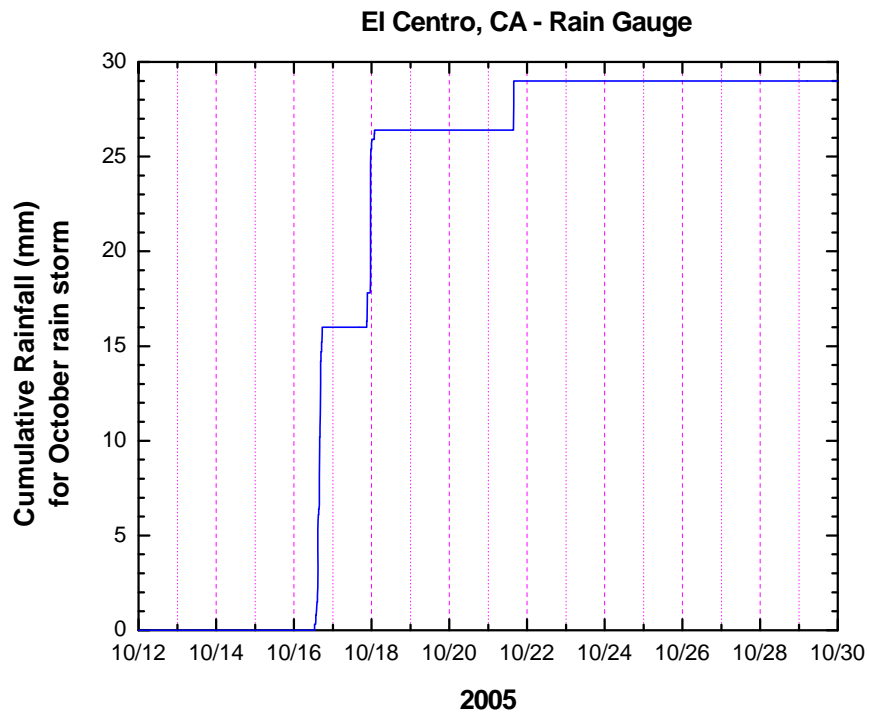
b. Rain events a few days before IOP #2.

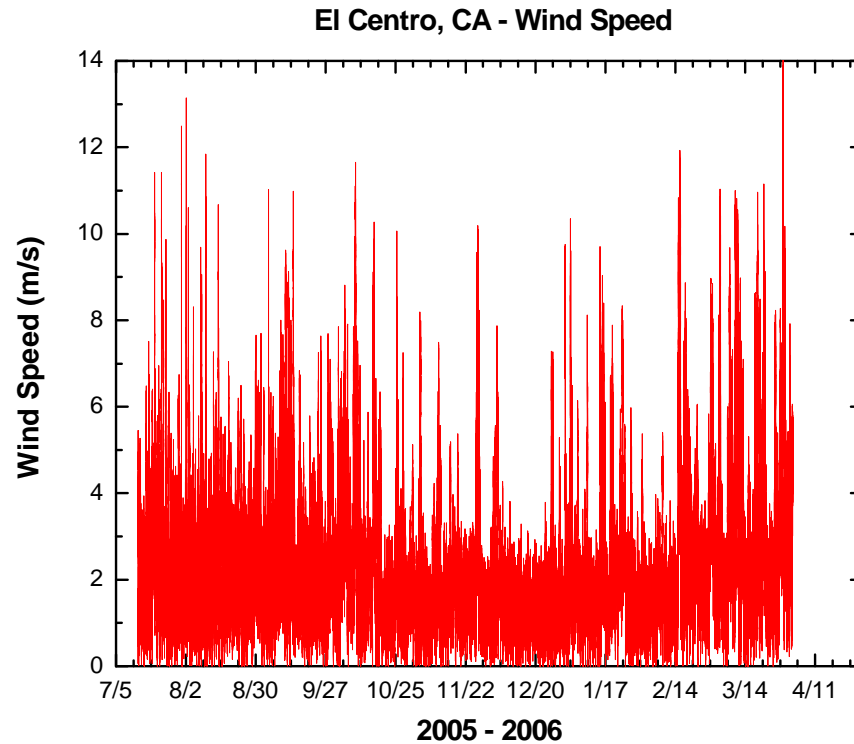Figure 11. Precipitation data from the observation station near the RAS.

El Centro, CA - Wind Speed

Figure 12. Wind speed observed from the weather station near the RAS averaged every 5 minutes for the entire monitored time.

4.4.4 Topography

The topography of the OLS is very flat, but gently sloping to the east and northeast for the majority of the RAS (Fig. 13). The elevation of the RAS centerline based from the total station data showed a gradual increase of 5.6 m from the beginning (east) to the end (west), as shown in Figure 14a. The overall grade of the center of the RAS from the beginning to the end is 0.5%, which is relatively flat. A laser profile was collected every 1 m in areas with mounds and every 5 m in flat areas. The spikes in the laser data display the mounds along the center of the RAS (Fig. 14a and 14b). The mounds are quite pronounced in some areas on the RAS and range in height and width. However, these spikes do not represent the entire mound and the centerline measurements didn't always occur on the peak (top) of the mound, but may have captured the sides or the edges. Transitional areas of relatively smooth or flat sections were observed between areas with mounds. In general, the eastern third of the runway has a large number of mounds, and the remainder of the RAS is relatively smooth and flat. Figure 14c illustrates typical surface undulations of a natural ground

on the flat areas (left photograph) and mound profiles (right photograph) measured with the profilometer. A detailed discussion regarding the mounds and the spacing between mounds is covered in Section 5.2.
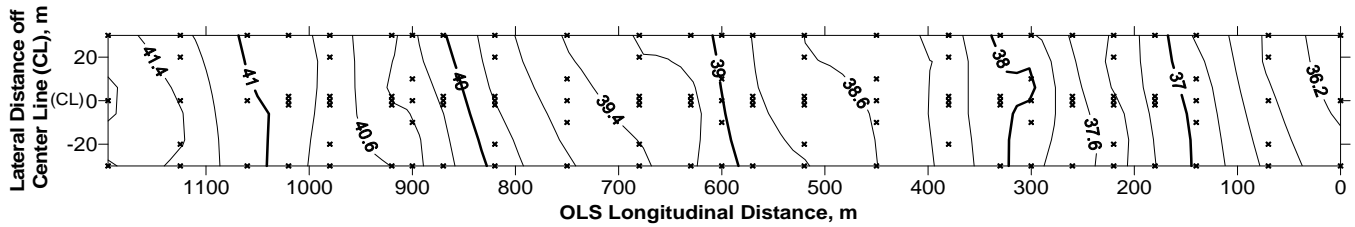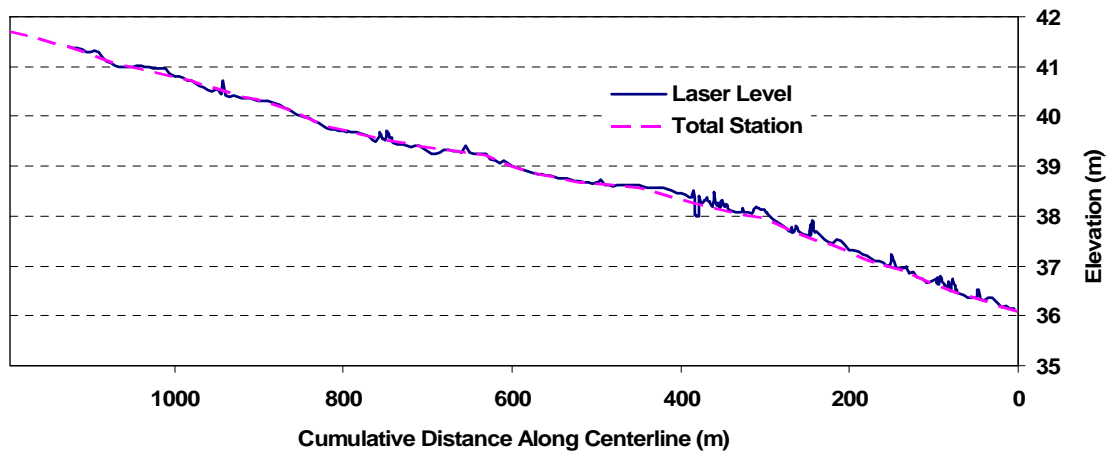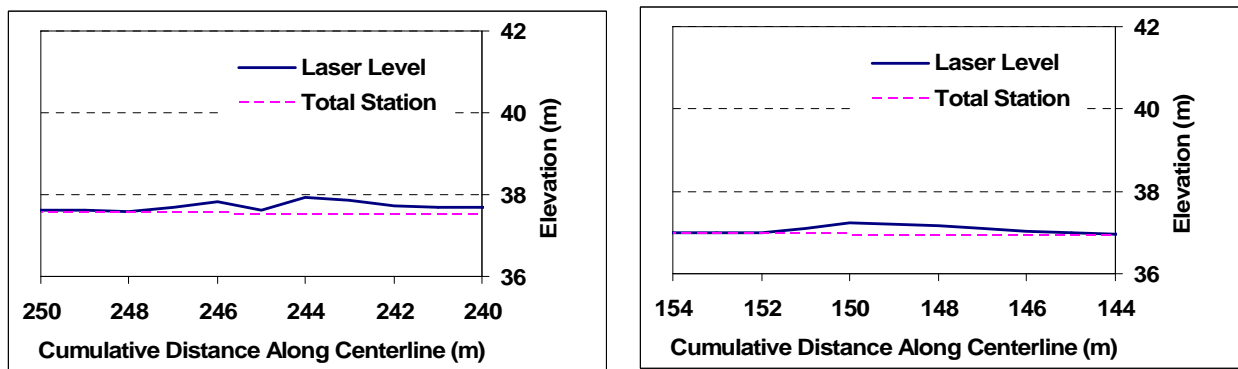

Figure 13. Contour map of the entire El Centro OLS. The x symbols show where elevations where taken (elevation in meters).

a. Elevation along the OLS centerline.

b. Surface roughness reflected from higher sampling using the laser level on mounded areas.

Figure 14. Elevation profile along RAS centerline.

c. Surface undulation using the profilometer on level areas (left) and mounds (right). The rods are spaced 2 cm apart and each rod is vertically marked at 1-cm intervals.

Figure 14 (cont'd).

Surface roughness along the centerline of the RAS is calculated using the Root Mean Square (RMS), equation (1) from the elevation data taken by laser level. The RMS value is determined to be 1.36 m along the centerline for the entire RAS.

In some areas on the OLS, mounds are 0.3–0.6 m (1–2 ft) high and 1.2–3.0 m (4–10 ft) across and 1.5–6 m apart. If mounds are considered as changes in slope, the grade from the laser data at El Centro RAS ranges from 0 on the flat areas to a maximum of 40% over short distance. These mounds can be considered abrupt change of grades.

The average lateral cross-sectional grade of the OLS is approximately 0.2%. A couple of typical lateral profiles of the OLS are shown in Figure 15. Overall, the lateral cross section of the OLS is very flat.
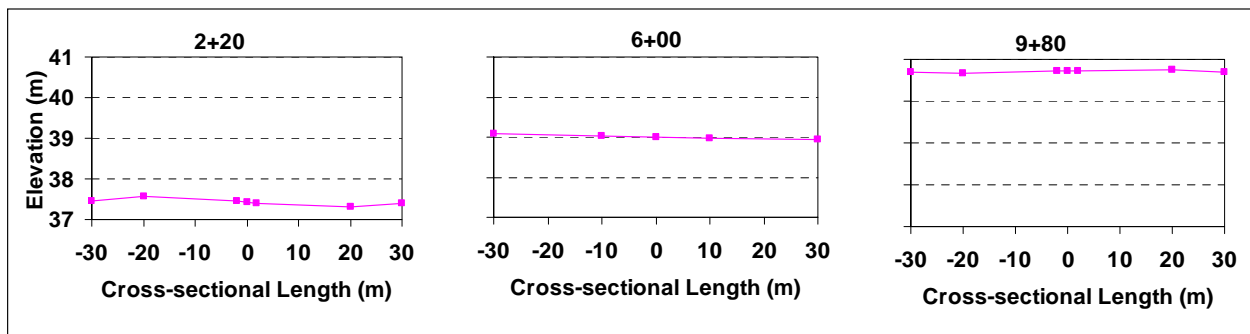

Figure 15. Typical transverse profiles of the RAS at El Centro.

5   Analysis and Results on Systematic Imagery Runway Assessment Site (SI-RAS)

5.1 Soil Characterization

5.1.1 Soil Type and Texture Profile

Figure 16 shows the soil exposed on the surface at four sampling points on the RAS. Significant amounts of exposed soil were commonly observed on the RAS. Granular materials such as stone of various sizes were on the surface. Several soil pits were shallower than planned because there were cemented layers in the soil. These cemented layers can be broken with effort using a pick with some pieces of crumbled soil. Also, because the soil is granular and dry, the tendency of the soil to slump back into the pit was unavoidable but was minimized by making the pit large.

a. 1+40 CL.   b. 3+80 2S.

c. 6+30 2S.   d. 9+80 2N.

Figure 16. Soil on the surface before digging the soil pits at four sampling locations on the RAS.

At sampling location 1+40 CL, the soil pit profile showed granular material embedded into fine sand near the surface (Fig. 17a). Below 0.30 m (12 in.) from the surface, the soil contained less coarse sand and more medium and fine-grained sand, as seen in Figure 17b. Soil samples were taken at depths of 0.08–0.10, 0.15, 0.30, 0.46, 0.56 m (3–4, 6, 12, 18, and 22 in.). The USCS soil type is classified as silty sand (SM) with a plasticity index of zero throughout the soil profile down to 22 inches. The gradation chart is shown in Figure 17c.
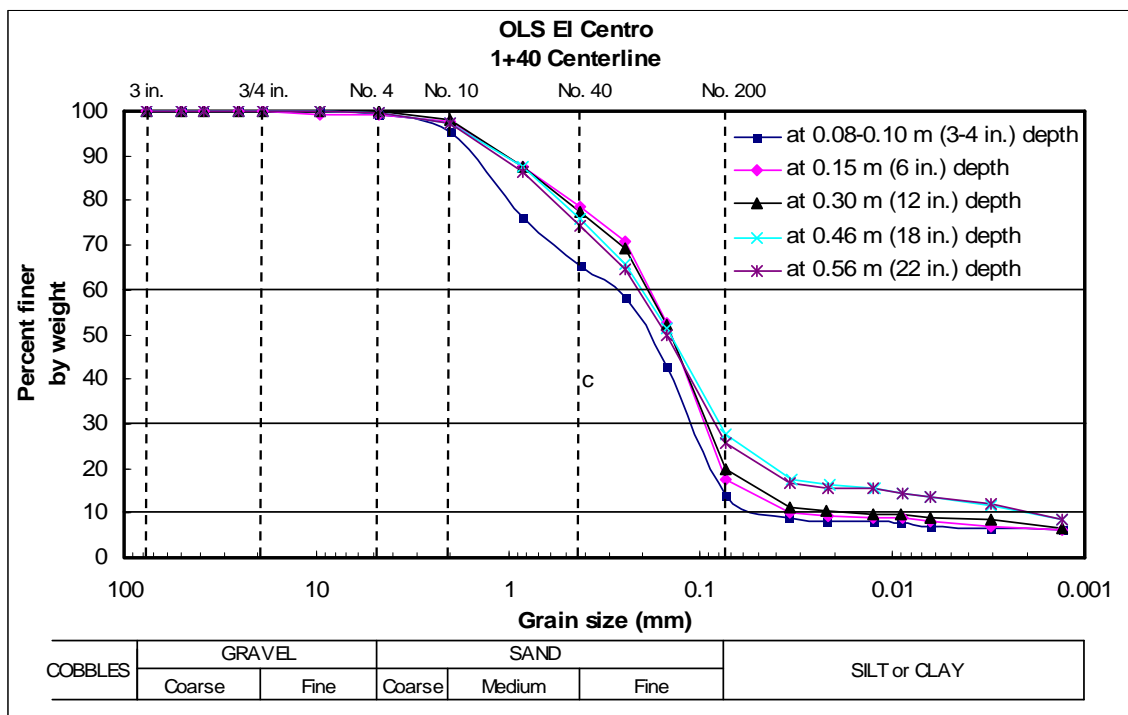

a. Soil from the surface down to 0.2 m (8 in.).

b. Bottom of pit at 0.56 m (22 in.) indicated on the measuring tape as zero.

Figure 17. Soil profile at 1+40 CL. A hard layer was encountered at approximately 0.46 m (18 in.) where a pick was used to break the cemented soil.

(c) Grain size distribution

Figure 17 (cont'd). Soil profile at 1+40 CL. A hard layer was encountered at approximately 0.46 m (18 in.) where a pick was used to break the cemented soil.

Cemented layers at various depths were found while digging the soil pit at 3+80 2S (Fig. 18a). The pit was dug down to 0.6-m (24-in.) depth (Fig. 18b). The results from the grain size analysis of the soils collected at station 3+80 2S are shown in Figure 18c. The gradation from the surface down to 0.30-m (12-in.) depth is classified as silty sand (SM). At 0.48- and 0.61-m (19- and 24-in.) depths, the soil samples are classified as well-graded sand with silt (SW-SM).

A photo of the soil profile taken at 6+30 2S during the first visit is shown in Figure 19a. The bottom of the pit was 0.6 m (24 in.) deep. Samples were collected for the gradation analysis during the first and second visits. A set from the soil pit during IOP #1 and another set from drive cylinder samples also were taken during IOP #2. The results of the grain size analyses of all the soils collected at 6+30 2S are shown in Figure 19b. The entire soil profile is classified as Silty Sand (SM) with higher percent fines passing the number 200 sieve in the top 0.3 m (12 in.) than in bottom.

a. Cemented layer encountered showing soil clods.

b. Entire soil pit.
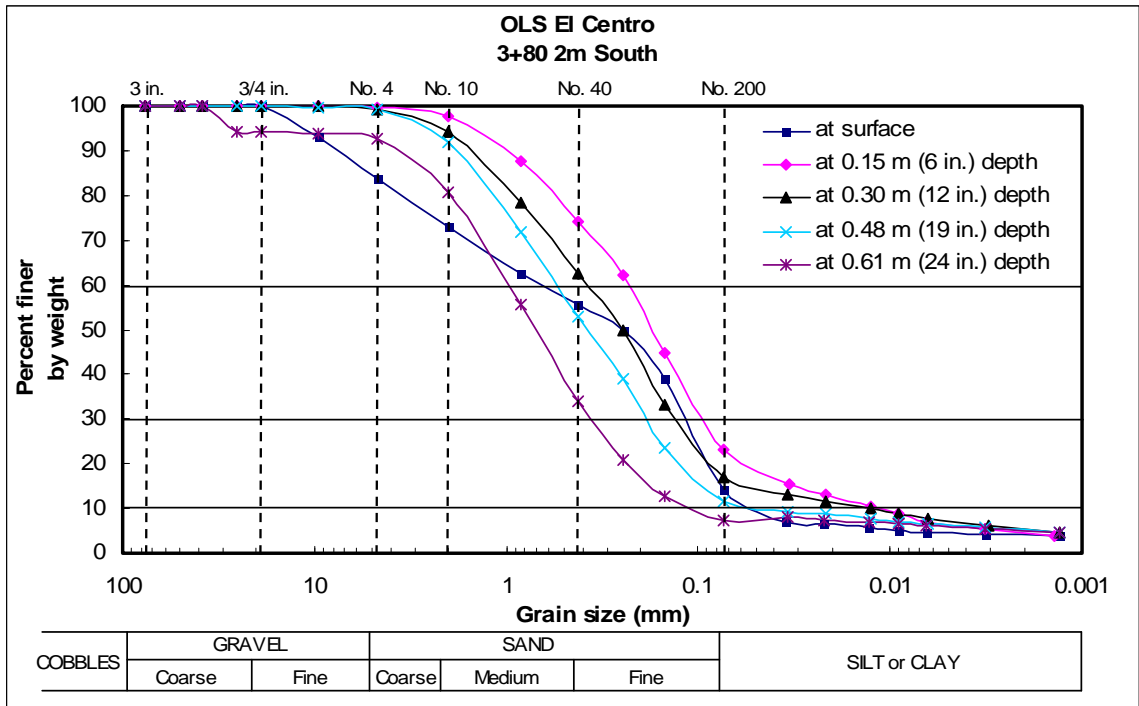
c. Grain size distribution.

Figure 18. Soil profile at station 3+80 2S showing cemented layer at different depths. The bottom of the pit is at 0.6 m (24 in.) below the surface. (Note that the tape is not standing vertically.)

a. Soil pit showing the bottom of the pit at 0.6 m (24 in.) below the surface. (Note that the tape is not standing vertically.)
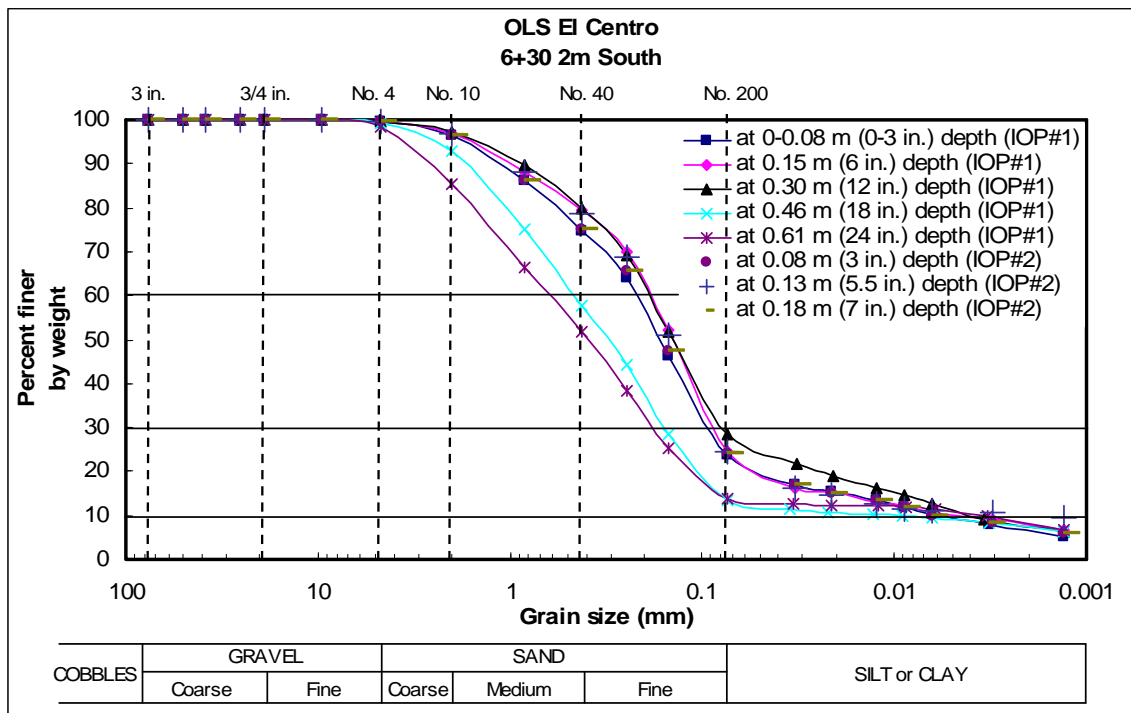
b. Grain size distribution.

Figure 19. Resulting soil profile at 6+30 2S.

At sampling location 9+80 2N, the soil pit was dug to a depth of 0.81 m (32 in.). Thin cemented layering was observed throughout the soil profile (Fig. 20a). Similarly, soil samples were taken at both IOP #1 and IOP #2. The first set of soil samples was taken when a pit was dug during the first IOP on July 11–15, 2005. The second set of soil samples were collected October 17–21, 2005 and were taken on an undisturbed area approximately 1 m away from the edge of soil pit during IOP #1. The result from the grain size analysis for all samples is given in Figure 20b. The soil profile at this location indicates a silty sand (SM) from the surface down to 0.51 m (20 in.), then well-graded sand with silt (SW-SM) to a depth of 0.71 m (28 in.), and then the soil changes to silty sand (SM) at a depth of 0.81 m (32 in.).

At sampling location 10+60 CL, soil was sampled using the drive cylinder at 0.20-m (8-in.) depth during IOP #2. The result from the grain size analysis can be seen in Figure 21. The soil type at that depth indicates a silty sand (SM) material.

a. Pit at 9+80 2N was dug down to 0.81-m (32-in.) depth.

Figure 20. Soil profile and grain size analysis at sampling location 9+80 2N.
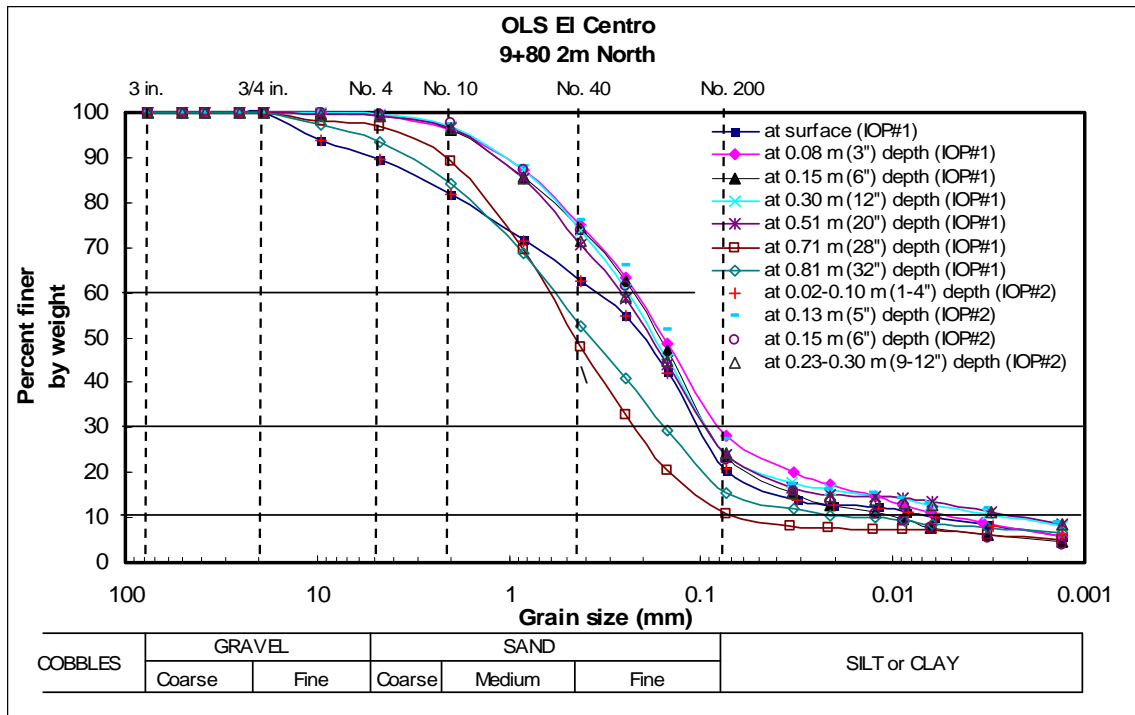
b. Grain size distribution.

Figure 20 (cont'd). Soil profile and grain size analysis at sampling location 9+80 2N.
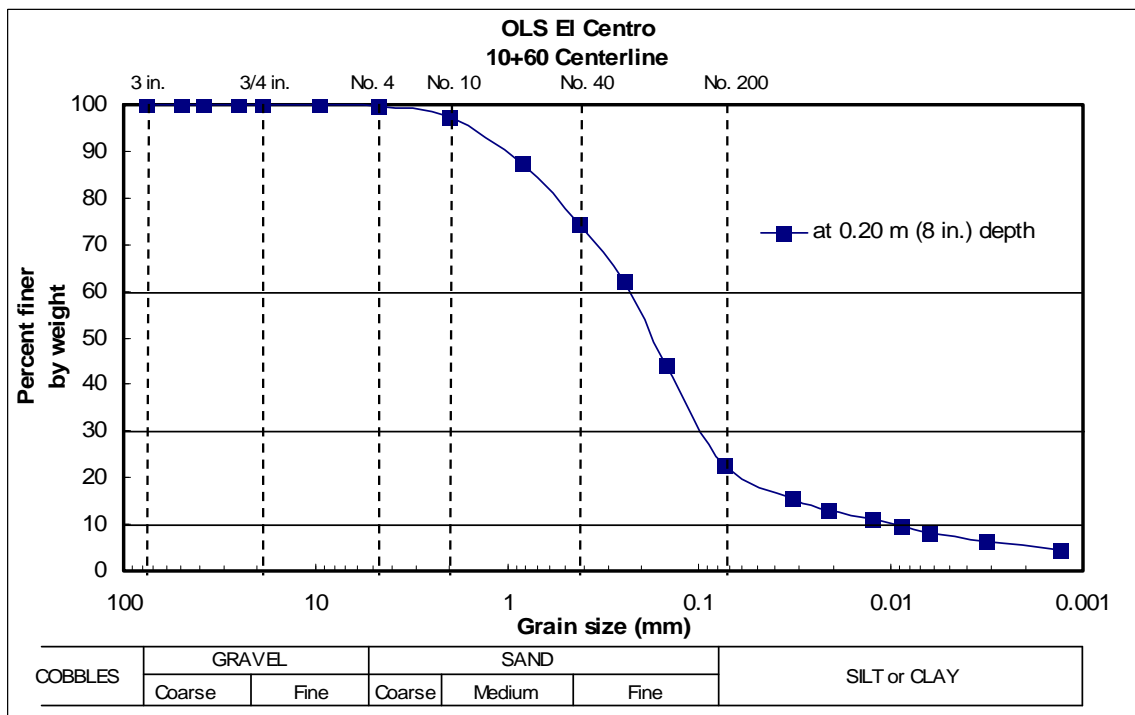

Figure 21. Grain size analysis at 10+10 CL taken from a core sample at 0.2-m depth.
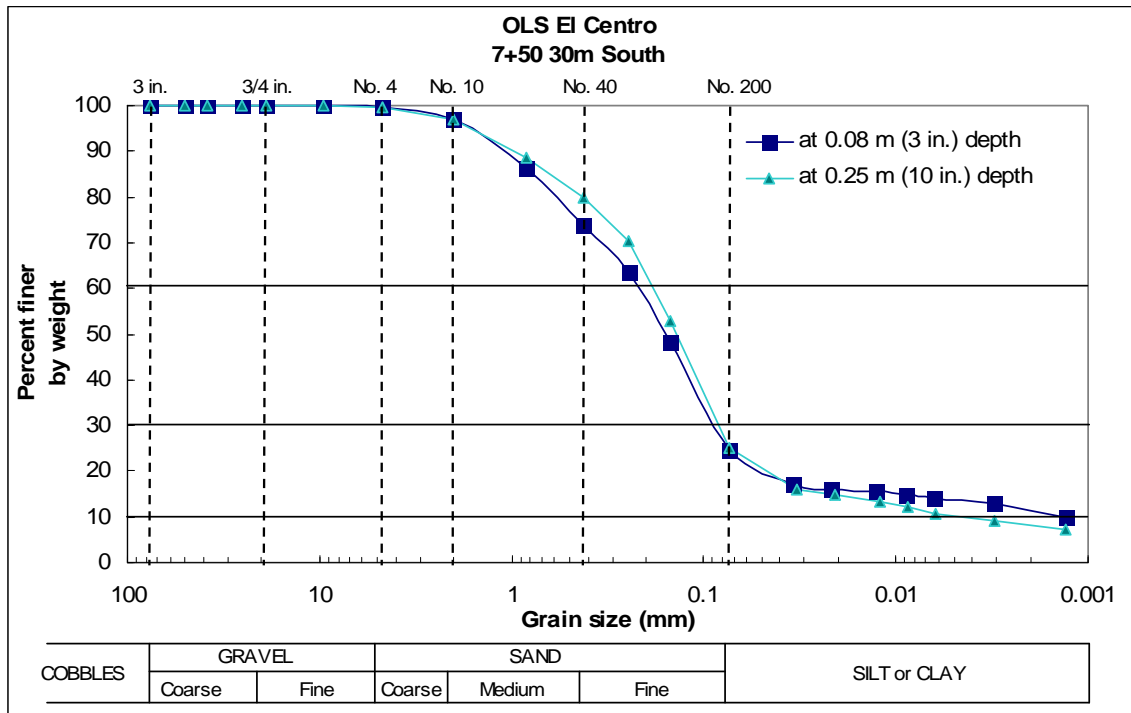
Figure 22. Soil profile and grain size analysis from drive cylinder samples at location 7+50 30S.

Soil samples at 0.08- and 0.25-m (3- and 10-in.) depth were extracted from the drive cylinder at sampling location 7+50 30S IOP #2. The results from the grain size analysis are given in Figure 22. The soil profile for this location indicates a silty sand (SM).

5.1.2 Munsell

The summary of the surface soil color for this RAS is listed in Table 7 (Munsell 2000).

Table 7. Munsell color of in-situ soil next to the surface.

Location	Color and Description
1+40 CL	10YR 8/2, Very Pale Orange
3+80 2S	10YR 6/3, Very Pale Orange
6+30 2S	10YR 8/2, Very Pale Orange
9+80 2N	10YR 8/2, Very Pale Orange

5.1.3 Density

Soil density measurements were made with the Troxler nuclear gage at 1+40 CL, 3+80 2S, 6+30 2S, and 9+80 2N during IOP #1 and are summarized in Figure 23. Aside from the loose surface layer (1440 kg/m³), density ranged from 1573 to 1709 kg/m³ (98.2 to 106.7 lb/ft³) with an average 1664 kg/m³ (103.9 lb/ft³). The average specific gravity was 2.63. There is no significant density variation between 3+80 2S, 6+30 2S and 9+80 2N except for the density at 1+40 CL and at the 0.76-m (30-in.) depth at 6+30 2S (Fig. 23). Density generally increased slightly with depth. Although a low density was found just above a very hard layer at the bottom of the pit. This variation in soil density is typical for in-situ or natural deposited soils with non-homogenous layering and cemented layers. Instrument error, spatial variability, and mineralogy may also contribute to the variability and were not examined in this report.
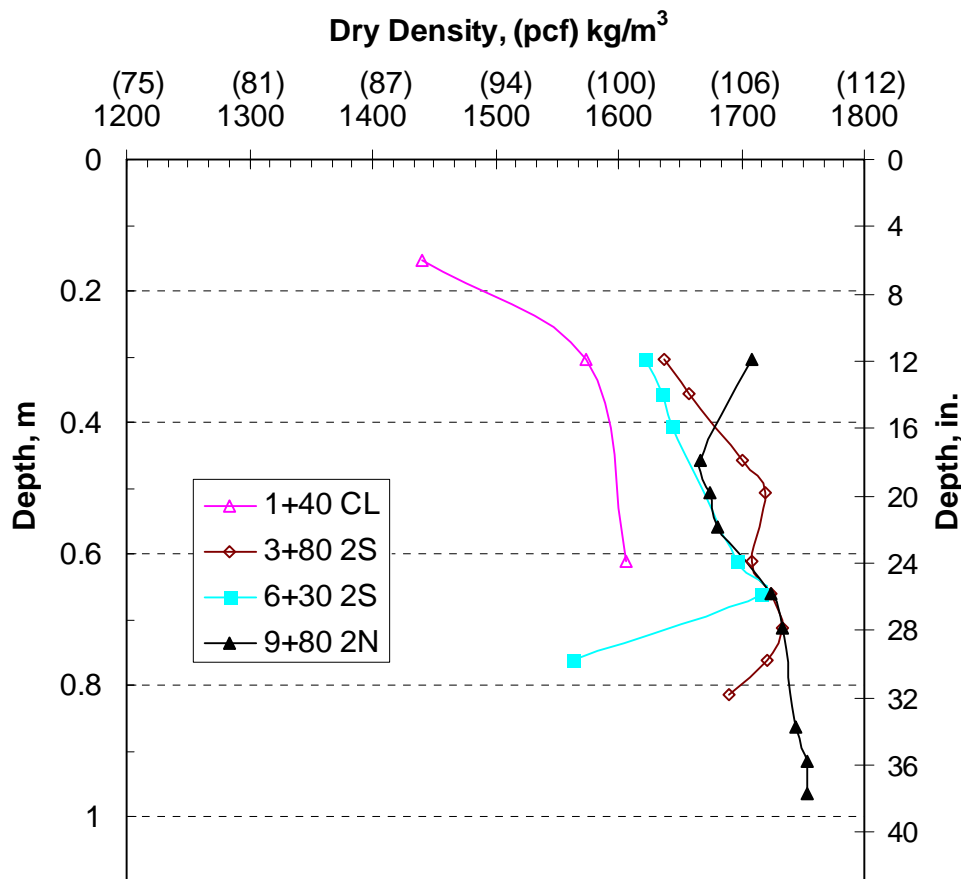

Figure 23. Dry density measurements from the nuclear gage in four soil pits at El Centro RAS during IOP #1.

5.1.4 Organics

Three replicate surface samples were conducted to measure the organic contents for sampling locations 3+80 2S and 9+80 2N, whereas only one sample was tested for 6+30 2S. The results from replicate tests are reported here as an average value. The organic content at stations 3+80 2S, 6+30 2S and 9+80 2N were 0.22, 0.38 and 0.78 percent, respectively. Because the RAS area has relatively low vegetation cover, it is to be expected that organic content is minimal.

5.1.5 Natural Resources Conservation Service (NRCS) Soils Information

RAS soils information published on Soil Survey Geographic (SSURGO) database produced by USDA, Natural Resources Conservation Service (NRCS), is bounded by two soil map units. Table 8 summarized the two soil map units present on the RAS with soil horizons information. The western portion of the RAS is classified as Rositas Sand with zero to two percent slopes and the USCS soil types vary from poorly graded sand (SP), poorly graded sand with silty sand (SP-SM), and silty sand (SM). The rest of the RAS is on a soil group called Antho-superstition Complex with USCS soil type ranging from silty sand (SM) to silt (ML).

Soil density information presented in Table 8 is from Soil Survey Geographic (SSURGO) Database produced by USDA, Natural Resources Conservation Service (NRCS), which measured on natural fabric samples (i.e., soil clods) by coating in saran resin, adjusting the water content on a tension table or pressure plate, and weighing in air and water. The bulk density is typically estimated from lab measurements on selected soils in the survey area and algorithms based on pedotransfer functions. The soil bulk density in the SSURGO data reported the representative soil density of the area in the range between 1600 and 1650 kg/m^3 (99.9 and 103.0 lb/ft^3) with volume determined at water content of 1/3 bar. Also the representative values for soil bulk density reported for coated soil clod vary from 1680 to 1730 kg/m^3 (104.9 to 108.0 lb/ft3), which are within the range of our measured densities from the Troxler nuclear gage.

5.1.6 Soil Characterization Discussion and Summary

The soils data reported in the SSURGO database nearly match the soil type determined on the RAS. A summary of the soil type, texture, along with

the percentage of fines density and specific gravity, is given Table 9. Generally, the soil is non-plastic silty sand (SM) to a depth of approximately 0.5 to 0.7 m. However, the soil was found to be well-graded sand with silt (SW-SM) at depths of 0.48 and 0.61 m (19 and 24 in.) at sampling location 3+80 2S, and at 0.71 m (28 in.) at sampling location 9+80 2N. The cemented layers found at El Centro RAS were at different depths and of irregular thickness. A thin cemented layer also was observed on the surface when the soil was relatively dry, shown in Figure 24. The chemical composition of the cemented layer was not examined for this project. However, it is important to indicate that there is a gypsum mine about 15 miles northwest of the site. Thus the soil deposit is most likely gypsum. In dry regions such as El Centro, cemented soil grains are formed by the accumulation of soluble minerals deposited by mineral-bearing waters that move upward, downward, or laterally by capillary action, driven by temperature gradients and commonly assisted in arid settings by evaporation. These cemented materials are formed near the surface, which in more extreme cases is a duricrust, or specifically for sulfate-rich deposits, as gypcrete or gypcrust (Rollings and Rollings 1996). The cemented layer was found to be easily disintegrated by a human footprint at this RAS.

Soil density measurements made from the Nuclear gage increased slightly with depth. Density ranged from 1573 to 1709 kg/m³ (98.2 to 106.7 lb/ft³) with an average 1664 kg/m³ (103.9 lb/ft³). Drive cylinder samples to measure density were made on the RAS; however, as determined later, density measurements from drive cylinders are reliable only for cohesive soils with a plasticity index of 21 and higher. The soil bulk density in the SSURGO data reported the representative soil density of the area is within the range of the measured densities from the Troxler nuclear gage.

Table 8. Soil information published by Soil Survey Geographic (SSURGO) Database.

Horizon Layer	Horizons	Distance from top of soil to upper bound of soil horizon cm	of soil to base of soil horizon cm	The oven dry weight of the less than 2 mm soil material per unit volume of soil at a water tension of 1/3 bar. Low Value g/cc	Representative Value g/cc	High Value g/cc	The oven dry weight of the less than 2 mm soil material per unit volume of soil at a water tension of 15 bar. Representative Value, g/cc	The oven dry weight of the less than 2 mm soil material per unit volume of soil exclusive of the desication crack, measured on a coated clod. Representative Value, g/cc	USCS
For Map unit number 101 (Antho-Superstition Complex)									
H1	1	0	20	1.55	1.6	1.65	1.7	1.68	SM
H2	2	20	152	1.6	1.65	1.7	1.63	1.73	ML, SM
For Map unit number 130 (Rositas Sand, 0 to 2 percent Slopes)									
H1	1	0	69	1.6	1.65	1.7	1.73	1.73	SP, SP-SM
H2	2	69	152	1.6	1.65	1.7	1.73	1.73	SM, SP-SM, SP

Table 9. Summary of the soils on the RAS in El Centro.

Soil Properties Sampling Station / Depth, m (inches)	1+40 CL USCS Type [A]	Percent Fines	Specific Gravity	Dry Density kg/m³	3+80 2S USCS Type [A]	Percent Fines	Specific Gravity	Dry Density kg/m³	6+30 2S USCS Type [A]	Percent Fines	Specific Gravity	Dry Density kg/m³	7+50 30S USCS Type [A]	Percent Fines	Specific Gravity	9+80 2N USCS Type [A]	Percent Fines	Specific Gravity	Dry Density kg/m³	10+60 CL USCS Type [A]	Percent Fines	Specific Gravity
Surface					SM	14.3	2.63									SM	20.4	2.64				
0.05-0.1 (2-4)	SM	14.1	2.66	1440	SM	21.3	2.64		SM	23.9	2.61		SM	24.8	2.62	SM	28.2	2.62				
0.15-0.2 (6-8)	SM	17.5	2.68		SM	23.2	2.61		SM	24.6	2.63					SM	23.7	2.64		SM	22.6	2.62
0.25-0.3 (10-12)	SM	20	2.62	1573	SM	16.8	2.62	1637	SM	28.5	2.62	1621	SM	25.1	2.63	SM	24.0	2.6	1709			
0.46-0.51 (18-20)	SM	27.5	2.61		SW-SM	11.5	2.65	1719	SM	13.4	2.6					SM	24.0	2.6	1674			
0.56-0.61 (22-24)	SM	25.6	2.62	1607	SW-SM	7.4	2.65	1709	SM	13.8	2.65	1696							1680			
0.71 (28)								1733								SW-SM	10.8	2.67	1733			
0.81 (32)								1690								SM	15.4	2.66	1744			

[A] Unified Soil Classification System type: Silty Sand (SM), Well-graded Sand with Silt (SW-SM); Non-plastic soils (Plasticity Index = 0)

Figure 24. Cemented materials found on the surface of RAS.

5.2 Seasonal Impacts

5.2.1 Surface Conditions

5.2.1.1 Surface Condition and Features

A walk-through visual survey along the RAS was conducted to determine the surface condition of the runway during IOP #1. From the visual survey, the observer noted vegetation type, vegetation cover, tire tracks or ruts, drainage, soil scouring from water or animals, landmarks, mounds, animal holes, artillery rounds, and anything else that could present a hazard to aircraft operations. A sketch was generated from the visual survey as shown in Figure 25 in approximately 150-m sections. Each sketch is a symbolic illustration of the surface features and is not drawn to precise scale. No additional visual surveys were conducted during subsequent visits because no significant changes were observed.
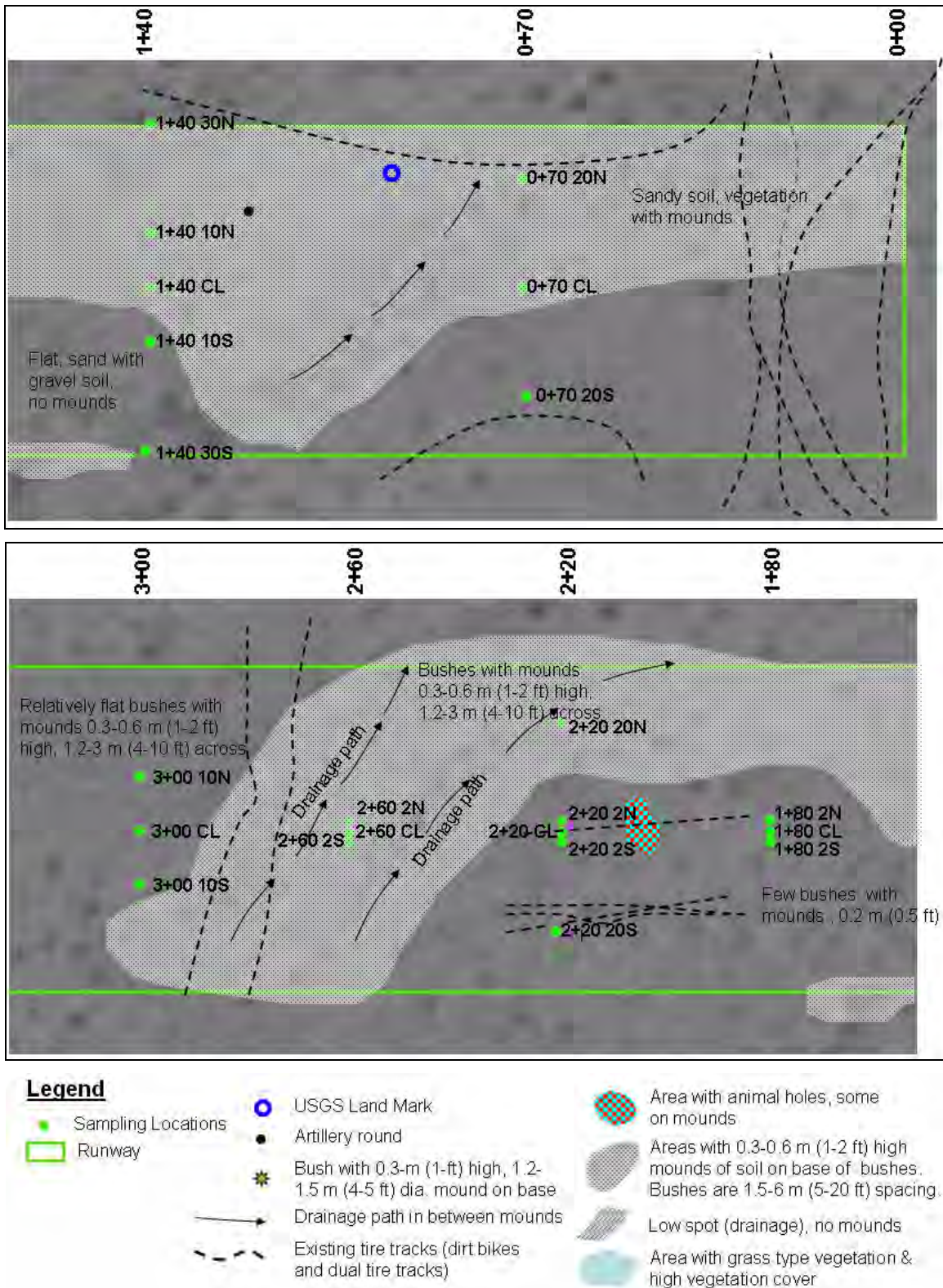
Figure 25. Symbolic representation of surface features from the visual survey along the RAS in sections.

Figure 25 (cont'd). Symbolic representation of surface features from the visual survey along the RAS in sections.

Figure 25 (cont'd).
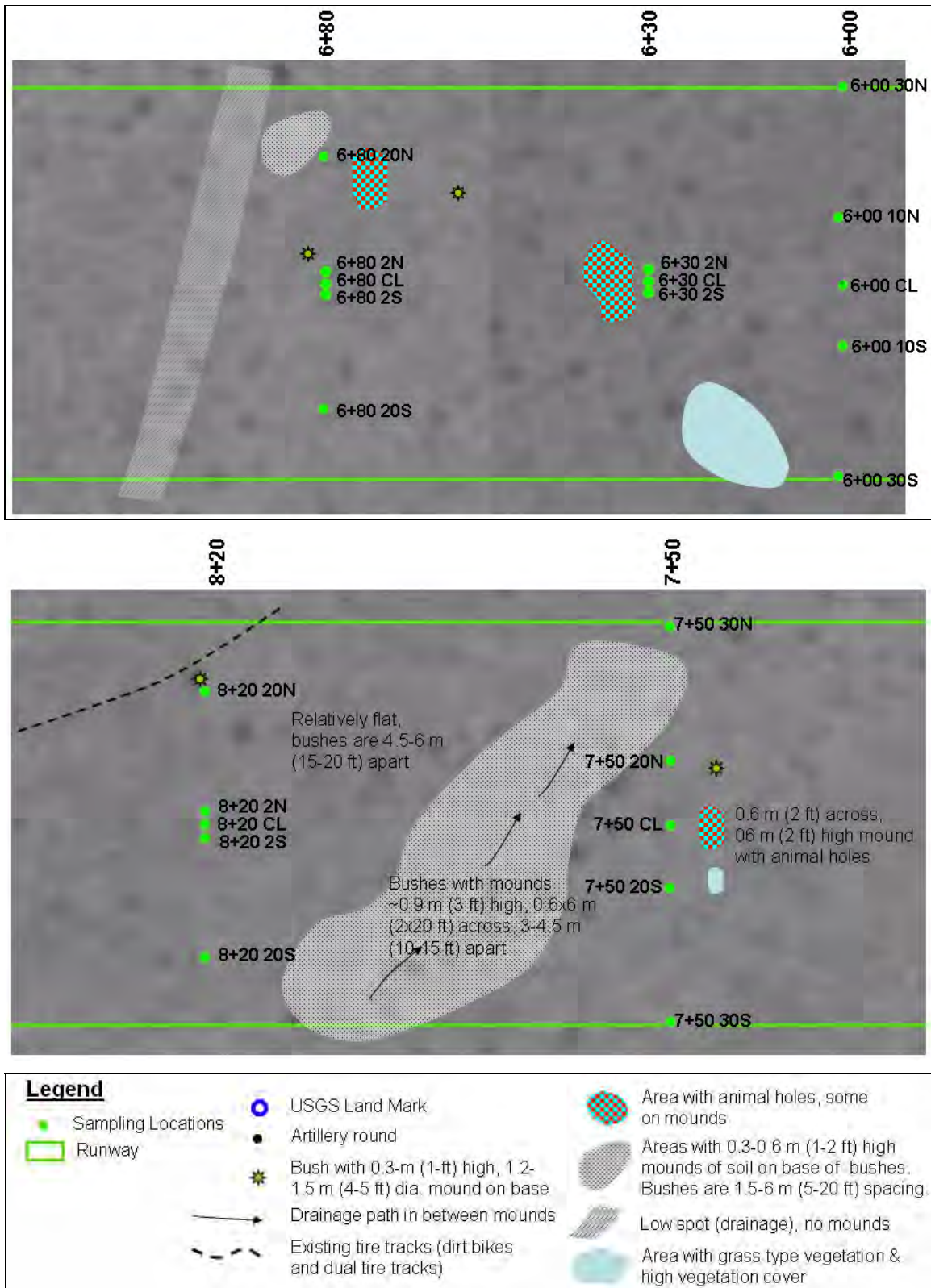
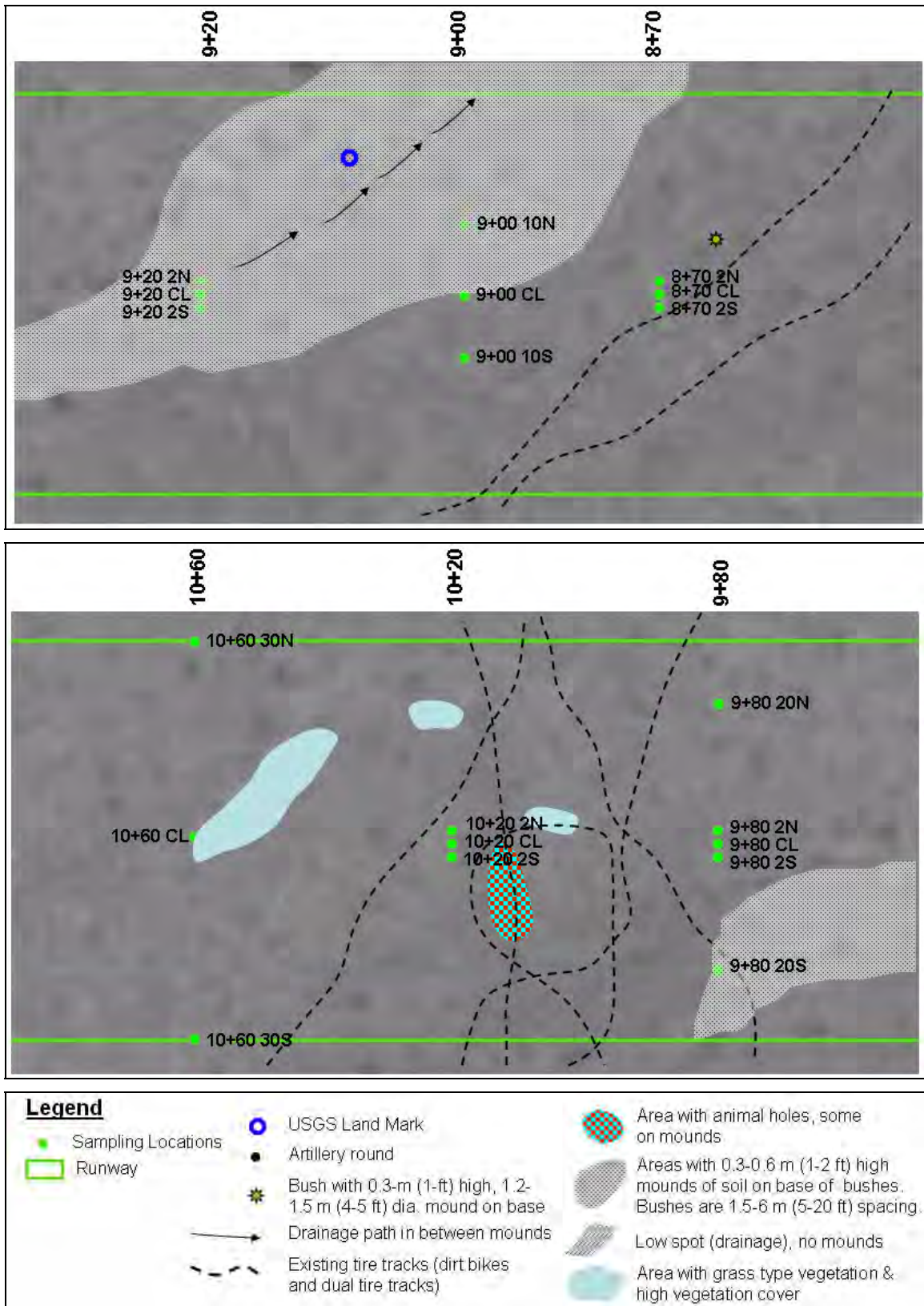Figure 25 (cont'd). Symbolic representation of surface features from the visual survey along the RAS in sections.

11+95

11+25

11+25 20N

11+25 CL

11+25 20S
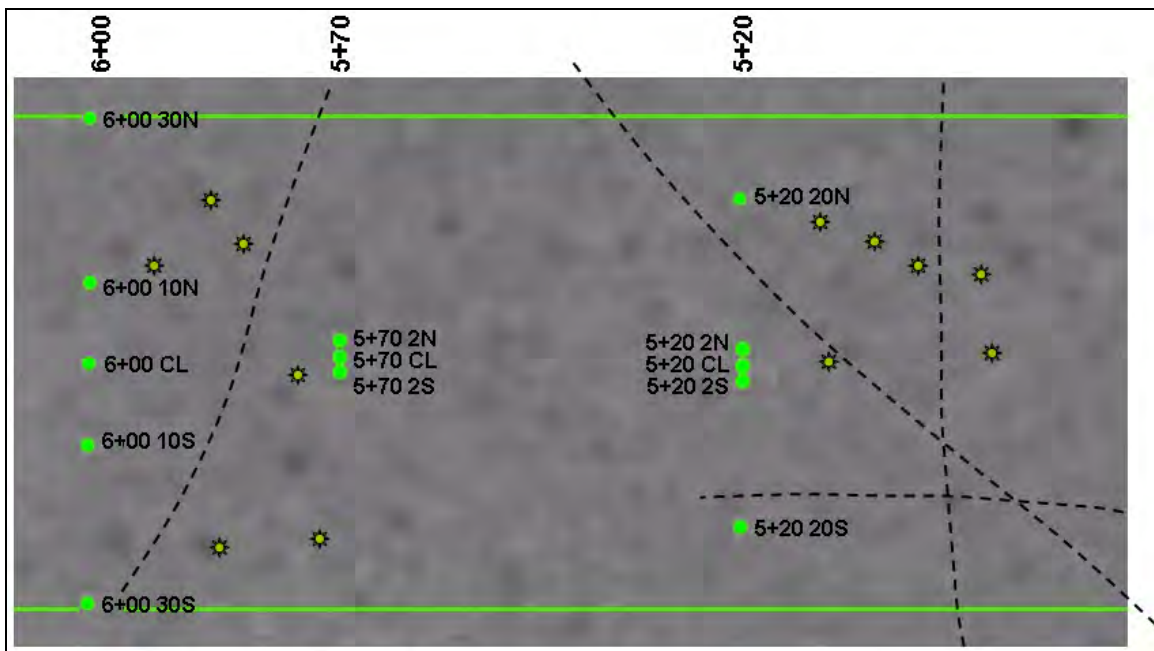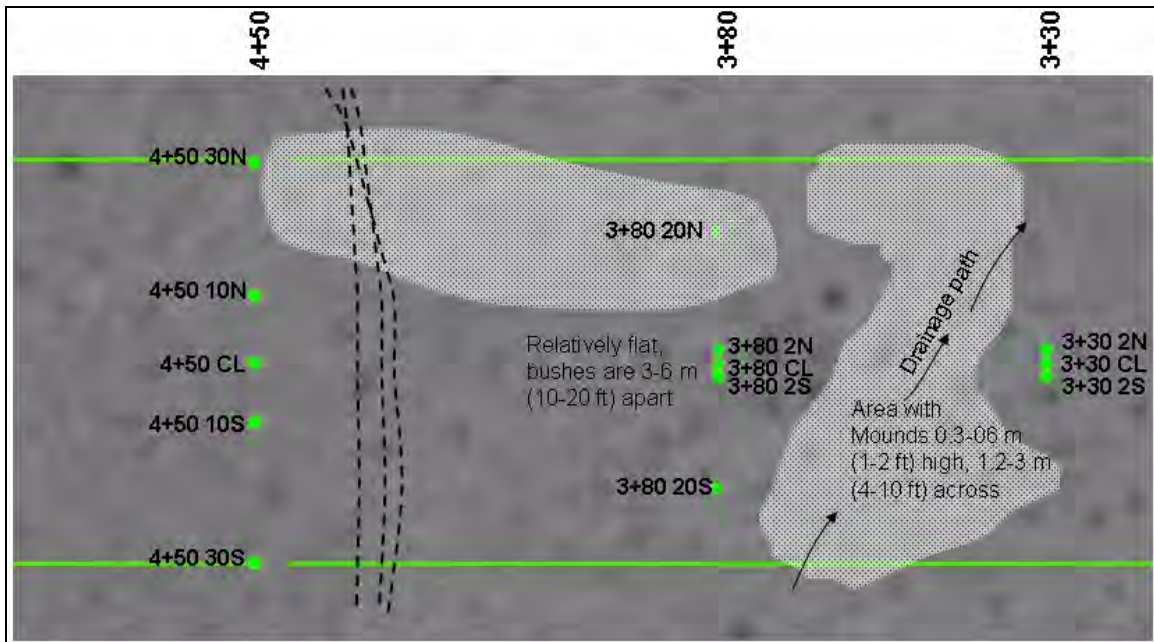
Legend

Sampling Locations

Runway

○ USGS Land Mark

● Artillery round

✳ Bush with 0.3-m (1-ft) high, 1.2-1.5 m (4-5 ft) dia. mound on base

→ Drainage path in between mounds

～ ～ Existing tire tracks (dirt bikes and dual tire tracks)

Area with animal holes, some on mounds

Areas with 0.3-0.6 m (1-2 ft) high mounds of soil on base of bushes. Bushes are 1.5-6 m (5-20 ft) spacing.

Low spot (drainage), no mounds

Area with grass type vegetation & high vegetation cover
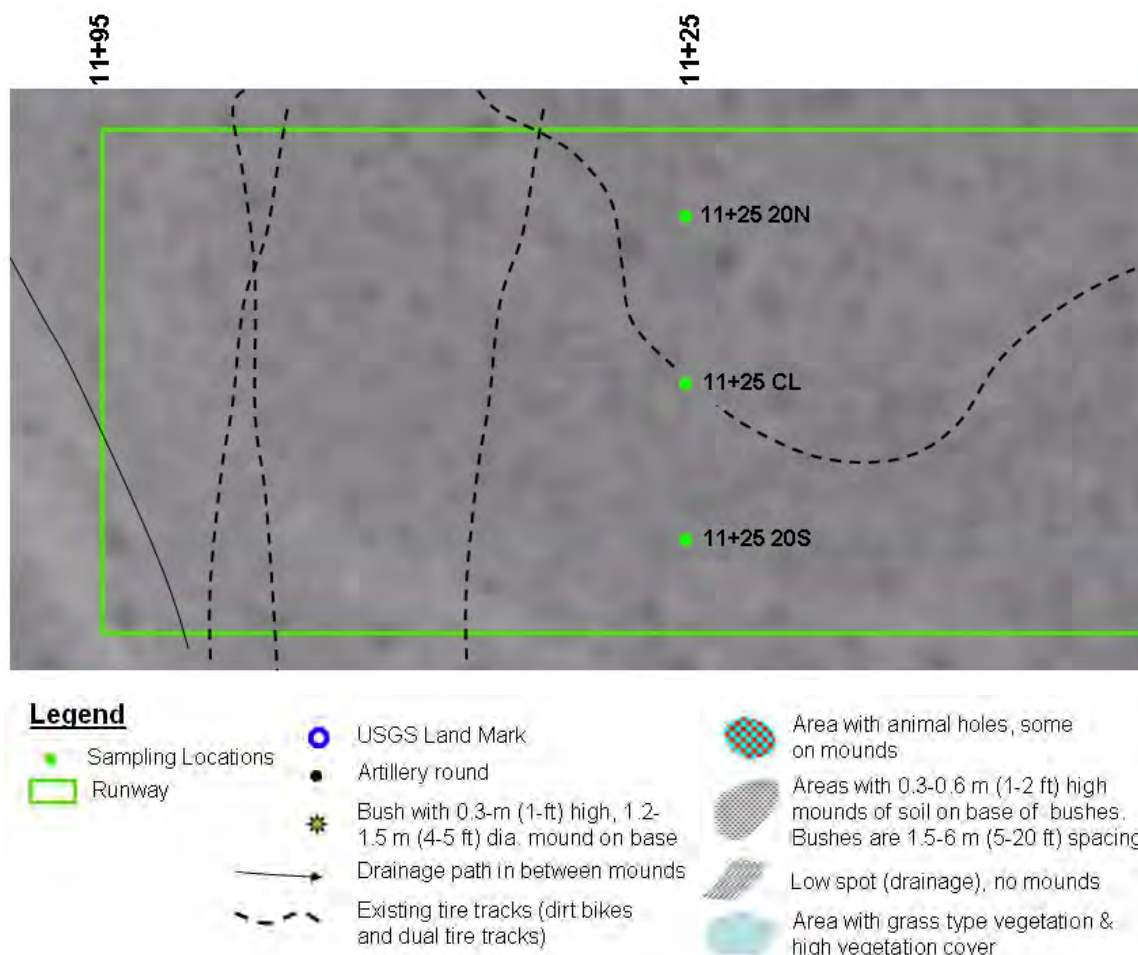
Figure 25 (cont'd).

At least a third of the RAS, primarily the eastern end (Stations 0+00 to 4+50 and 7+50 to 9+80), was covered with soil mounds surrounding the base of bushes, such as seen in Figure 26a. These mounds ranged in height from approximately 0.3 to 0.6 m (1–2 ft.), varied from 1.5 to 3 m (5–10 ft) across, and are spaced from 1.2 to 6 m (4–20 ft) apart peak to peak. However, small transitional areas with fewer mounds were found from stations 3+00 to 4+50. From stations 4+50 to 7+50, the soil mounds are less frequent, but occasionally one or two mounds were encountered. Areas with mounds are observed from station 7+50 to the western end of the RAS, but mostly the west of the RAS has few soil mounds present.

There were some animal mounds and holes within the RAS, as seen in Figure 26b. These holes ranged in size from 0.025 to 0.2 m (1–in.) in diameter. When we stepped on an animal burrow area, our shoes sunk in and

created a depression. The animal burrows consisted of connected animal holes with series of small tunnels creating soil voids. The depth of the burrows was difficult to survey and was not investigated.

a. Mounds at base of vegetation between stations 0+70 and 1+40.

b. Soil and animal burrow.

Figure 26. Surface features such as mounds, animal burrows, and gravels were observed on the RAS at El Centro.

c. Loose gravel-sized material on the surface of the western portion of the OLS.

Figure 26 (cont'd).

A more detailed compilation of photos taken during IOP #1 is shown in Appendix B. Although a thorough survey of the surface features was conducted during IOP #1 (Fig. 25), features such as the soil mounds, animal burrows, etc., remained in the same vicinity during IOP #2 and IOP #3.

5.2.1.2 Vegetation Type and Height

The primary vegetation types on the RAS and the nature of their distribution are described below for each of the vegetation types in Figure 27. The vegetation types remained the same every season even though they went through a seasonal growing cycle.

The vegetation height of each plant was measured in the photos in Figure 27. With the exception of the *Fouquieria Spenden Engelm* (Octotillo), *Larria Tridentata* (Creosote bush), and *Grayia* (dune species), most of the vegetation on the RAS was less than 0.5 m in height. The *Fouquieria Spenden Engelm* (Octotillo) can reach 6 m (20 ft high) or taller and the

base (part of the plant right above the surface) of the plant can reach about 0.6 m (2 ft) wide, with spikes or large thorns along the branches. The creosote bushes are the dominant plant in the area and can be as high as 1.8 m (6 ft). The *Grayia* (dune species) are typically found on areas with finer sand and can be 1.5 m (4 ft) tall. We were warned by the Range Control personnel that both the *Grayia's* thorny branches and creosote's sharp dead roots can puncture a vehicle tire and we experienced a tire blowout during IOP #1 while driving along the side of the RAS.

Larria Tridentata (Creosote bush).

These bushes are the most common bush and are seen everywhere. Some have mounds under them, and others do not.

Grayia (dune species).

These are common on the eastern portion of the RAS. Normally the bushes have soil mounds under them.

Eriogonum inflatum (backwheat).

There are a few of this plant on the RAS.

Oenothera deltoicles (evening primrose).

This plant is scattered around the RAS.

Figure 27. Typical vegetation types on the RAS at El Centro and surrounding area.

Fouquieria Spenden Engelm (Octotillo).

There are a few of these bushes outside of the RAS. They have large thorns along the branches.

Phacelia Humilis.

This plant can be seen in some areas of the RAS.

Festuca Octoflora (6-week fescue).

This plant can be found growing on coarser sandy soil and is common on the western portion of the RAS.

Plantago Ovata.

This is a very common plant that grows between bushes on the RAS.

Phacelia.

This plant is rarely seen on the RAS.

Figure 27 (cont'd).

5.2.1.3 Vegetation Cover and Greenness

The variation in vegetation cover along the RAS is evident from the photos (Fig. 28). From Stations 0+00 to 3+80, the bushes such as the *Larria Tridentata* (creosote bush) and *Grayia* (dune species) are at an average spacing of 2.5 m (8 ft), and the crown of the vegetation is roughly 1.5 m (5 ft). The bushes for the rest of the RAS are quite spread out with an approximate average spacing of 6 m (20 ft) (Fig. 29). The percent vegetation cover for the bushes is added and is summarized in Table 10.

| At 3+80 CL due west. | At 3+80 CL due east. |

| At 6+00 CL due west. | At 6+00 CL due east (personnel sampling at 5+70 2N). |

Figure 28. Selected sampling locations displaying the distribution of vegetation cover on the RAS.

At 9+80 CL due west (personnel sampling at 10+20 N).

At 9+80 CL due east.

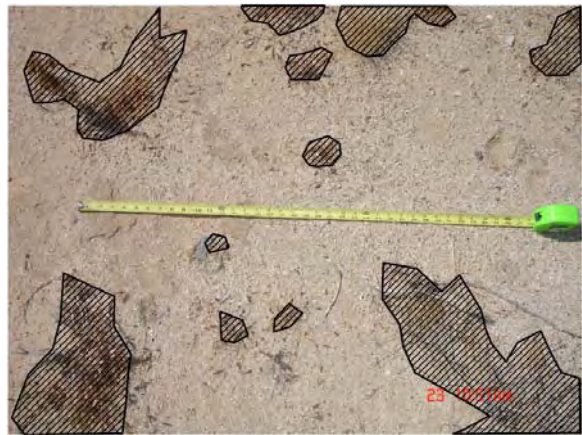Figure 28 (cont'd).

2+60 CL.

7+50 CL.

6+00 CL.

9+80 CL.

Figure 29. Vegetation cover calculated from the photos taken at respective sampling locations. (Hatched polygons are digitized areas of plant cover.)

Table 10. Vegetation cover summary from photos taken on the RAS at selected sampling locations.

Sampling Locations	2+20 CL	2+60 CL	3+00 CL	3+80 CL	6+00 CL	6+80 CL	7+50 CL	9+80 CL	11+25 CL
Vegetation Cover, % (low-height)	15	16	27	11	8	8	18	20	6
Vegetation Cover, % (bushes)	24	24	25	24	4	4	6	5	5
Total Veg. Cover, %	39	40	52	35	12	12	24	25	13

There was no seasonal variation in vegetation cover on the RAS at El Centro (Fig. 30). Most of the plants appeared dried or dead during summer, fall, and spring visits. In terms of vegetation greenness, only the creosote bushes remained green every IOP. Some plants flowered during IOP #3 (spring), including the creosote bushes and *Octotillo*.

a. IOP #1 (July 14, 2005).

Figure 30. Vegetation cover during three IOPs. Photos were taken at Station 6+00 along the centerline due east.

b. IOP #2 (October 18, 2005).

c. IOP #3 (April 24, 2006).

Figure 30 (cont'd).

5.2.1.4 Surface Water

No surface water was observed on the RAS during any IOP. Puddles of water were observed on the low-lying areas outside of the RAS from a rain storm that occurred days before IOP #2. Erosion and deposition on the soil surface indicated that water flowed through the OLS during that rain event (Fig. 31).

Figure 31. Surface run-off erosion and deposition features from the recent rain storm prior to IOP #2.

5.2.1.5 Rutting

Typical tracks found on the OLS were from four-wheeled and two-wheeled (dirt bike) vehicles. Tire tracks noted are sketched on Figure 25. Some tracks were as deep as 10 cm (4 in.) (Fig. 32).

Figure 32. Existing ruts on the RAS from recreational vehicles.

5.2.1.6 Dust

When the ground is disturbed, dust is quite common when fine particles become airborne, especially in the dry environment. At El Centro RAS, dust was observed while digging pits and backfilling (Fig. 33a) during IOP #1. Significant dust clouds occurred when driving vehicles (40 psi tire pressure) at speeds of 13.4–15.6 m/s (30–35 mph) on unpaved trails (Fig. 33b). The vehicle was barely visible by the observer and this was of course depending on the condition of the road such as areas of sand pockets and wind. But within 30 s after vehicles passed, dust clouds dissipated as a result of slight winds (Fig. 33c), giving clear visibility of the road from approximately 200 m (650 ft). During IOP #2, no dust was observed because rain storms occurred prior to the field visit.

a. Dust generated during digging (IOP #1).

b. Vehicle approaching showing significant dust behind it (IOP #3).

c. Dust diminishing within half a minute after vehicle passed (IOP #3).

Figure 33. Dust observation and susceptibility at El Centro RAS.

5.2.1.7 Surface Conditions Discussion and Summary

The surface conditions and their ratings for the OLS are summarized in Table 11, which is based on Table 2 in Section 3. Some of the ratings are considered subjective and other distress types do not apply, particularly for an OLS (i.e., jet blast erosion or stabilized layer failure). Cemented layer could be considered as a stabilized layer; however, the layers are irregular and non-uniform through out the RAS.

Table 11. OLS rating for surface condition for all seasons.

	Surface Categories	Rating
1	Potholes	**Green and Amber:** < 100 to 230 mm (<4 to 9 in.) deep and > 380 mm (15 in.) in diameter
2	Loose aggregate	**Amber:** Covers about 1/10 and 1/2 of RAS
3	Ruts	**Green:** Ruts are insignificant and are not along the wheel paths.
4	Rolling resistance material	**Amber:** > 195 mm (7.75 in.) deep
5	Dust	**Amber:** Partially obstructs visibility, appr. 400 m (¼ mile)
6	Jet blast erosion	Not applicable on the RAS becausethere is no scouring caused by jet blast erosion
7	Stabilized layer failure	Not applicable on the RAS
8	Animal burrows	**Green and Amber:** Number of animal holes between 3 and 6 with 25-m- (1-in.-) dia. holes, in a 10- by 10-m area, but mostly spaced farther than 200 m.
9	Mounds	**Red:** Third of RAS has mounds greater than 230 mm (9 in.) high and greater than 380-mm- (15-in.-) diameter
10	Vegetation	**Amber:** Bushes are less than 0.5 m (1.5 ft) high and less than 1-in. diameter with vulnerability for vehicle tires puncture.
11	Standing water	**Green:** No water ponding
12	Surface drainage paths	**Green:** Exist but < 100 mm (4 in.) deep
13	Surface debris and organics materials	**Green:** Minimal organics on the RAS
14	Snow depth	**Green:** Zero snow cover

Creosote bushes have flexible branches that can be pushed down when a vehicle is driven over them. Thus, the vegetation on the RAS in El Centro will not limit landing of transport aircraft. Vehicle tires can be punctured by the *Grayia* and creosote bushes. However, aircraft tires contain several plys and can most likely handle these type of plants. Using "Green, Amber, Red," the RAS can be rated "Amber." Additional rolling resistance during take is likely to occur on the RAS as a result of unconfined loose aggregate and fine-grained soils.

Few areas with animal burrows were observed on the RAS. If the OLS is subjected to aircraft loading, uneven soil compaction may take place and localized soil failure can occur. The subjective rating for the OLS in terms of surface condition is considered to be marginal. Using "Green, Amber, Red," the RAS can be rated from "Green to Amber."

Granular materials, coarse gravel, and stones ranging in size from 0.025 to 0.2 m (1 to 7 in.) are observed to be prevalent on the surface of the RAS. Rocks larger than 0.1 m (4 in.) must be removed from the operational surface according to AFCESA's criteria. Loose aggregates are considered to be a potential cause of FOD, which can damage aircraft components such as the engines, tires, etc. The El Centro RAS can be rated as "Amber" for FOD based on the presence of coarse gravel and stones.

Dust is certainly an issue in the semi-arid environment. The large amount of fine particles in the soil (ranging from 11 to 28% of less than 0.075 mm in size) can be airborne for a couple of minutes. Dust was observed to partially obstruct visibility. The RAS is rated as "Amber" because dust will generally clear up within half a minute for visibility of approximately 200 m (650 ft).

The RAS contains Green for at least 7 of 14 categories, three Amber ratings, and one Red rating. The surface categories can be summarized as "moderate" (according to Table 4 in Section 3).

5.2.3 Soil Moisture

Soil moisture was measured using several methods in both volumetric and gravimetric units with considerable variation among measurement methods (Appendix C). Sampling locations where soil moisture was measured at various depths during all IOPs are listed in Table 4.

5.2.3.1 Dynamax (ML2, PR2)

During IOP #1, soil moisture contents taken by the HH2 (ML2) probe were measured only in the soil pits. Soil moisture content readings were taken three or more times at each location for replication. In order to capture the moisture profile, soil moisture contents were measured at the surface and at various depths (e.g., 0.08, 0.15, 0.3, 0.6, 0.9 m [3, 6, 12, 24, 36

inches]). Depending on the sampling locations, the instrument tines had difficulty extending into the soil because of cemented layer or stones.

The soil moisture profiles from the replicate readings during the first IOP, seen in Figure 34, showed that moisture varied up to 6% volume. Soil moisture near the surface ranged between 2 and 4% by volume throughout the RAS; depending on the location, the moisture gradually increased up to 18% with depth, then slightly decreased below 0.6 m. The average soil moistures were calculated for each location (Fig. 35) and moisture profiles reflected the low values in July for dry summer conditions in the area.
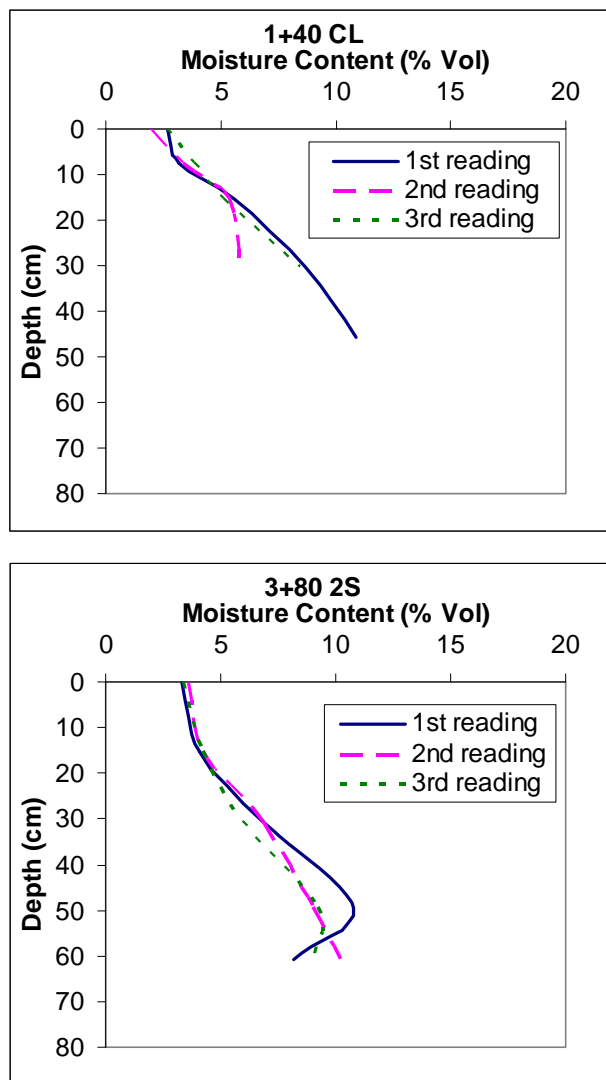
Figure 34. Moisture profiles taken from Dynamax ML2 probes during the first IOP.
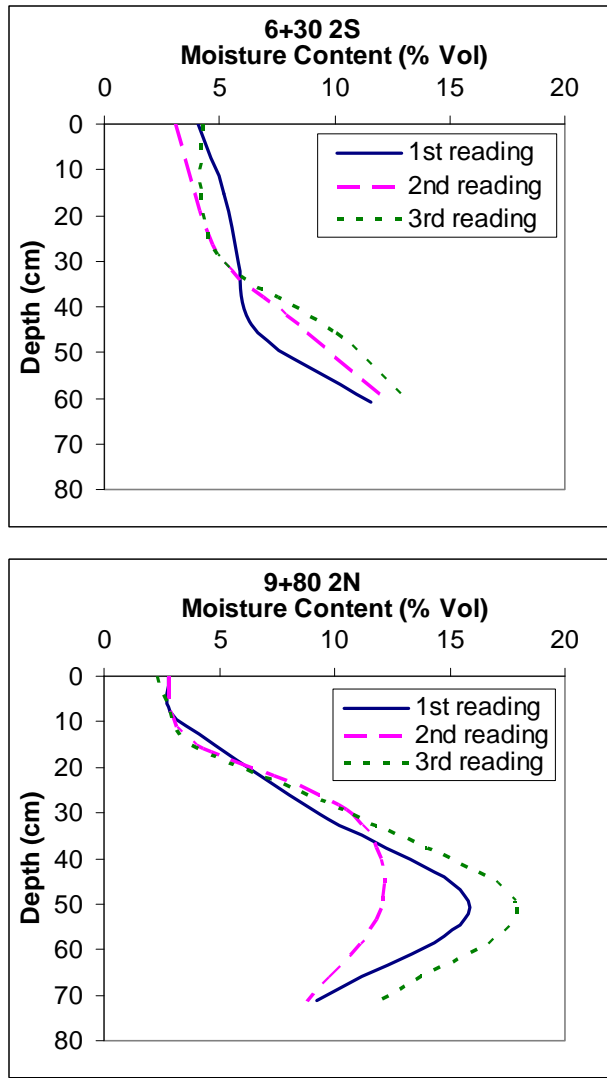
Figure 34 (cont'd). Moisture profiles taken from Dynamax ML2 probes during the first IOP.
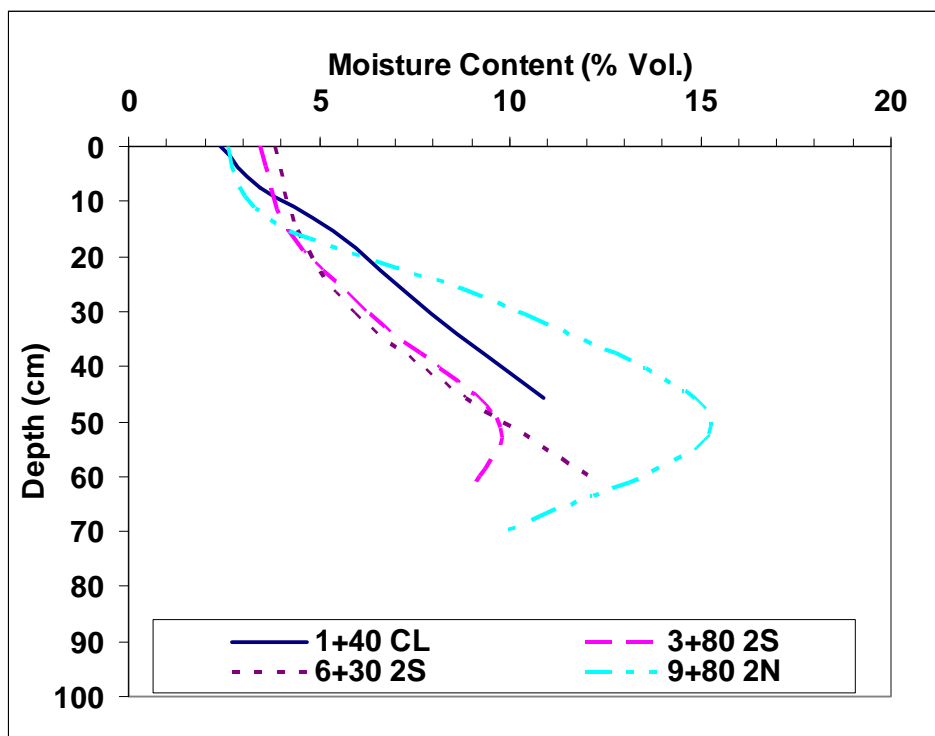
Figure 35. Average soil moisture profiles from the Dynamax ML2 probes taken during IOP #1 (July 2005).

The soil moisture profile from the average of all the readings with depth using the HH2 (ML2) probe taken during IOP #2 (October IOP) are shown in Figure 36. During this IOP, soil moisture measurements were taken at 77 sampling locations as shown by dots in the contour profile. The surface moisture is approximately five to six times wetter than during IOP #1, with a range from 10 to 26%. Moisture content dramatically changed with depth, where some sections of the RAS were wetter than others. These pockets of "wetter areas" were related to surface runoff of water onto low lying areas of the RAS topography. Contours for soil moisture below 0.3 m can be questionable due to the limited number of moisture sampling locations at those depths because of the cemented layer.

Weather records during IOP #2, and before, showed rain storm events occurred in the area with total accumulation of 29 mm of rainfall over a period of five days, ending the morning of our field measurements. These rainfall events explain some, if not all, of the moisture changes observed during the second visit (IOP #2).
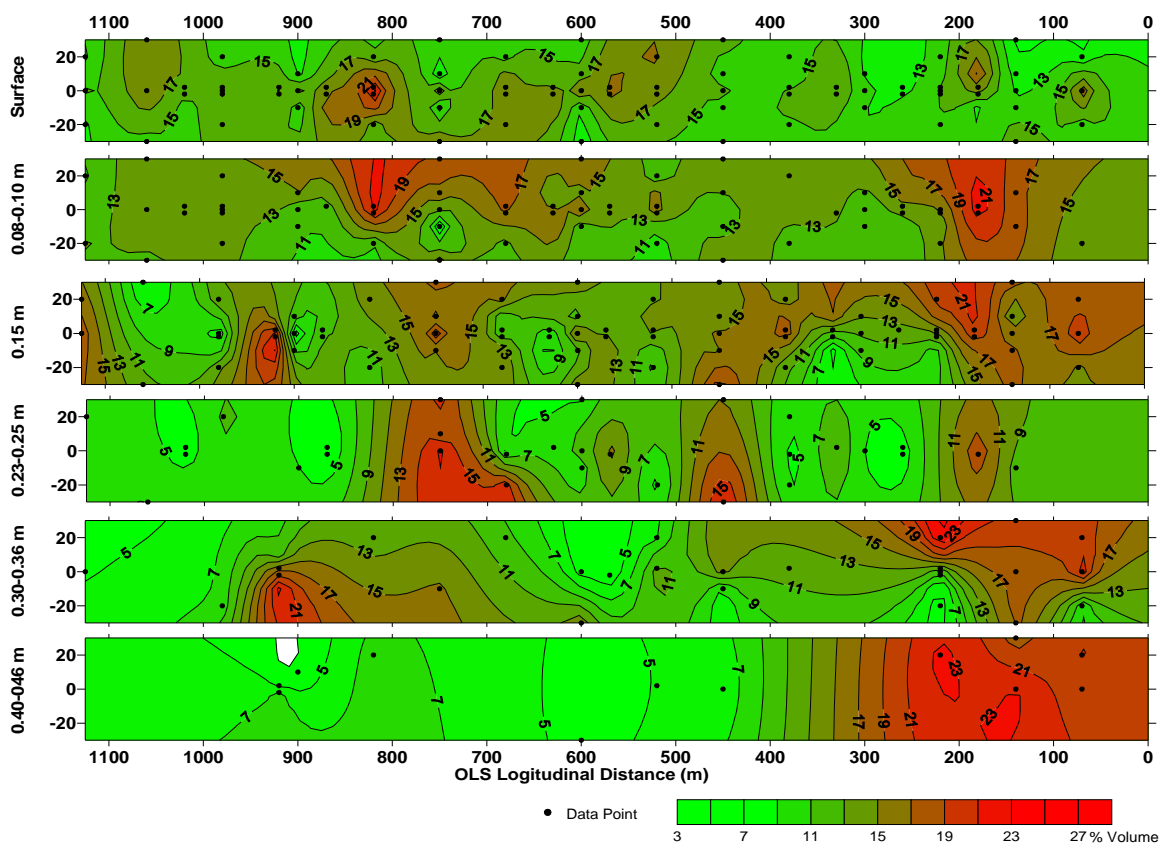
Figure 36. Profiles of soil moisture from the ML2 Dynamax, taken in October 2005 as shown in contours.

Only surface moisture using the ML2 was taken during IOP #3, ranging from 3 to 6% for the average value of data for each sampling location.

The surface moisture contents from the three IOPs indicate a very dry summer, significant moisture in the soil in the fall, and a dry spring (Fig. 37). During IOP #2 (in October 2005), the vegetation also was relatively greener than during IOP #1 (July 2005) and IOP #3 (April 2006).
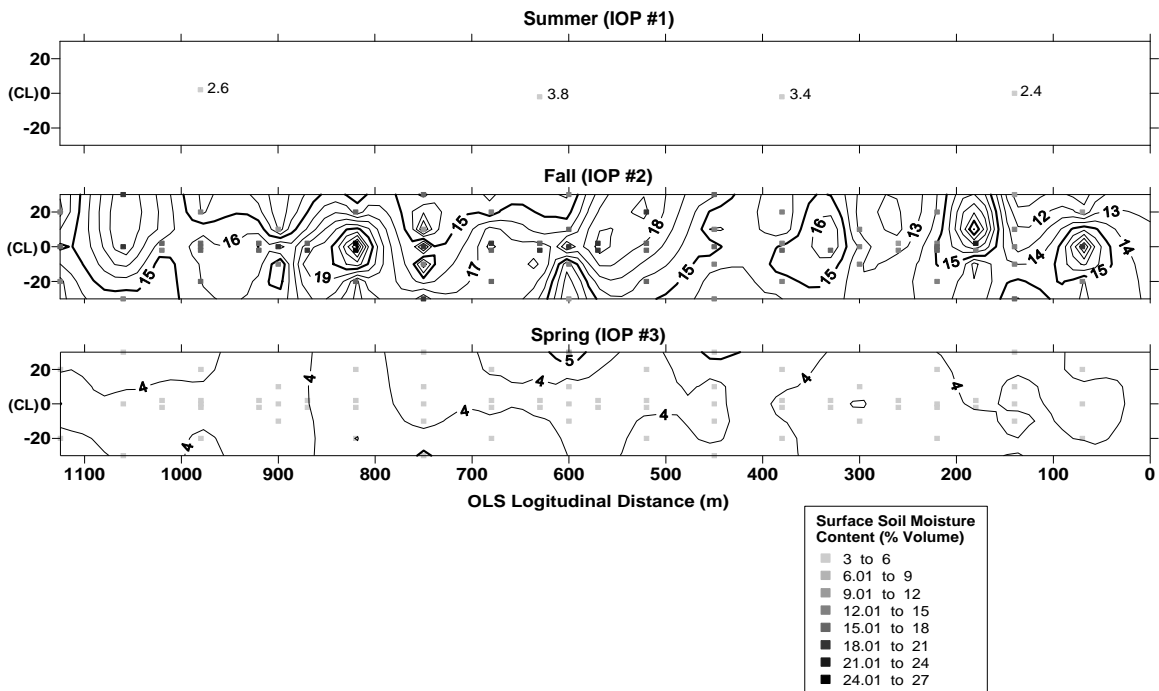
Figure 37. Surface soil moisture content comparisons between three field visits.

Figure 38 exhibits the soil moisture profiles from the Dynamax PR2 sensors installed near the weather station. The soil moisture profiles from the PR2 are similar to moistures observed from the ML2. There is a large jump of soil moisture at 5-cm and 15-cm depths from the precipitation (Fig. 38a). Soil moisture from the PR2 at 5-cm depth during the third IOP is 3.5% volume (Fig. 38b), which is very similar to the ML2 measurements on the RAS (Fig. 37).
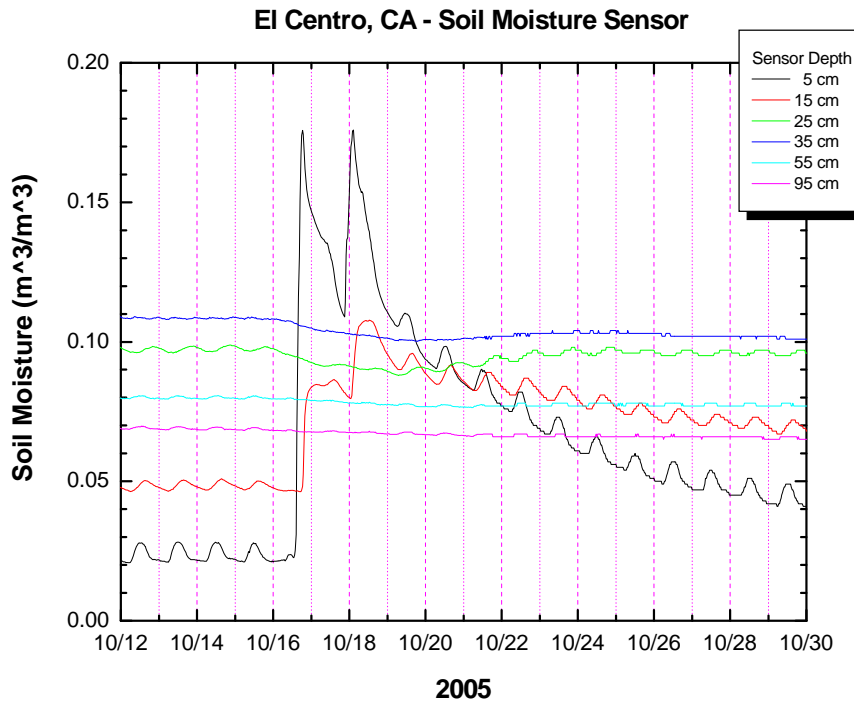
a. Days prior and during IOP #2.
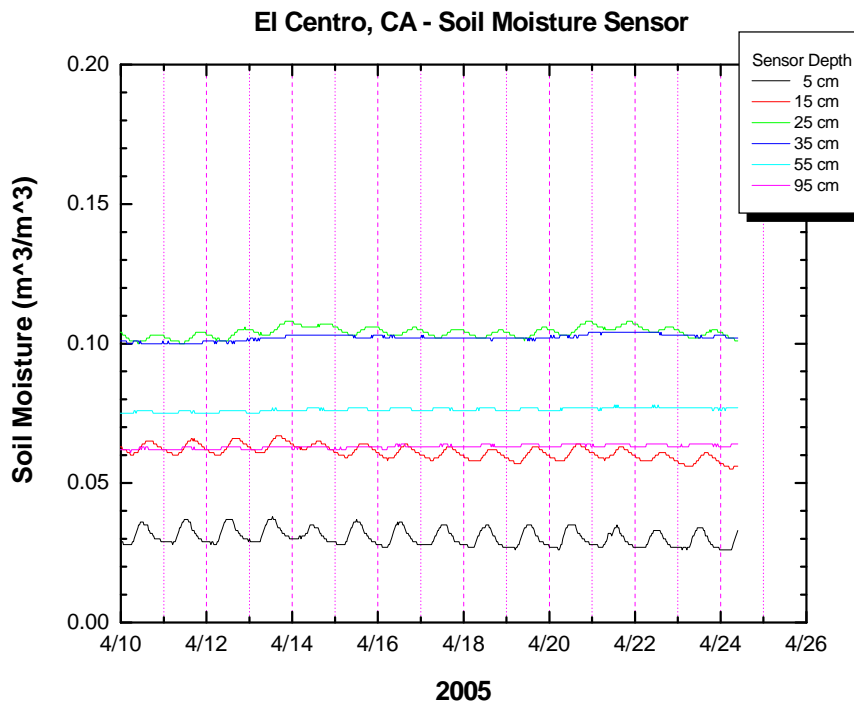
b. Days prior and during IOP #3.

Figure 38. Soil moisture data from the Dynamax, PR2 installed at the weather station.

5.2.3.2 Gravimetric Soil Moisture Contents (including drive-cylinder soil samples)

Profiles for soil moisture contents obtained from the gravimetric samples (calculated using equation 2) taken during summer and fall are reported in Figure 39. The soil moisture content profiles for IOP #1 (July 2005) ranged from 1 to 5% by weight, which reflected a very dry condition. During IOP #2, the soil was moister, with soil moisture near the surface ranging from 8 to 10%, and then varying with depth at several locations.
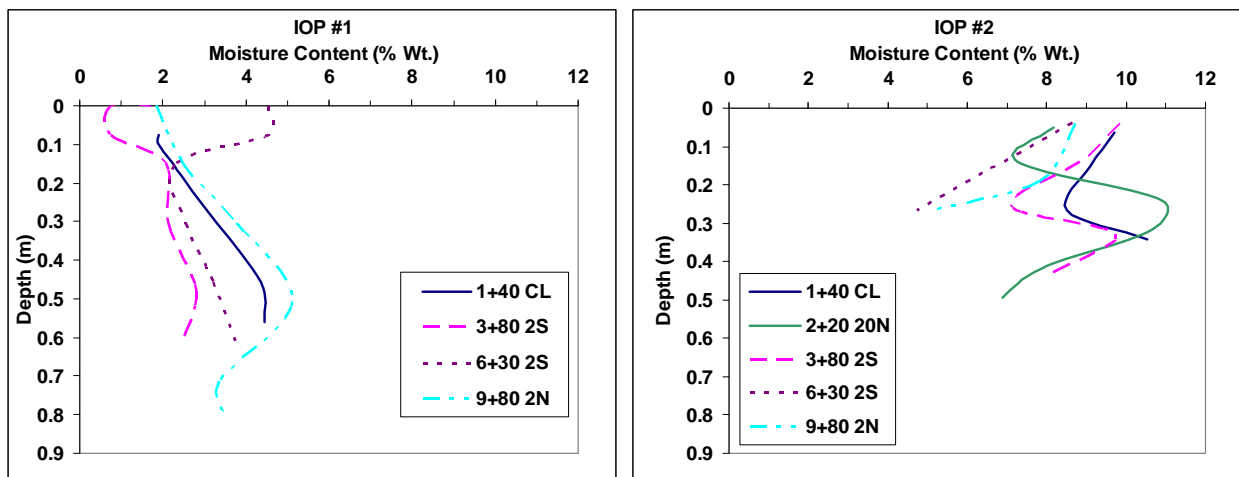
Figure 39. Soil moisture profiles using the gravimetric method from samples taken in July 2005 (IOP #1) and in October 2005 (IOP #2).

Gravimetric moisture contents can be converted to percent volume using the corresponding dry density of the soil layer taken from the nuclear density gage. Soil moisture contents measured between the Dynamax ML2 and the gravimetric soil samples are found to be within 2 to 5% water content of one another for IOP #1 (Fig. 40a). Soil moisture measurements obtained during IOP #2 showed significant scattering in some sampling locations as can be seen in Figure 40b. Although both measurements were taken relatively in the proximity, the scattering could be attributed to instrument and sampling errors and possibly to spatial variability.
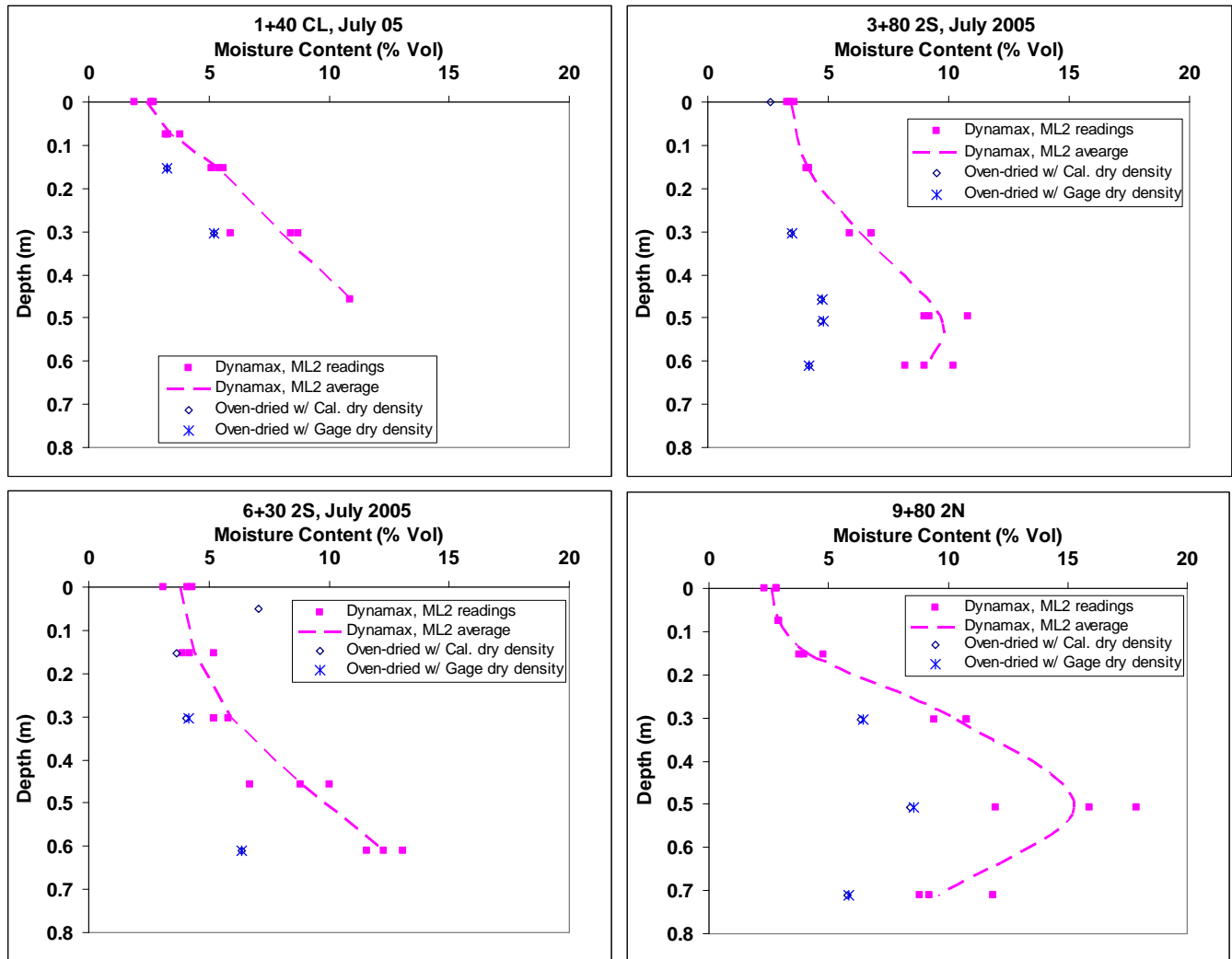
a. IOP #1, July 2005.

Figure 40. Gravimetric moisture contents converted to percent volume along with soil moisture profiles measured using the Dynamax, ML2.
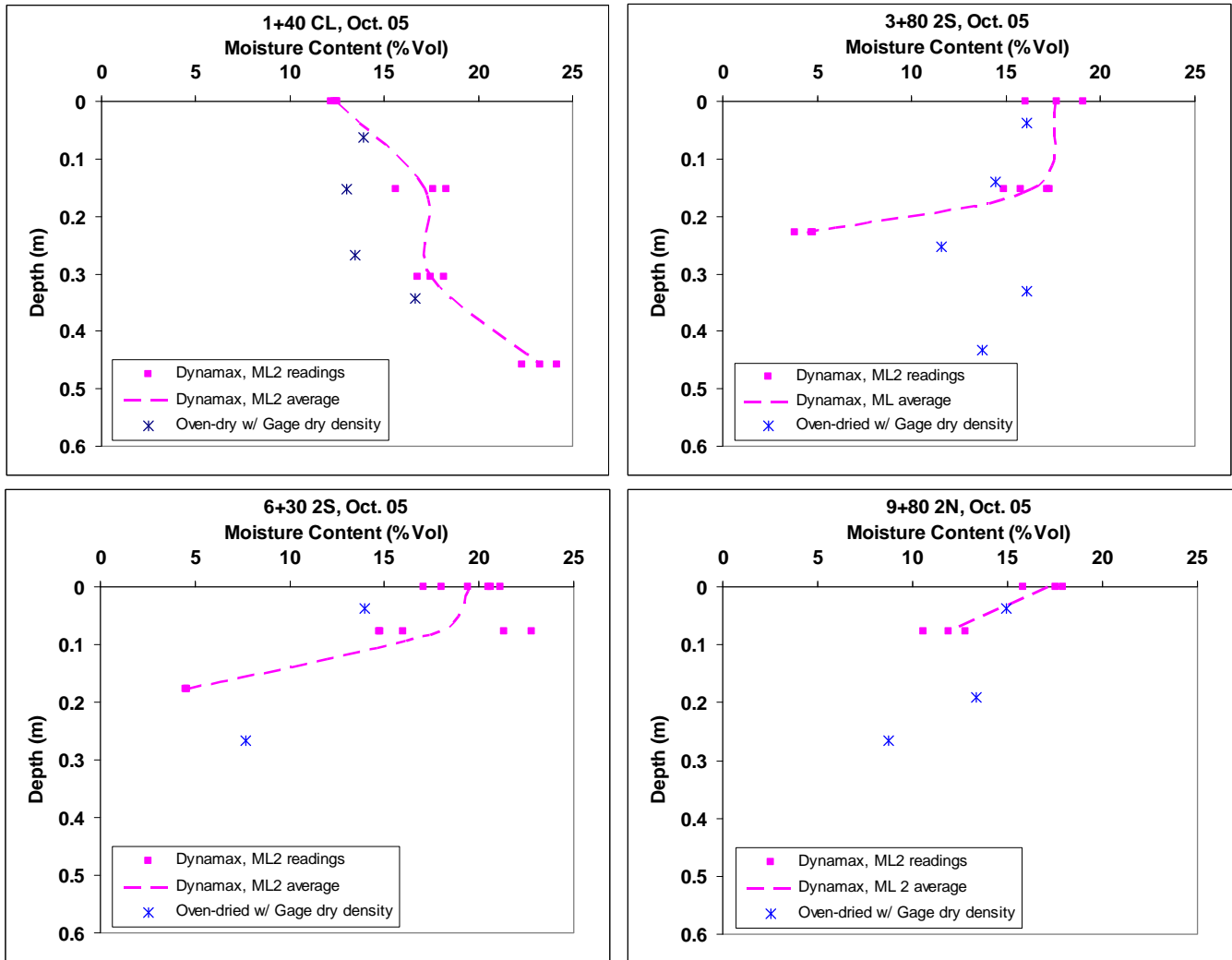
b. IOP #2, October 2005.

Figure 40 (cont'd).

5.2.4 Soil Strength

5.2.4.1 Dynamic Cone Penetrometer (DCP)

An Excel macro procedure was developed to average the CBR profiles for each sampling location within each of the following depth ranges:

- 0 to 0.15 m (0 to 6 in.);

- 0.15 to 0.30 m (6 to 12 in.);

- 0.30 to 0.45 m (12 to 18 in.);

- 0.45 to 0.6 m (18 to 24 in.);

- 0.60 to 0.75 m (24 to 30 in.) and;

- 0.75 to 0.9 m (30 to 36 in.).

These increments enable easy comparisons of the data. The CBR data for each IOP are graphed using contour plots, and the sampling locations are marked using shading and shapes denoting the CBR value (Fig. 41).

As described in Section 5.1, cemented layers were observed while pits were dug. These layers have irregular thickness and their depths are varied with sampling location. The cemented layers were noticeable while using the DCP where the rod would penetrate at a slow rate. DCP penetration showed that the cemented layers and their strength were variable with location on the RAS.

During IOP #1 (in July 2005), 81 DCP profiles were measured on the entire RAS (Table 6). CBR values of the top layer (0 to 0.15 m or 0 to 6 in.) were greater than 20 and up to 38 in a small area in the western corner and at a few other sample locations. For most of the RAS the surface layer CBR values are in the teens, with a few less than 10 and minimum of one (Fig. 41a). Of the 81 DCP profiles, at least 48 of those have CBR values of less than 10, and there are nine sampling locations with CBR strengths of less than or equal to two.

At depths of 0.15 to 0.30 m (6 to 12 in.), 25 of 81 locations have CBR values less than 10; four of these locations have CBR values less than or equal to two. In general, the soil strength increased below the surface layer and in some locations at deeper depths, such as areas surrounding stations 7+50 and 2+00, with relative high CBR values in the 30s and 40s (Fig. 41a). Based on our observations in the soil pits, the cemented layer is the main source of the soil strength increase at depth.

The soil strength for 0 to 0.15 m (0 to 6 in.) and 0.15 to 0.30 m (6 to 12 in.) during IOP #2 in October 2005 ranged from zero to 29, and one to 53 percent CBR, respectively (Fig. 41b). Of 70 DCP profiles, 63 of the sampling locations have surface layer CBR values less than or equal to 10, and two-thirds of these measurements have CBR values less than 2. Similarly, an

increase in soil strength is discerned from the CBR values at 0.15- to 0.30-m (6- to 12-in.) depth, with 50% of the locations having CBR values greater than 10, and at least 10% of the locations on the RAS having CBR values of two or less. The changes in soil strength with depth most likely are influenced by the cemented layer in certain parts of the RAS, as described earlier (Fig. 41b).

There were 77 DCP profiles taken during IOP #3 (April 2006). The CBR profiles for IOP #3 are shown in Figure 41c. The CBR for 0−0.15 m (0−6 in.) and 0.15−0.30 m (6−12 in.) ranged from 2 to 33, and 2 to 44, respectively. Soil strength profiles below 0.15 m (6 in.) are comparable to the strengths for IOPs #1 and #2 at these depths. The soil strength for 0−0.15 m to 0.30 m (6−12 in.) depth ranged between three and 32 (% CBR), and at 70% of the sampling locations the CBR is less than or equal to 10.
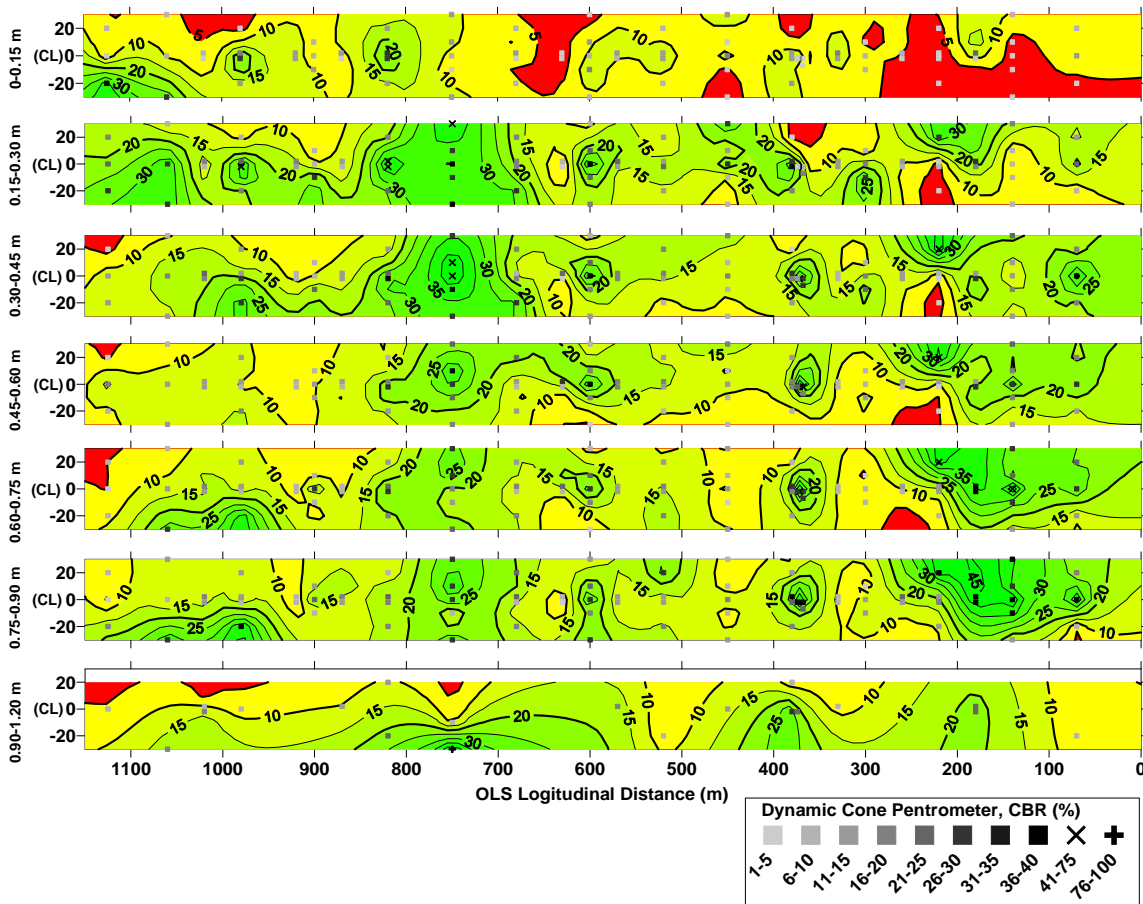
a. CBR contours for each depth range (July 2005).

Figure 41. Soil strength contours measured using the Dynamic Cone Penetrometer for all IOPs on El Centro RAS.
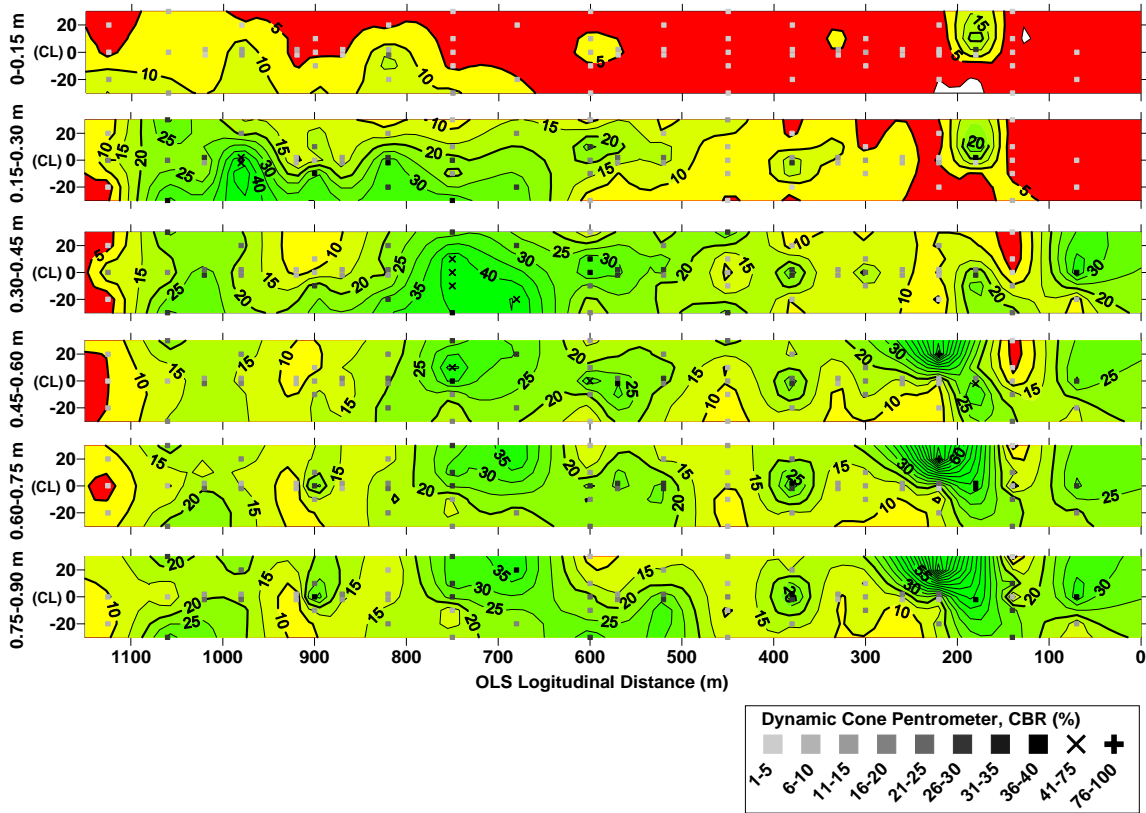
b. CBR contours for each depth range (October 2005).
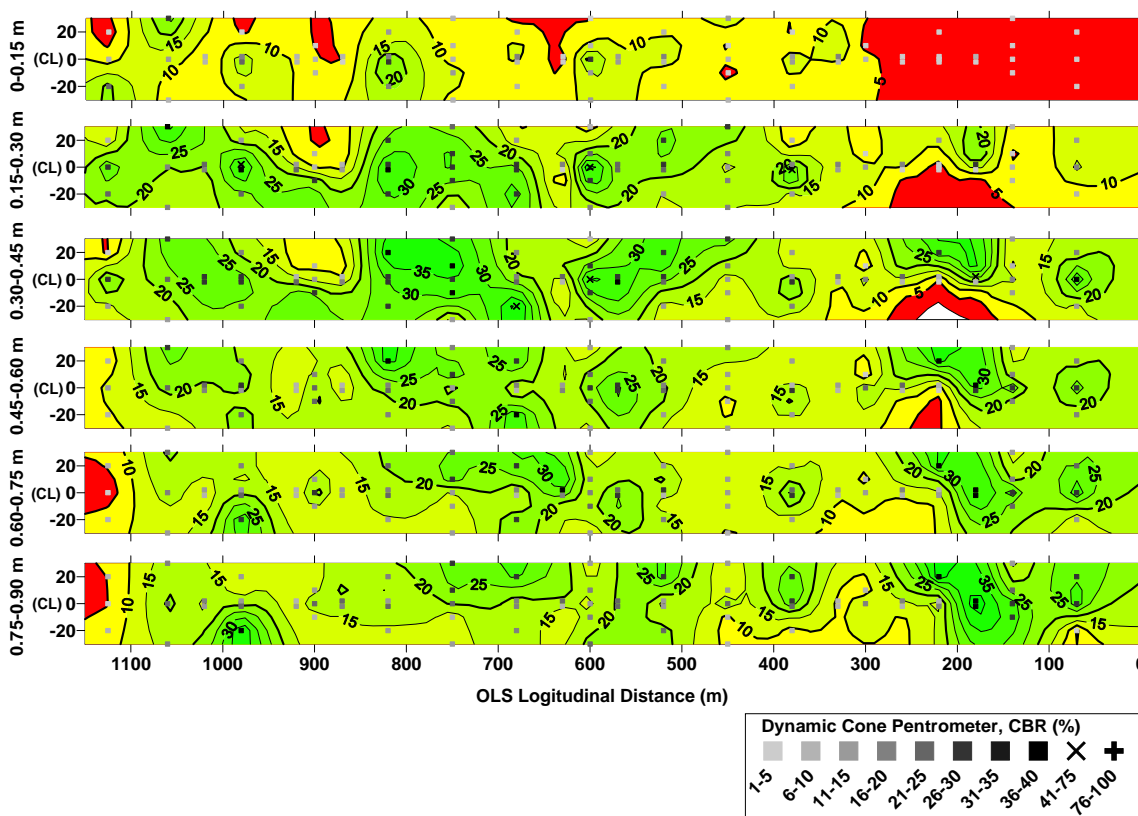
Figure 41 (cont'd). Soil strength contours measured using the Dynamic Cone Penetrometer for all IOPs on El Centro RAS.

c. CBR contours for each depth range (April 2006).

Figure 41 (cont'd).

In general, the surface layer CBR values are low and not reliable due to the lack of confinement in the soil. CBR values vary with depth, which are solely controlled by the irregular and discontinuous cemented soil layers. CBR values also differed with the topography of the RAS. In the upper depths (from the surface down to 0.3-m depth), the soil strength is lower elevation (the eastern part of the RAS) than in the higher elevation (the western part of the RAS). The area with lower soil strength is quite significant during IOP #2 (Fig. 41b), where the water from the rain event drained toward the lower elevation (Fig. 36), evident from the surface runoff patterns shown in Figure 31. The CBR can have variations within a soil type. The eastern part of the RAS consisted of fine coarsed-grained gravel and sand on the surface, with higher vegetation cover than the other section of the RAS.

CBR profiles from all the DCP data for all IOPs are compiled in Appendix D. The profiles for each sampling location can be compared for seasonal changes. Typical DCP profiles taken at sampling locations 2+60 2S and

7+50 CL are shown in Figures 42 and 43, respectively. At sampling loca-
tions 2+60 2S, the soil displayed low strength profiles from the surface
down to 0.35 m, with CBR less than 10. Below it, the soil strength varied,
depending on where the DCP was taken at that specific location (Fig. 42).
While at 7+50 CL, the cemented layer can be easily detected from the DCP
profiles below 200 mm (Fig. 43). Despite changes in soil moisture for IOP
#2 in October, the soil strength profiles at the two locations vary little with
seasons.
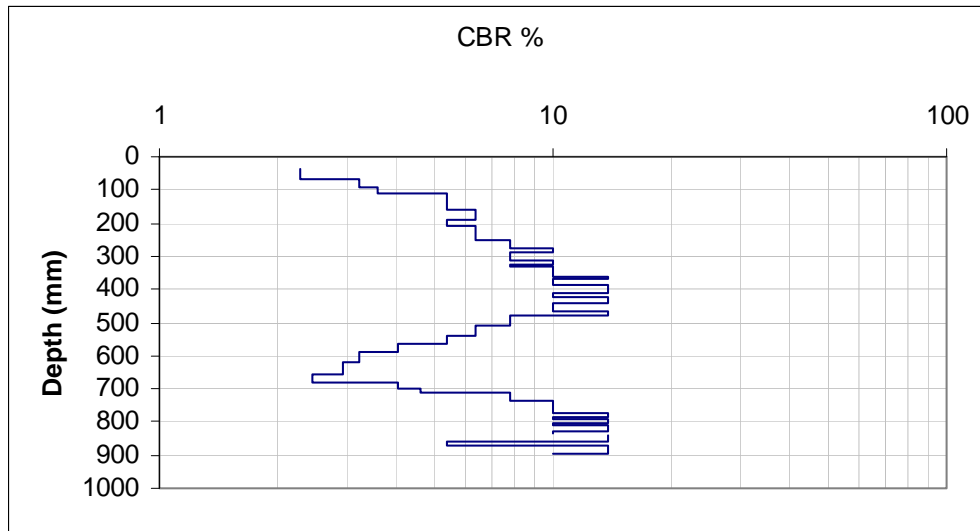
a. 2+60 2S, IOP #1 (July 2005).
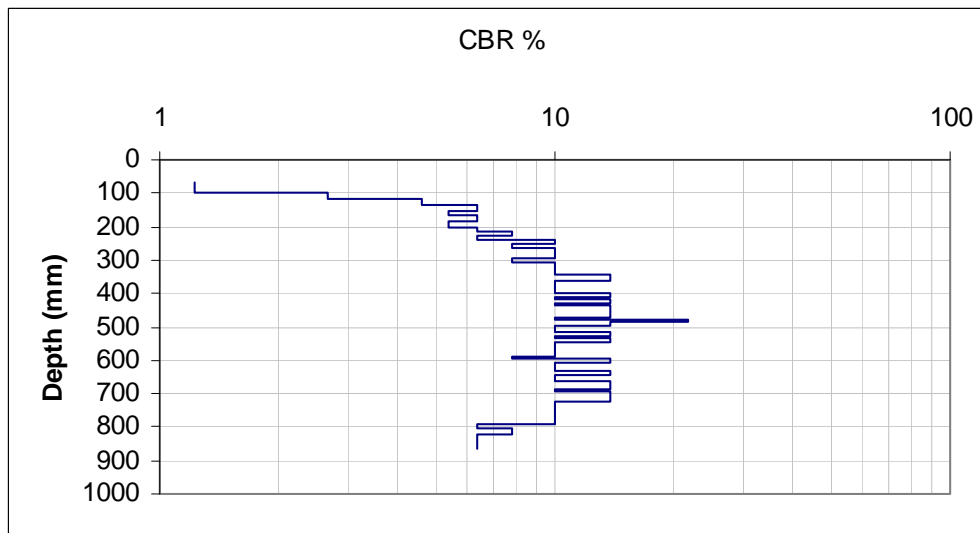
b. 2+60 2S, IOP #2 (October 2005).

Figure 42. CBR profiles at sampling location 2+60 2S taken during three IOPs at El Centro.
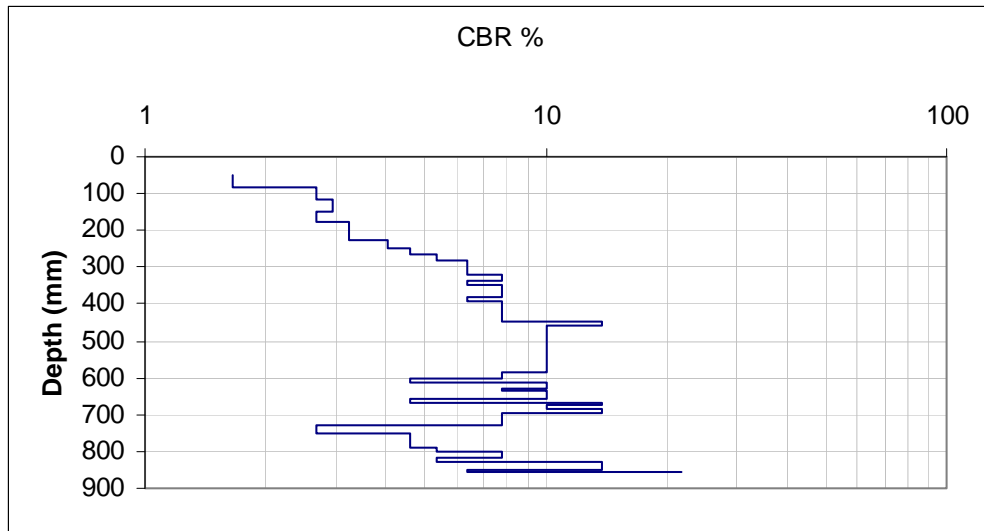
c. 2+60 2S, IOP #3 (April 2006).

Figure 42 (cont'd).
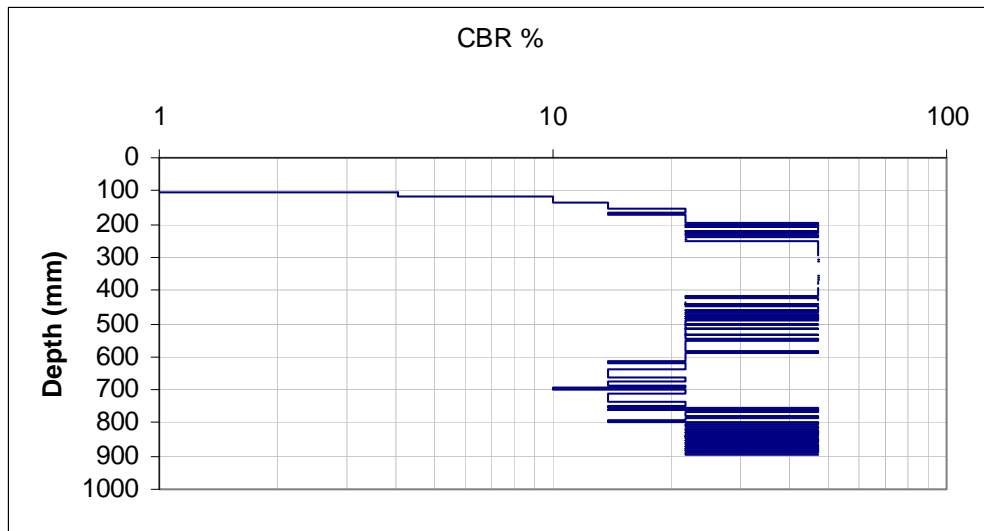
a. 7+50 CL, IOP #1 (July 2005).

Figure 43. DCP profiles at sampling location 7+50 CL taken during three IOPs at El Centro.
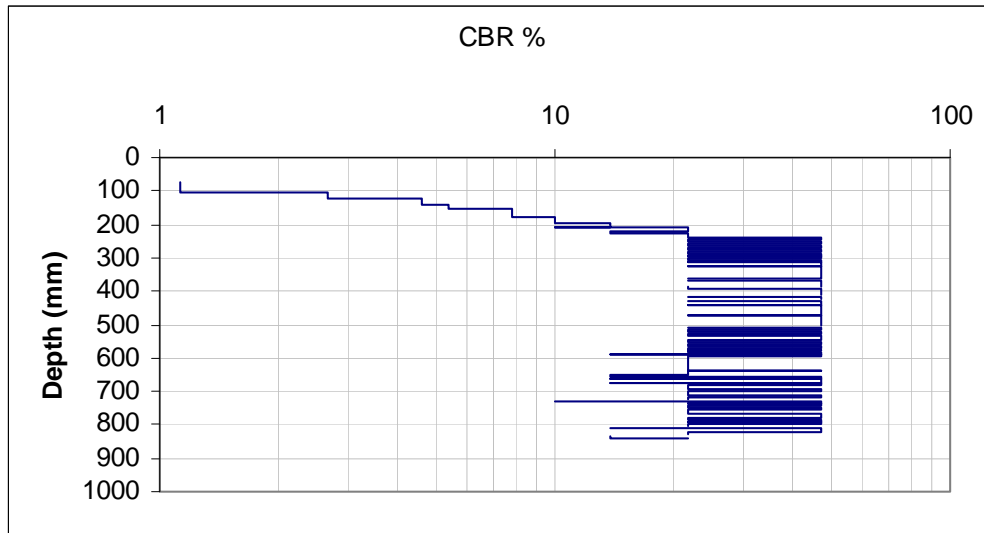
b. 7+50 CL, IOP #2 (October 2005).
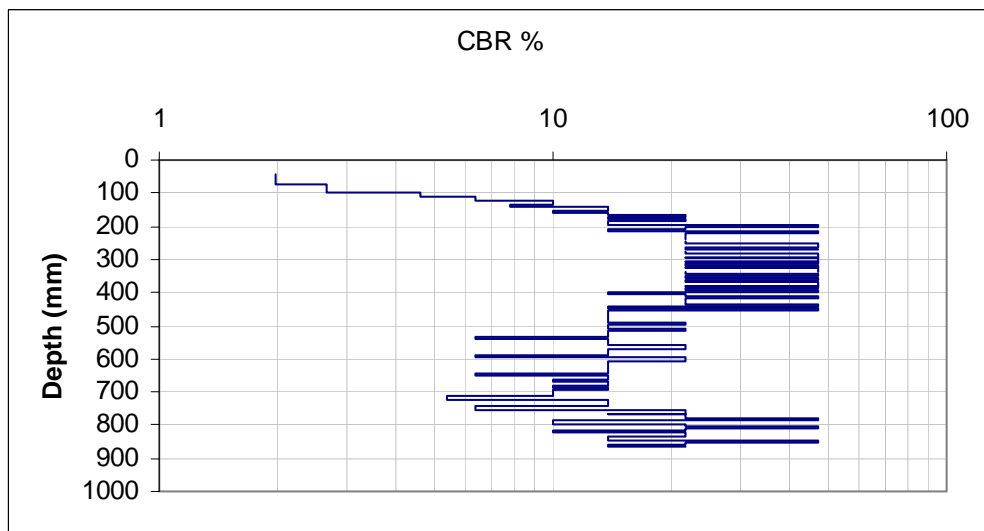
c. 7+50 CL, IOP #3 (Spring 2006).

Figure 43 (cont'd). DCP profiles at sampling location 7+50 CL taken during three IOPs at El Centro.

5.2.4.2 Clegg Hammer

CIV/L readings should increase for each subsequent drop as described in Section 4, and that was not always the case when the CIH_L (0.5-kg hammer) was used on the RAS. We discussed this issue with the equipment manufacturer, who stated that it is not uncommon to have the fourth reading lower than the third reading for certain soil conditions due to the effect of organic materials (Brown and Crandell, personal communication). The surface can be relatively strong enough that there is virtually elastic re-

bound from the first two blows, where it is more difficult to observe stiffness differences. In some cases, the first one or two blows flatten and compact, and too many blows pulverize and loosen the immediate surface or may continue to compact the material. On this RAS, we found compaction of soil with significant depth of hammer indentation after conducting a set of tests and on a surface with thin-crust layer where the soil was pulverized after the third and fourth drops. There also are several possibilities of why the third blow reading is sometimes higher than the fourth blow (Crandell, personal communication). First, if loose material falls into the impact crater, this too can cause a downwards bias. Second, the material might begin to spring back, (such as soils with organic materials), causing sufficient cushioning to cause the readings to appear lower. Lastly, it is possible that subsequent blows are retarded sufficiently by hitting the rim of the crater formed by previous blows.

Table 12. Examples of CIH$_L$ datasets calculations. (Rows highlighted in yellow are datasets with decreasing fourth readings.)

Location, IOP	0.5 kg Clegg Hammer Readings:					CBR Values calculated using Equation 3				
	1st	2nd	3rd	4th		1st	2nd	3rd	4th	
2+20 CL, IOP#1	10.6	10.1	11.1	9.9	⇒⇒⇒	2	2	3	2	
	11.2	13.9	14.5	14.4	⇒⇒⇒	3	4	4	4	
	8.9	10.0	10.0	10.7		2	2	2	2	
						2	3	3	3	Average CBR
4+50 CL, IOP#2	6.0	7.0	8.2	8.8		1	1	2	2	
	6.9	8.5	9.6	9.3	⇒⇒⇒	1	2	2	2	
	5.6	7.4	9.4	9.0	⇒⇒⇒	1	1	2	2	
	5.6	6.9	8.3	8.6		1	1	2	2	
						1	1	2	2	Average CBR
1+40 CL, IOP #3	17.2	18.6	17.6	16.2	⇒⇒⇒	4	5	5	4	
	12.3	19.5	19.1	16.7	⇒⇒⇒	2	6	5	4	
	7.1	11.7	14.2	15.2		1	2	3	4	
	18.4	23.6	22.0	19.2	⇒⇒⇒	5	8	7	6	
	14.3	18.9	20.1	18.6	⇒⇒⇒	3	5	6	5	
	14.4	18.2	17.9	17.5	⇒⇒⇒	3	5	5	5	
						3	5	5	5	Average CBR

Equation 4 was applied on datasets with decreasing readings, and in most cases showed insignificant differences in average CBR values between the third and fourth drops (Table 12). Nevertheless, Equation 4 was used to convert the fourth readings to CBR for all of the datasets regardless of whether the values were increasing or decreasing. The CBR for each sampling location was computed by averaging the calculated CBR values from all the datasets for that sampling location. The distribution of the Clegg CBR values for each IOP is shown in Figure 44. The minimum and maximum CBR values are found to be 2 and 9, 1 and 4, and 2 and 10 for each

subsequent IOP. The higher soil moisture during IOP #2 seemed to cause a decrease in surface soil strength for the wet season, and we also noticed the disappearance of the near-surface cemented layer (shown in Fig. 24) when the soil was wet.
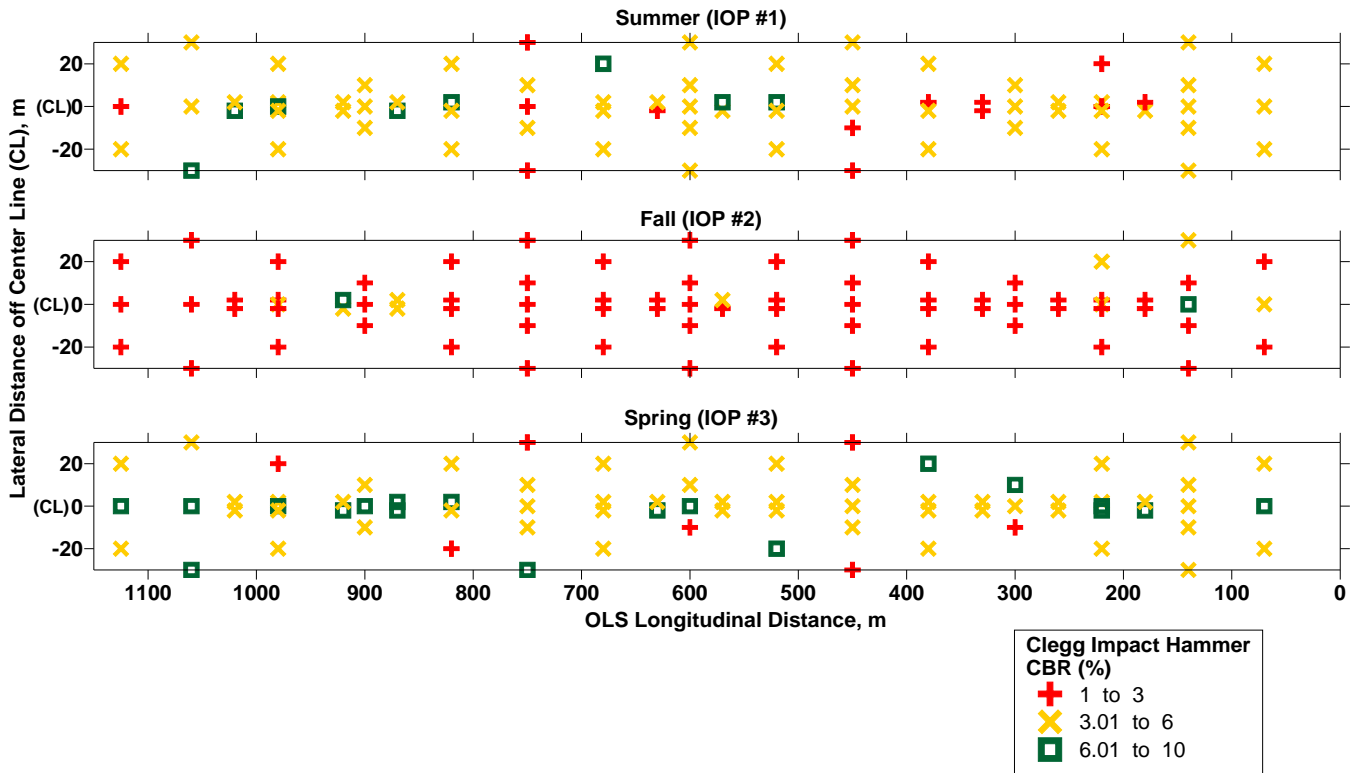
Figure 44. Soil strength for top 0.15 m (6 in.) measured using the light Clegg impact hammer expressed in CBR (%) for the El Centro RAS.

5.2.4.3 Drop cone

The force calculated using equation 5 from the Drop cone measurements for the entire RAS for three IOPs can be seen in Figure 45. Most of the areas presented very little resistance, resulting in force values of 0.6 to 0.8 kN (135 and 180 lb$_f$). Forces greater than 1 kN (225 lb$_f$) occurred primarily during IOP #3, with a few high strengths measured during IOP #1 and no high strength values during IOP #2. Some of the higher resistances are most likely attributed to the cemented materials on the surface from soil prior to summer and spring visits.
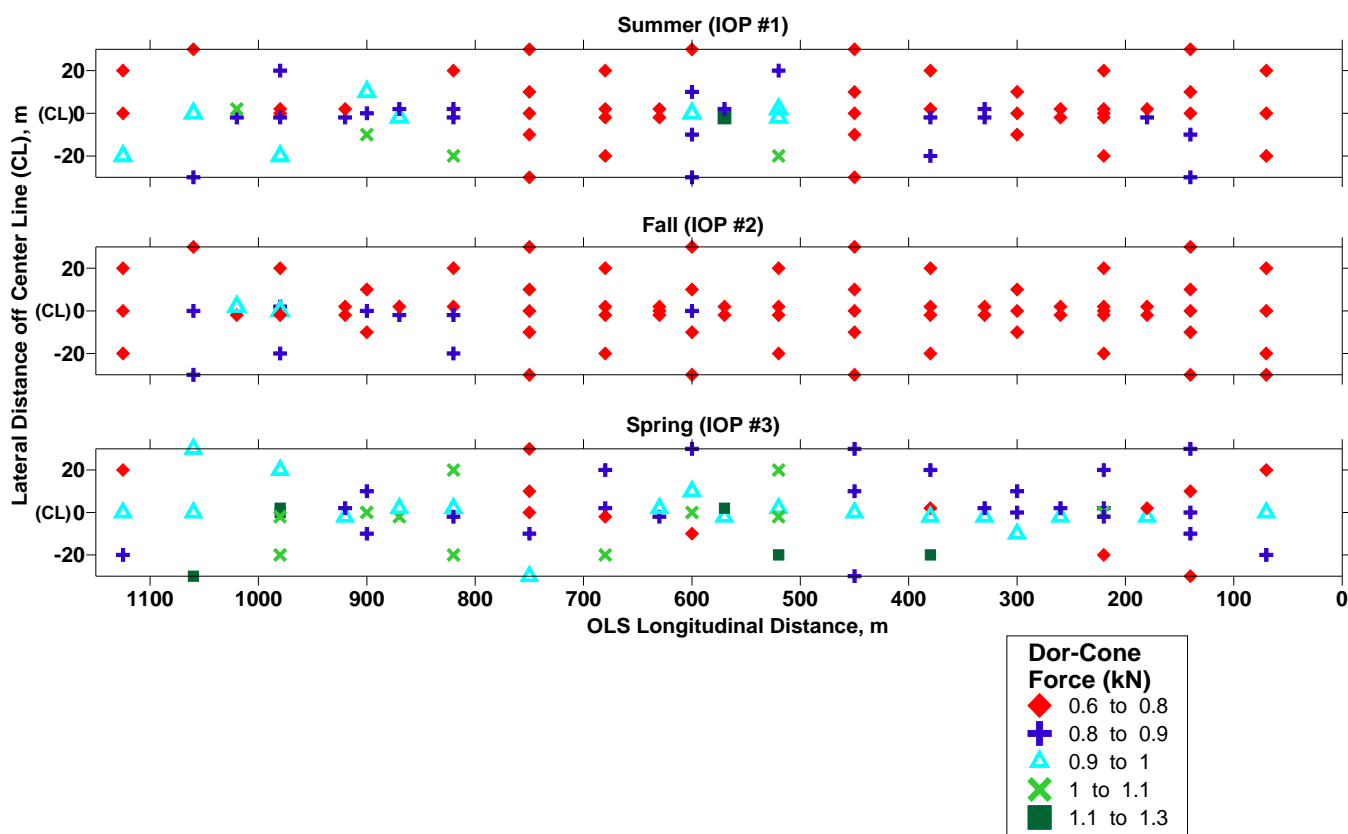
Figure 45. Calculated Drop cone force indicating the surface soil strength throughout the RAS during the three IOPs.

5.2.4.4 Soil Strength Summary

The surface CBR values between the DCP and the 0.5-kg Clegg hammer showed significant differences. It is important to note that each instrument has a correlation to provide the CBR values as indices. The 0.5-kg Clegg hammer provides a CBR value only for the upper layer of the soil based on hammer dynamic impact onto the soil surface, whereas the DCP is based on penetration resistance and provides CBR values as far down as 1 m (3 ft) below the surface. Because of low confining at the upper portion of the soil layer, the DCP CBR values for the 0- to 0.15-m (0- to 6-in.) depths can be questionable. However, DCP is the standard tool for measuring soil strength by AFCESA for airfield design and evaluation. The CBR profiles of the weak areas on the OLS determine the suitability for specific aircraft and number of passes.

The typical process for evaluating a contingency airfield using the AFCESA is breaking a CBR profile in layers, because an existing runway normally consists of various subsurface structures (i.e., base, subbase, subgrade).

The same procedure was applied to the selected DCP profiles in order to determine the various layers of CBR values on the OLS for natural soils. Figures 46, 47, and 48 are actual CBR profiles along with the average CBR values defining the layers for IOP #1, IOP #2, and IOP #3, respectively. These CBR profiles are representative of the weak areas on the RAS as indicated by low CBR values. The distributions of low CBR values are of limited extent spatially and some of these locations are along the center line of the RAS. Most low strength layers are located in the upper portion of the soil layers with depth ranging from 50 to 600 mm. At least one DCP profile during IOP #1 (in July 2005) contained a CBR value of one from the surface down to a depth of 450 mm for sampling location 6+30 2S (Fig. 46). Several CBR profiles at El Centro RAS showed low soil strength in the upper portion, then the CBR increased with depth, for example 2+20 CL (Fig. 46). In some locations, the strength was mostly uniform, with a small soft layer (Fig. 47 and 48).

Table 13 summarizes the distribution of CBR values based on number of DCP profiles and 0.5-kg Clegg measurements for all IOPs. The CBR for 0- to 0.15-m (0- to 6-in.) depths was excluded in the analysis because of the lack of confinement at the top of the surface layer that affects the DCP measurements, and assumed that the CBR for the surface is equal to the CBR at 0.15- to 0.3-m depth. To evaluate the loading capacity of the RAS, the analysis was based on the DCP profiles of minimum (Fig. 49a) and 15th percentile of minimum CBR values (Fig. 49) for 0.15-m (6 in.) incremental layers. For design, it is common practice to take the representative CBR profile by obtaining the 15th percentile of the minimum CBR values from all the DCP data collected in the test area. The 15th percentile of the minimum CBR profiles at the SI-RAS shows low CBR on the surface, then slight increase in CBR with depth down to 0.45 m, and also uniform at deeper depths (Fig. 49b). The fall (IOP #2) CBR values for the surface down to 0.3 are lower than summer (IOP #1) and spring (IOP #3). Strength for the surface layer from the DCP showed that only 11%, 31%, and 4% of the DCP data on the SI-RAS have CBR values of 2 or less for the summer, fall, and spring seasons, respectively (Fig. 49c). Considerable amounts of DCP measurements on the SI-RAS have CBR values of 5 or less for the surface; however, the values significantly decrease with depth (Fig. 49d).
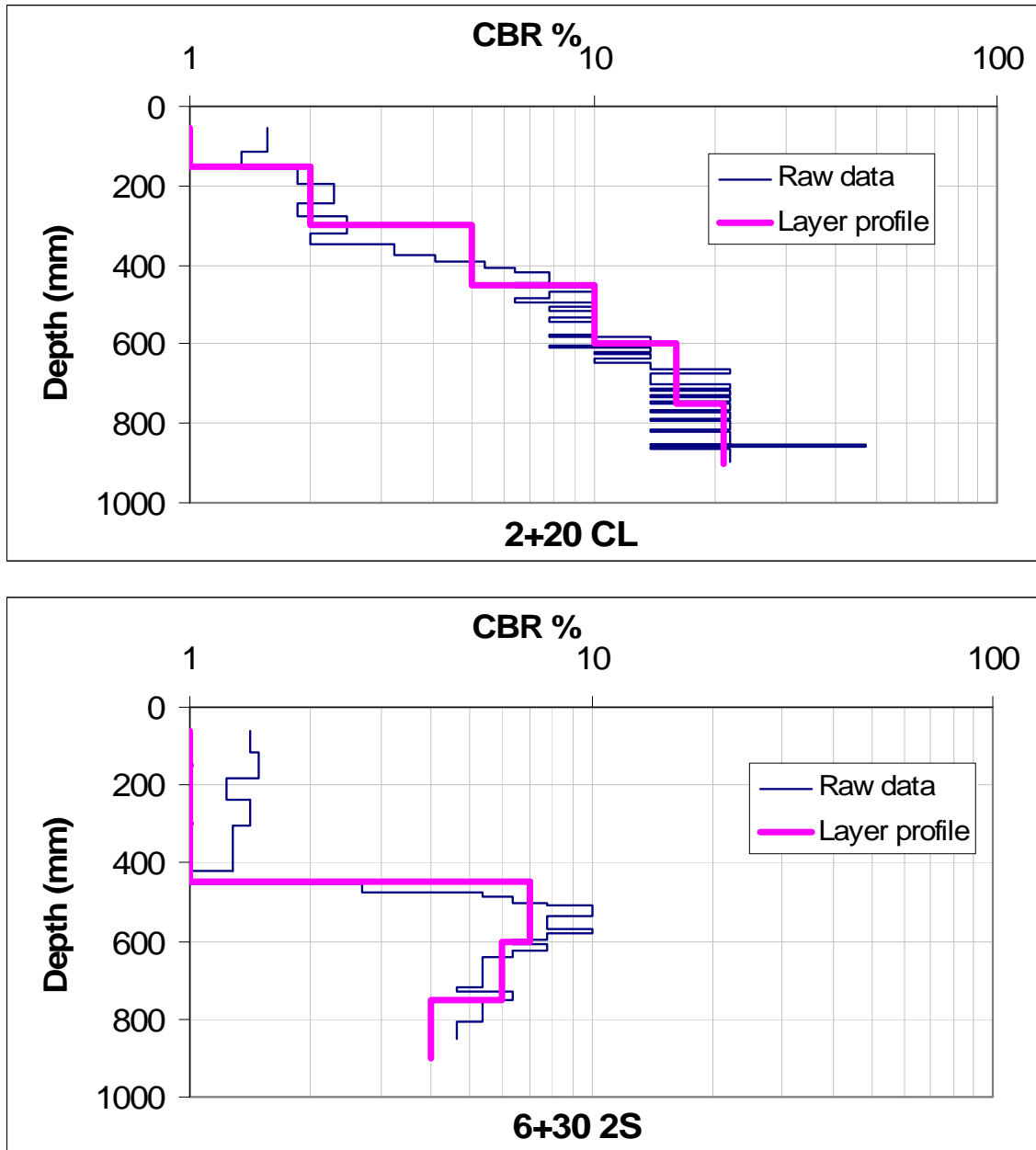
Figure 46. Selected CBR profiles showing layers with weak soil strength (IOP #1 at the El Centro RAS).
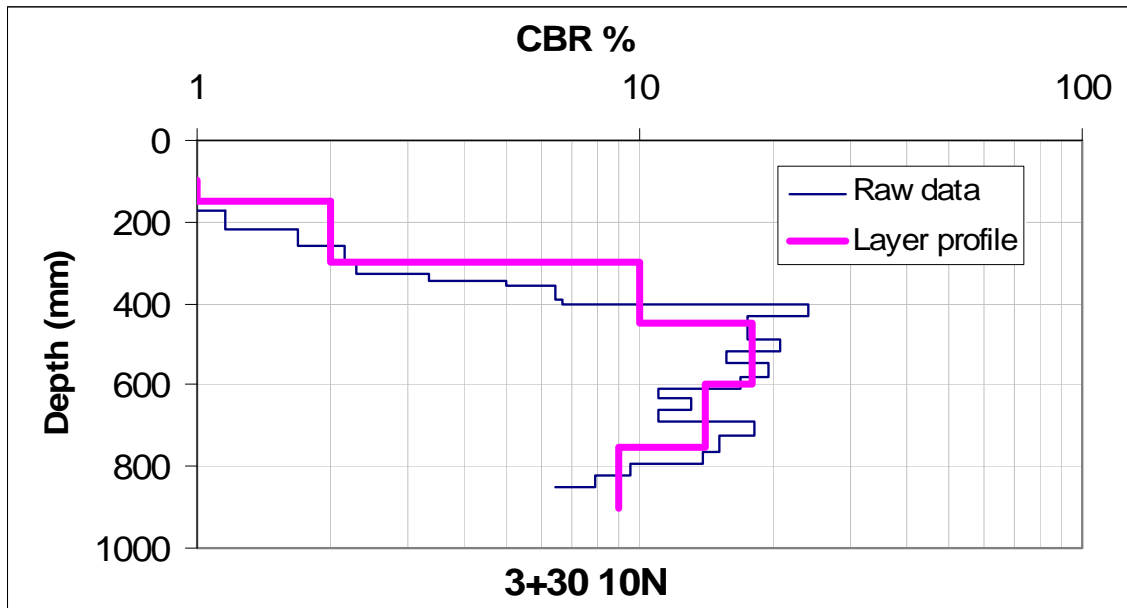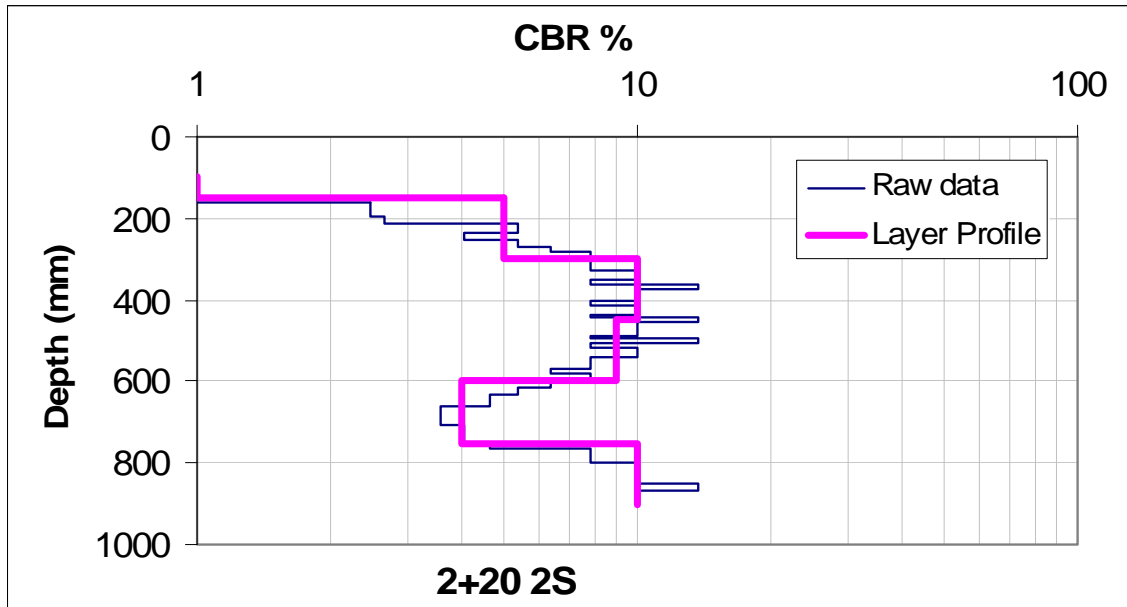
Figure 47. Selected CBR profiles showing layers with weak soil strength (IOP #2 at the El Centro RAS).
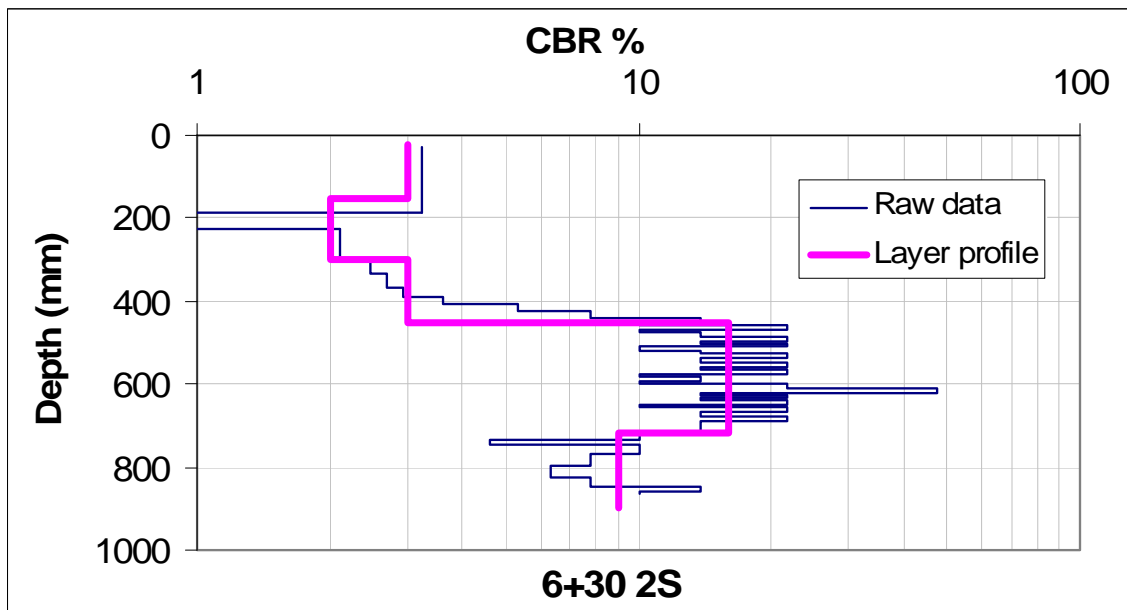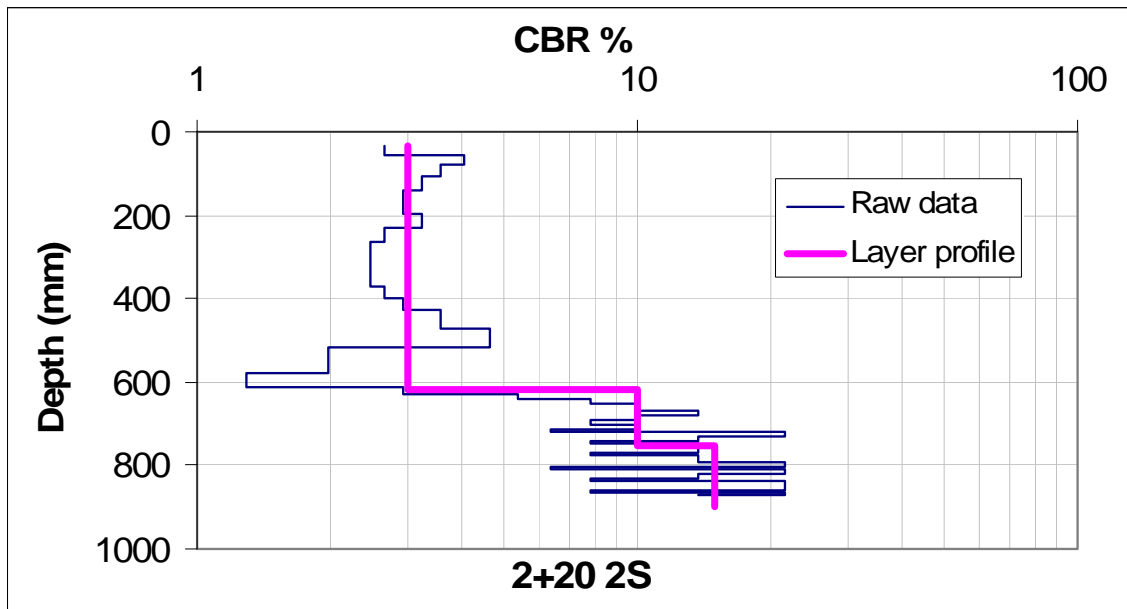
Figure 48. Selected CBR profiles showing layers with weak soil strength taken during IOP #3 at the El Centro RAS.

Table 13. CBR distribution calculated from the DCP profiles and CIH$_L$ (0.5-kg hammer) at El Centro RAS during all IOPs. Shaded numbers are CBR values less than 5.

Station	IOP#1, July 2005 Avg. CBR within 15 cm bins							IOP#1 Avg. CBR within 30 cm bins				IOP#2, October 2005 Avg. CBR within 15 cm bins						IOP#2 Avg. CBR within 30 cm bins			IOP#3, April 2006 Avg. CBR within 15 cm bins						IOP#3 Avg. CBR within 30 cm bins			CBR 0.5 kg Clegg Hammer		
	0-15	15-30	30-45	45-60	60-75	75-90	90-120	0-30	30-60	60-90	90-120	0-15	15-30	30-45	45-60	60-75	75-90	0-30	30-60	60-90	0-15	15-30	30-45	45-60	60-75	75-90	0-30	30-60	60-90	IOP#1	IOP#2	IOP#3
0+70 CL	10	21	37	26	31	40		17	32	33		2	3	40	31	31	39	3	35	34	4	16	35	28	34	34	13	32	34	4	2	7
0+70 20N	6	14	16	19	24	20		12	18	22											5	11	15	18	25	29	10	17	27	6	2	4
0+70 20S	3	6	19	14	11	5	6	5	17	8	6	2	5	7	14	18	11	4	10	16	3	6	13	16	10	4	5	15	9	5	1	6
1+40 CL	4	6	11	34	45	44		5	27	45		1	3	4	6	7	8	2	5	7	3	6	16	30	34	32	5	25	33	5	3	5
1+40 10N	3	6	13	19	24	34		5	17	30		1	1	2	4	17	27	1	3	23	3	4	10	16	19	23	4	13	20	5	2	5
1+40 10S	4	9	15	17	26	37		7	16	33		1	4	11	17	24	28	3	15	26	4	8	12	18	22	33	7	15	28	6	1	4
1+40 30N	10	19	22	21	28	35		17	21	32		1	2	2	2	3	2	2	2	2	2	8	10	13	12	14	7	12	13	6	2	4
1+40 30S	3	9	14	10	13	15		7	12	14		3	8	22	21	21	28	5	22	22										5	1	4
1+80 2N	20	26	12	11	35	46	22	24	11	42	22	29	38	17	16	40		35	16	40	5	30	41	37	37	43	26	39	40	4	1	4
1+80 2S	4	17	29	29	37	43	22	14	29	40	22	1	4	32	43	39	46	4	38	41	4	4	8	27	36	44	4	22	40	6	1	7
2+20 CL	1	2	5	10	16	21		2	8	19		1	6	12	11	22	21	6	11	22	3	2	5	9	17	15	3	8	16	3	2	7
2+20 2N	2	5	10	12	15	14		4	11	14		1	3	6	9	20	22	3	8	21	3	5	9	7	8	8	4	8	8	5	1	5
2+20 2S	2	5	5	5	10	17		4	5	14		1	5	10	9	4	10	5	9	8	3	3	3	3	10	15	3	3	13	4	1	6
2+20 20N	3	35	45	42	43	43		31	44	43		1	2	10	76	92	100	2	43	94	3	12	34	38	37	44	10	36	41	4	3	6
2+20 20S	1	2	3	5	7	10		2	4	9		0	1	4	7	15	18	1	5	15										4	1	4
2+60 2N	6	12	13	13	13	20		10	13	17		2	9	12	15	13	20	8	14	17	5	16	21	22	15	17	13	22	16	4	2	3
2+60 2S	4	7	11	7	6	12		6	10	10		4	8	12	12	12	8	7	12	10	2	5	8	10	8	10	4	9	9	5	1	4
3+00 CL	7	17	16	6	9	13		14	12	11		5	11	24	18	13	12	9	21	13	8	14	18	20	13	16	12	19	14	4	2	4
3+00 10N	4	6	8	5	3	5		5	7	4		1	2	10	18	14	9	2	14	12	3	4	5	4	8	6	4	5	7	6	2	7
3+00 10S	7	32	23	13	9	13		27	19	11		2	8	13	16	14	15	6	15	15										5	1	3
3+30 2N	15	13	9	8	9	8	8	14	9	9	8	7	13	13	11	10	11	11	12	10	16	16	15	15	14	8	16	15	12	4	1	3
3+30 2S	11	12	10	8	8	8		12	9	8		3	7	11	8	11	8	6	10	10	6	10	8	9	9	9	9	8	9	3	1	3
3+68 2S	4	7	34	41	34	36		6	38	35																						
3+68 7S	4	18	28	19	27	21		14	24	25																						
3+72 2S	20	36	43	44	46	42		31	44	44																						
3+74 2S	3	4	14	23	30	35	22	3	20	33	22																					
3+80 2N	10	25	29	19	27	36		21	24	32		3	10	28	25	37	37	8	26	37	11	18	15	8	25	34	16	12	29	4	1	3
3+80 2S	15	37	20	20	19	22	31	32	20	21	31	3	29	33	33	33	30	25	33	32	14	42	31	27	28	22	37	29	26	6	1	4
3+80 20N	1	2	4	11	7	10	5	2	9	9	5	1	3	6	13	17	13	3	10	16	4	5	11	13	13	26	5	12	21	6	1	6
3+80 20S	13	17	11	8	13	15		16	10	14		5	4	8	14	12	15	4	11	13	6	12	16	14	11	7	10	15	9	4	1	3
4+50 CL	15	30	16	14	12	17	14	25	15	15	14	4	5	9	11	12	15	5	10	13	6	13	12	12	11	22	11	12	17	4	1	3
4+50 10N	3	12	8	8	7	6		10	8	6		3	6	9	8	10	10	5	8	10	4	17	18	12	10	11	14	15	10	4	1	4
4+50 10S	3	8	10	8	4	6		7	9	5		1	6	9	9	6	8	5	9	7	3	17	12	8	12	7	14	10	11	3	2	4
4+50 30N	15	32	20	20	10	8		27	20	9		5	14	31	23	12	11	10	27	12	13	26	27	19	10	11	22	24	11	5	1	2
4+50 30S	2	8	10	9	11	13		7	9	12		3	5	28	8	9	13	4	18	11	9	15	13	11	9	9	13	12	9	3	1	3
5+20 2N	14	13	19	19	17	13		13	19	15		4	24	34	28	26	22	20	31	24	16	25	31	18	26	14	22	26	22	8	1	4
5+20 2S	12	25	15	14	14	10		20	14	12		5	12	17	17	26	35	9	17	30	9	22	23	24	6	12	18	24	9	6	1	6
5+20 20N	6	11	18	13	10	27		10	16	21		5	9	19	17	13	15	7	19	14	8	26	33	18	14	33	21	27	26	4	2	5
5+20 20S	9	11	8	10	18	16	6	10	9	17	6										7	14	13	15	19	23	12	14	22	5	2	6
5+70 2N	14	23	19	20	15	12	18	20	19	14	18	5	24	33	23	30	14	20	29	24	11	22	31	28	21	21	18	30	21	8	2	5
5+70 2S	7	11	16	19	14	10		10	18	13		5	10	30	36	22	17	9	33	20	11	23	37	33	28	20	19	35	25	6	2	6
6+00 CL	10	40	40	39	30	33		34	39	32		8	20	38	41	31	24	17	40	29	26	44	41	25	15	13	39	35	15	6	1	7
6+00 10N	10	22	23	20	21	23		19	22	22		7	31	35	19	14	14	18	27	14	9	22	26	22	18	16	18	24	17	5	1	4
6+00 10S	15	22	20	17	17	19		20	18	18		4	17	22	17	18	18	10	20	18	14	33	29	21	21	17	28	25	19	5	1	3
6+00 30N	1	7	6	10	7	11		7	8	9		1	5	8	13	9	7	4	11	9	5	6	9	11	12	12	6	10	12	4	1	3
6+00 30S	8	17	10	4	4	27		14	9	23		2	6	15	10	23	35	5	13	27	12	16	14	13	10	22	14	14	18	6	1	1
6+30 2N	3	10	20	26	23	10		8	23	19											5	18	21	14	39	25	15	18	34	6	2	6
6+30 2S	1	1	1	7	6	4		1	7	5											3	2	6	16	18	9	2	13	15	3	1	6
6+80 2N	15	19	10	14	15	22		17	12	19											17	26	18	19	18	16	23	18	17	6	2	4
6+80 2S	3	19	17	5	7	9		16	13	8											6	26	23	9	8	15	22	19	13	4	1	4

|																																
6+80 20N	5	17	19	22	15	20		14	20	18		3	18	26	30	41	40	12	29	40	5	10	17	30	30	32	9	25	31	7	1	6
6+80 20S	6	31	32	15	16	17		27	26	17		5	28	46	22	17	20	18	37	18	7	33	44	37	27	18	28	41	24	5	1	5
7+50 CL	9	38	44	31	17	33		34	39	27		3	27	42	39	28	31	24	41	29	7	31	33	15	11	22	27	26	18	3	2	5
7+50 10N	11	31	44	36	30	34		26	41	32		4	15	46	45	34	33	12	46	33	8	31	40	31	31	26	26	36	29	5	1	4
7+50 10S	4	28	38	24	15	10	6	25	32	13	6	3	14	42	17	10	6	9	31	8	14	26	37	23	11	9	22	32	10	4	2	3
7+50 30N	11	42	34	20	26	27		36	29	26		3	7	26	25	26	32	5	26	27	5	22	33	19	24	26	18	27	25	4	1	2
7+50 30S	14	35	30	15	24	30	47	30	24	27	47	12	35	40	19	17	20	30	32	19	8	14	12	13	11	15	12	13	13	3	1	7
8+20 2N	27	41	23	18	23	23		37	21	23		8	32	24	21	19	14	27	23	17	17	33	31	19	16	11	28	26	15	10	1	10
8+20 2S	27	42	38	29	30	18		37	34	25		24	35	15	18	20	13	32	17	18	32	38	29	22	24	24	36	26	24	5	1	3
8+20 20N	15	17	12	9	11	9	11	16	11	10	11	4	10	22	15	12	10	8	19	11	13	26	39	39	21	19	22	39	20	6	1	5
8+20 20S	13	23	23	14	17	16	22	20	19	16	22	10	33	34	23	20	20	20	28	20	20	30	29	17	13	12	26	24	12	4	2	3
8+70 2N	11	13	13	14	9	18	10	12	14	15	10	5	14	13	16	13	18	12	15	15	6	6	5	10	11	22	6	8	17	6	2	6
8+70 2S	5	9	12	9	9	10		7	11	10		4	11	13	11	10	13	9	12	12	4	11	16	14	11	16	9	15	14	8	2	7
9+00 CL	6	8	9	11	25	25		7	10	25		2	6	8	13	34	41	5	11	37	6	7	11	21	27	24	6	17	26	6	1	6
9+00 10N	7	6	8	6	7	13		6	7	10		1	21	7	7	17	24	15	7	20	4	6	9	15	15	12	5	13	14	6	1	5
9+00 10S	11	28	20	10	7	9		23	17	8		10	37	26	17	11	12	21	21	12	6	26	27	21	12	10	21	24	11	5	1	4
9+20 2N	15	17	7	7	7	7		16	7	7		6	9	8	8	7	6	8	8	7	9	10	9	9	8	10	10	9	9	6	2	6
9+20 2S	10	14	8	6	8	6		13	7	7		1	8	9	7	8	7	7	8	7	10	20	24	10	10	11	17	19	10	7	3	6
9+80 CL	28	38	15	11	17	16	8	36	13	16	8	7	31	15	15	17	16	17	15	17	13	29	21	26	23	20	24	24	22	8	3	8
9+80 2N	17	23	13	11	11	11		21	12	11		15	46	18	10	8	12	29	13	9	19	41	28	26	13	12	34	27	12	5	2	4
9+80 2S	33	45	27	6	8	8		41	21	8		14	53	16	16	19	23	32	16	21	22	37	32	13	21	21	33	26	21	6	1	4
9+80 20N	2	7	10	12	14	14		6	11	14		5	16	22	19	20	23	11	21	21	3	14	17	19	17	14	13	18	16	4	1	3
9+80 20S	10	17	32	16	40	43		14	26	42											10	22	22	24	35	42	18	23	39	6	1	8
10+20 2N	6	17	21	12	18	15	5	14	17	17	5	8	25	24	14	12	14	16	19	13	6	23	29	20	14	16	19	25	15	6	2	4
10+20 2S	4	9	18	13	11	11	18	8	16	11	18	3	15	29	21	24	23	10	26	24	6	17	29	18	10	12	14	24	11	7	1	3
10+60 CL	9	35	20	13	12	9		29	17	10		6	22	16	9	8	9	14	12	9	11	20	23	22	17	22	16	23	19	7	1	8
10+60 30N	7	9	9	7	7	14		9	8	12		7	31	26	23	24	26	18	25	24	28	37	28	27	21	17	33	28	19	5	1	3
10+60 30S	28	33	13	13	28	34	18	31	13	32	18	13	37	31	16	23	33	32	25	28	7	17	15	10	13	16	14	13	15	7	1	6
11+25 CL	5	21	13	17	5	4	5	17	15	4	5	3	17	15	5	2	10	12	9	7	7	30	27	11	1	5	25	24	4	4	1	8
11+25 20N	6	17	3	4	5	9		14	3	8		4	6	2	5	9		5	4	9	2	10	3	7	6	5	8	6	5	5	1	4
11+25 20S	38	29	12	8	8	18		34	11	15		15	1	0	5	8	7	12	4	8	22	20	13	9	8	7	21	12	8	6	2	4
Total Count	81	81	81	81	81	81	20	81	81	81	20	70	70	70	70	70	68	70	70	70	74	74	74	74	74	74	74	74	74	77	77	76
Minimum	1	1	1	4	3	4	5	1	3	4	5	0	1	0	2	2	2	1	2	2	2	2	3	3	1	4	2	3	4	3	1	2
Maximum	38	45	45	44	46	46	47	41	44	45	47	29	53	46	76	92	100	35	46	94	32	44	44	39	39	44	39	41	41	10	3	10
15th percentile of Minimum	3	7	8	7	7	9	6	6	9	8	6	1	4	8	8	9	9	4	9	9	3	6	9	10	10	9	5	11	9	4	1	3
% w/ CBR <= 10	59	31	26	32	31	23	40	35	26	25	40	90	47	27	26	21	24	59	24	20	69	24	19	19	18	22	31	14	16	100	100	100
% w/ CBR <= 5	36	9	7	7	6	5	15	14	4	5	15	74	26	9	7	4	1	34	9	1	38	12	5	3	1	4	16	3	3	53	100	64
% w/ CBR <= 2	11	5	1	0	0	0	0	5	0	0	0	31	9	6	1	1	1	9	1	1	4	3	0	0	1	0	1	0	0	0	95	3

Although the 0.5-kg Clegg hammer CBR values do not match with DCP data, the distribution of the Clegg CBR data show similar seasonal trends, i.e., weaker soil surface during the rainy season of IOP #2. Because the 0.5-kg Clegg hammer is not commonly used, further assessment and correlations are suggested between these instruments, including sensitivity analysis for additional soil types and conditions.

The influence of soil moisture in the fall season (October 2005) showed a significant decrease in surface soil strength as discerned from the DCP (Fig. 49), Clegg hammer, and Drop cone data. The DCP data show decreased strength of deeper layers during IOP #2. Total precipitation observed during the period was 29 mm, all immediately prior to IOP #2.

Applying the PCASE program (version 2.08) using the evaluation module for unsurfaced runway on subgrade soils, the results showed only one pass is allowed with varying allowable loads for C-17 using the 15th percentile of minimum CBR profiles. The C-130 is able to land on the RAS up to 48 passes with 62 ton (137 kips) of allowable gross load during summer, 42 tons (93 kips) of allowable gross load during fall, and up to 19 passes with 58 tons (127 kips) of gross load during spring using the 15th percentile of minimum CBR values (Table 14). This analysis was based on CBR profiles for 0.15-m (6-in.) incremental layers using profiles of minimum and 15th percentile of minimum CBR values from the DCP data during the three field visits as shown in Figures 49a and 49b.

The evaluation using the charts established in ETL 2002-19 (AFCESA 2002a) calculated different loading capacity and number of passes for C-17 and C-130 compared to the PCASE results. This analysis was based on 0.15-m (6-in.) thickness using the minimum and 15th percentile of CBR values. The loading capacity using the minimum CBR is outside the range of the charts for C-130 and C-17, therefore no values are reported (Table 14).

The weak areas with low percent CBRs are the controlling factor for determining w the runway is capable for aircraft traffic. The capability for aircraft landing operations on El Centro OLS can be summarized based on *estimated* CBR analysis as marginal for landing a C-130 during summer and spring but unacceptable during fall when rainfall occurred. The OLS cannot support the C-17 aircraft because of soil strength criteria.

Minimum CBR values

a. 15th percentile of the minimum CBR profiles.
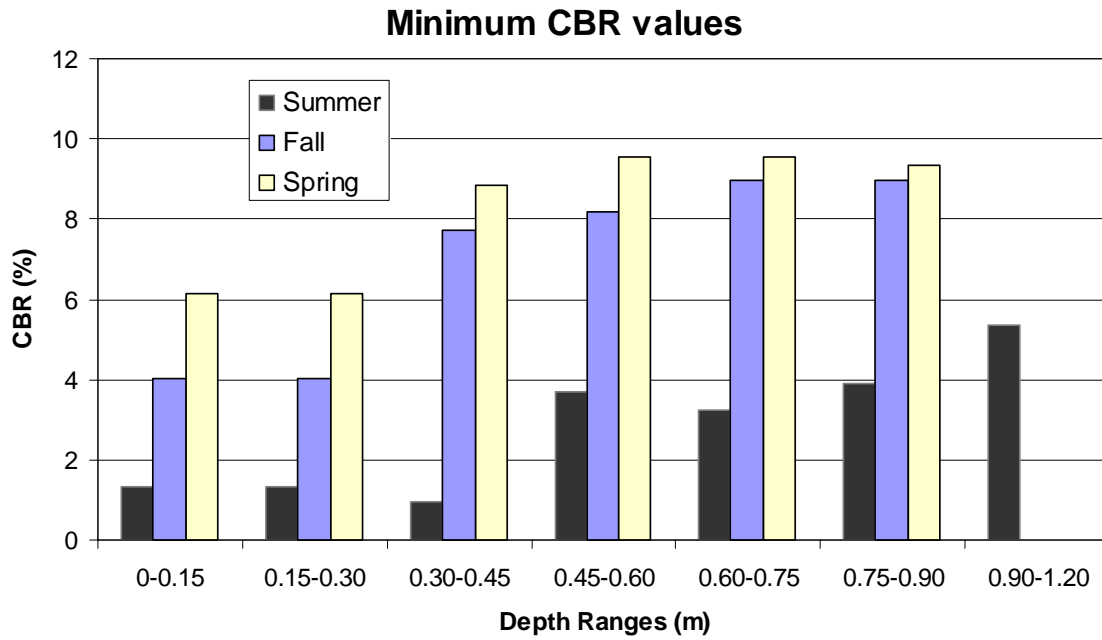
15th Percentile of Minimum CBR values
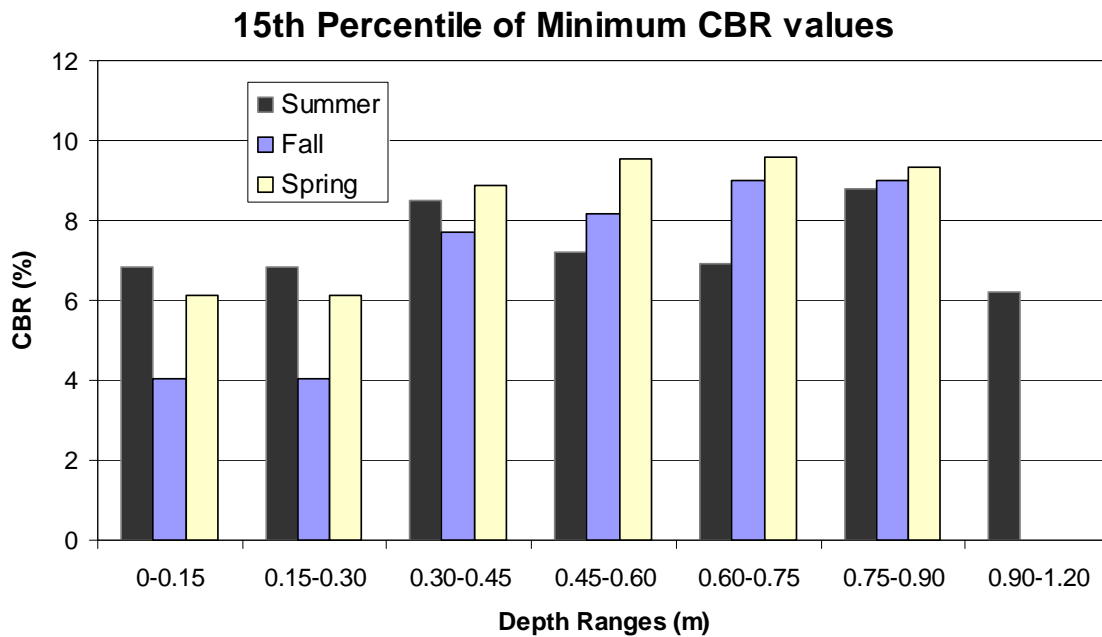
b. 15th percentile of the minimum CBR profiles.

Figure 49. CBR values at each depth range at SI-RAS.

Distribution (%) of CBR Values Less than or equal 2
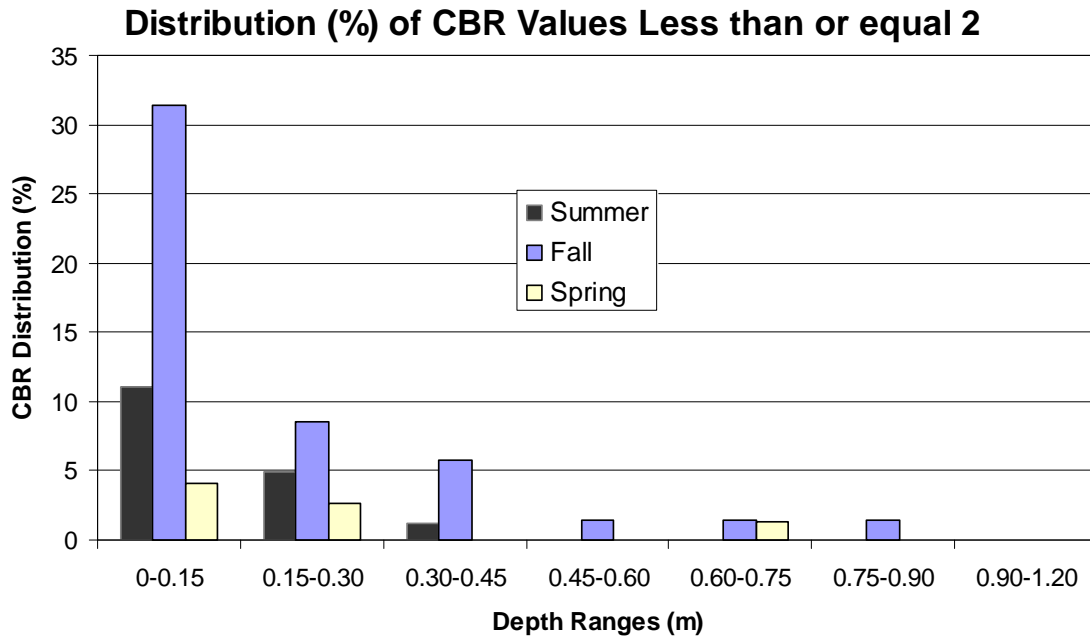
c. Amount of DCP measurements with CBR value of 2 or less.

Distribution (%) of CBR Values Less than or equal 5
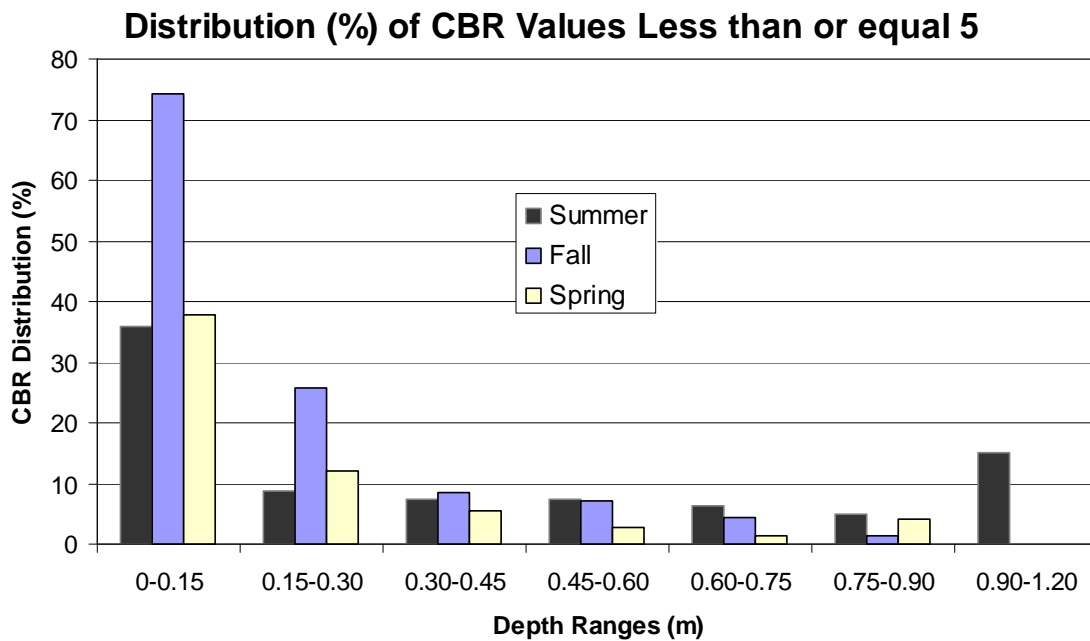
d. Amount of DCP measurements with CBR values equal or less than 5.

Figure 49 (cont'd). CBR values at each depth range at SI-RAS.

Table 14. PCASE loading capacity results for three seasons.

	Aircraft	Summer		Fall		Spring	
	Estimated CBR Values/Profile	Minimum	15th Percentile of Minimum	Minimum	15th Percentile of Minimum	Minimum	15th Percentile of Minimum
Charts (EIL 2002-19)	C-130 AGL, metric ton (kips) Number of Passes		79 (175) 70		68 (150) 10		70 (155) 60
Charts (EIL 2002-19)	C-17 AGL, metric ton (kips) Number of Passes		208 (460) 10		131 (290) 10		159 (350) 10
Analysis using PCASEE	C-130 AGL, metric ton (kips) Number of Passes	0.4 1	62 (137) 48	0.2 (0.4) 1	42 (93) 2	20 (45) 1	58 (127) 19
Analysis using PCASEE	C-17 AGL, metric ton (kips) Number of Passes	0 0	107 (236) 1	0 0	92 (202) 1	40 (88) 1	120 (265) 1
C17	Minimum weight = 126.6 metric ton (279,000 lb), maximum weight = 265 metric ton (585,000 lb)						
C130	Minimum weight = 31 metric ton (69,000 lb), maximum weight = 79 metric ton (175,000 lb)						
n/a	Outside the range of the chart						

6 Conditions at Precision Corrected Imagery Runway Assessment Site (PCI-RAS)

Shift on RAS location was found at El Centro as a result of georeferencing level of imagery. The runway location, as presented in Figure 50, appears to be visually shifted on the Earth's surface. However, the UTM coordinates have identical values when examined with GIS tools. Because of the variation in levels of geoprocessing between the Landsat imagery (systematic or basic level) and the Orthophoto (precision corrected imagery - high level), there are differences in the placement of runway locations. The coordinates of the several distinct features were obtained from the Landsat7 Systematic and the coordinates of the corresponding feature were also obtained from the Orthophoto. An average for the offset values representative of this area was computed based on the individual feature's values. The Precision Corrected Imagery Runway Assessment Site (PCI-RAS), white outlined in Figure 50, has easting and northing coordinates of 605454m, 3639122m and 604257m, 3639122m for east and west OLS end points, respectively. Coordinates are UTM Zone 11N projection, WGS 1984 datum. The RAS using precision corrected imagery (PCI-RAS) is shifted 172 m to the east and 291 m to the north. A verification survey was conducted at the PCI-RAS location.

A verification assessment was conducted on 26 and 27 July 2007 to examine the site to determine whether the surface features and soil characteristics are similar on both locations. The assessment was mainly to spot-check the PCI-RAS. Tests conducted included soil strength test (10 DCP profiles and 0.5-kg Clegg measurements), soil moisture using the HH2 instrument, soil type analysis, and a brief walk-through along the OLS.
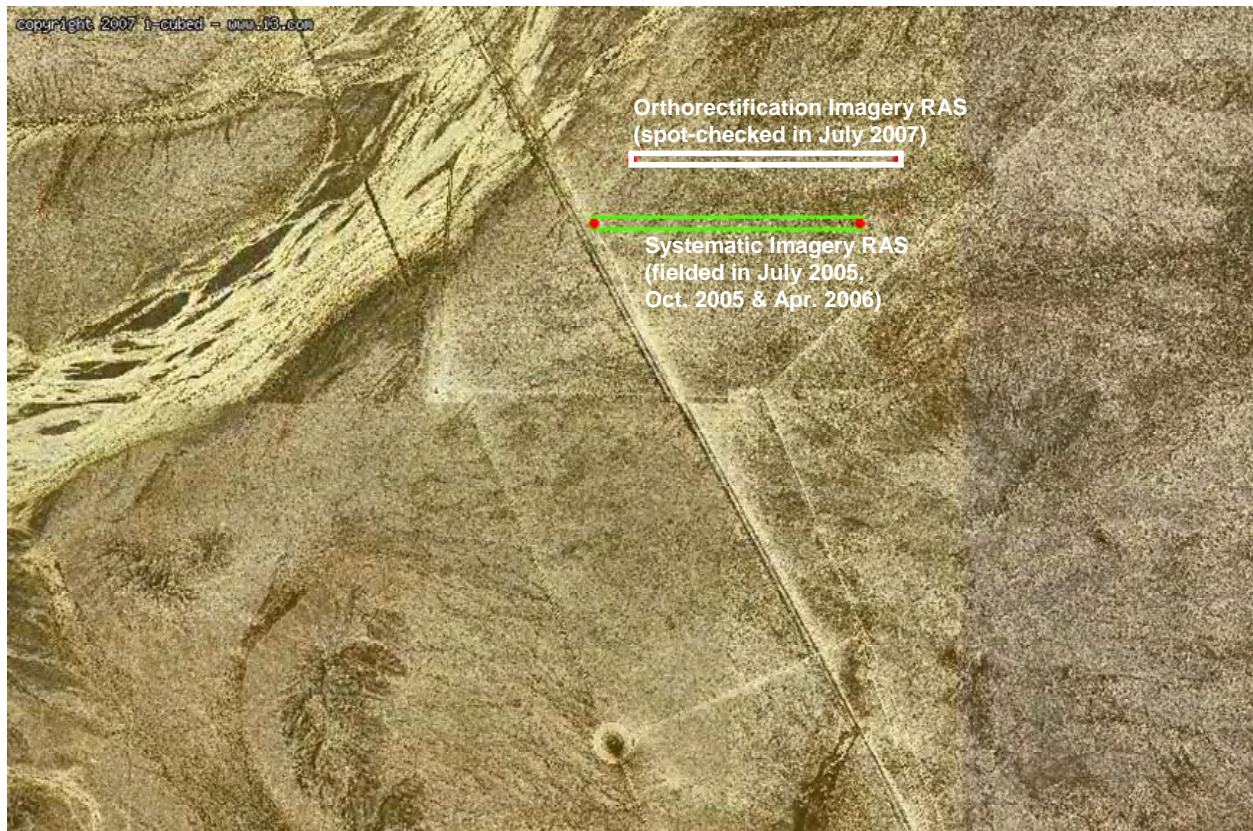
Figure 50. Shift on RAS location as a result of georectification level of imagery. El Centro RAS Precision Corrected Imagery (PCI-RAS) is shown in white and Systematic georeferenced (SI-RAS) in green. Field work was conducted at the SI-RAS and spot-check survey was conducted at the PCI-RAS (white box outline).

6.1 Precision-Corrected Imagery RAS (PCI-RAS) Surface Condition

Results from walk-through indicated that the PCI-RAS is relatively smoother than the SI-RAS. Figure 51 represents the view of RAS while the observer was standing 600 m west of the east end point of the PCI-RAS, which is relatively flat and smooth with very few mounds. The PCI-RAS has less pronounced mounds than the SI-RAS area, as shown in Figure 52a. The mounds ranged from 1.5 to 2.5 m (5 to 8 ft) across and approximately less than 0.15 m (0.5 ft) high. Animal burrows or holes are observed and are scattered on this area (Fig. 52b). Vehicle tire tracks are also found crossing the RAS (Fig. 52c). In most areas, the vegetation cover is very low and vegetation distribution and type are similar to the SI-RAS. Creosote bushes are spaced an estimated average of 7.5 m (25 ft) apart. Granular materials such as stones greater than 0.6 m (2 in.) are present in sections of the RAS (Fig. 52d); in slightly lower areas, stones are not so prevalent.

a. Looking north at 600 m west of the east end point of the PCI-RAS. DCP was conducted in the middle of the mounded area with animal hole.
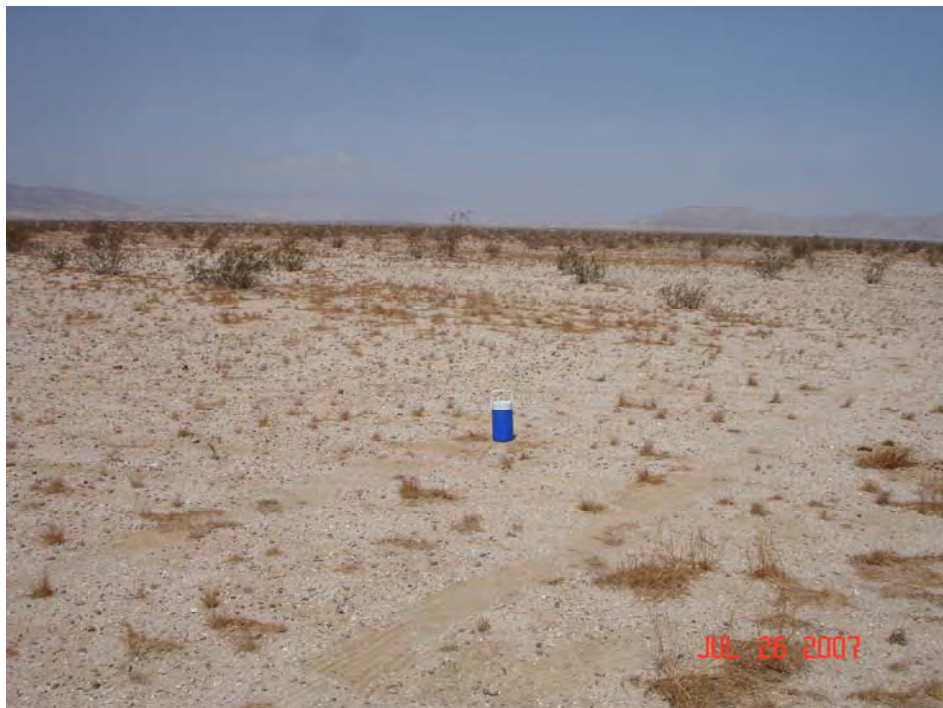
b. View looking west at 600 m west of the east end point of the PCI-RAS. Blue water jug is approximately 6 m (20 ft) away.

Figure 51. View at 600 m west from the east end point of the PCI-RAS displaying the RAS in various directions and distribution of vegetation cover on the area.
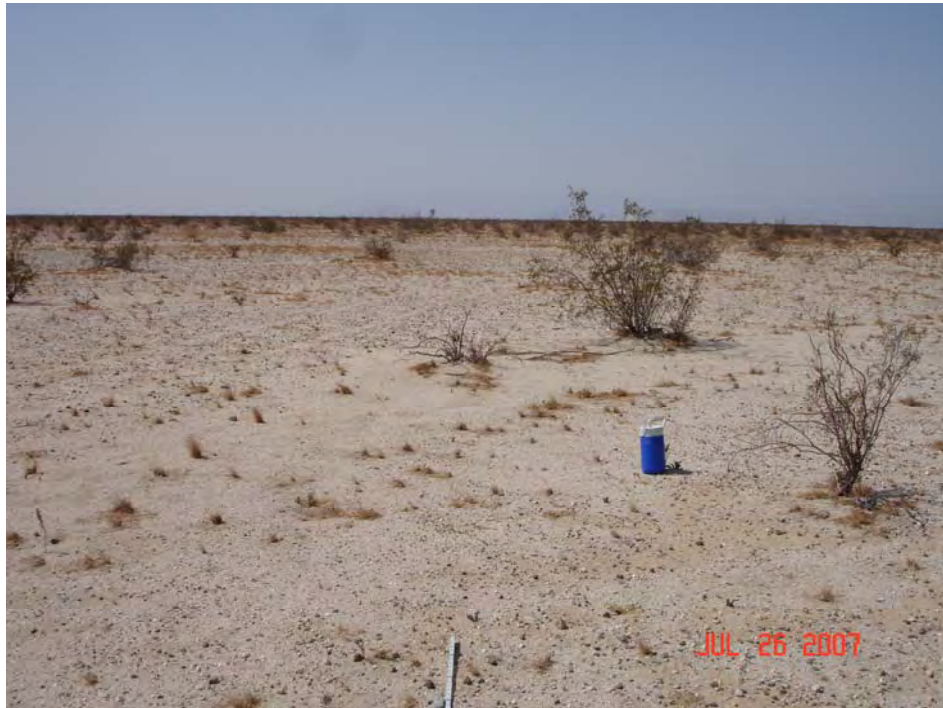
c. View looking south at 600 m west of the east end point of the PCI-RAS. Water jug is at approximate distance of 6 m.

d. View looking east at 600 m west of east end point of the PCI-RAS. Blue water jug is approximately 6 m (20 ft) away.

Figure 51 (cont'd).

a. Mounds on the OLS.

b. One of several animal holes observed on the PCI-RAS, showing a depression after a footstep.

Figure 52. Surface conditions observed on the PCI-RAS.

c. Existing tire tracks crossing the RAS.

d. Stones and gravel-size materials present in sections of the RAS.

Figure 52 (cont'd).

6.2 PCI-RAS Soil Information

Both OLSs are mapped on the NRCS soil data (e.g., SSURGO data) to determine whether the PCI-RAS have the same soil type. Figure 53 shows the similarity of the soils for both locations.

Soil samples were taken along the center of the PCI-RAS at 100 m, 500 m, 800 m, and 1000 m west of 605626E (Fig. 54). Samples were collected at the surface, 0.15-m (6-in.), and 0.3-m (12-in.) depths and were sent to a laboratory for grain size analysis. Figure 55 shows the grain size analysis for the soil samples taken at four locations along the center of the OLS. The soil type is primarily silty sand (SM) with a trace of gravel from the surface sample (at 500 m). The soil type on this RAS is the same as the SI-RAS.
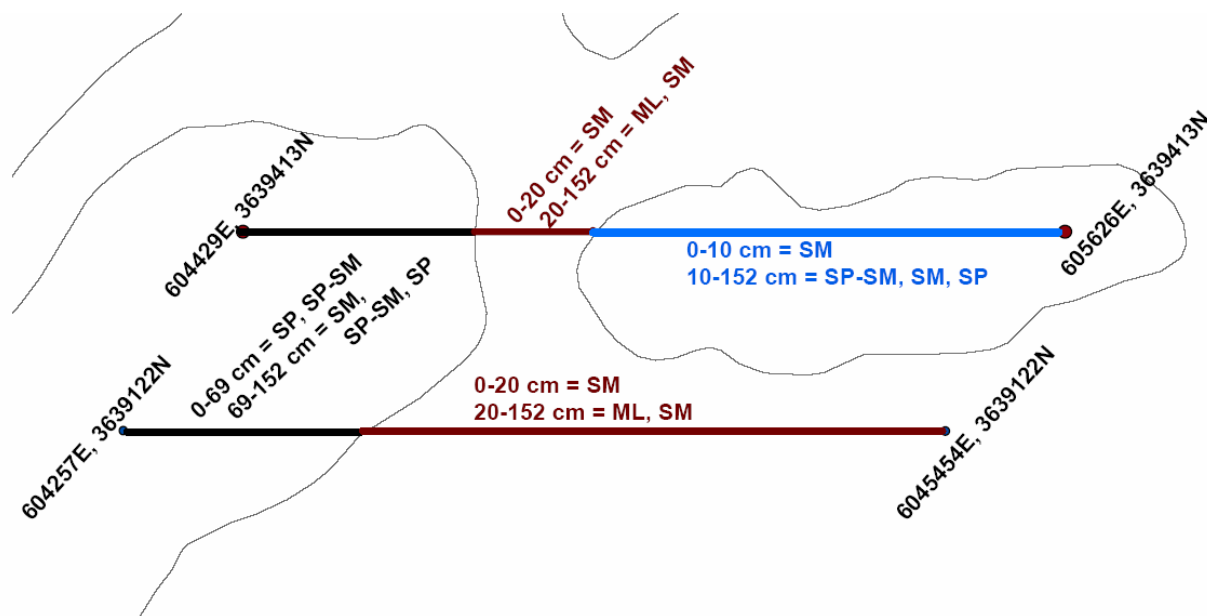
Figure 53. Soil type information from SSURGO data.

Soil sample collection at 800 m west

Soil profile at 800 m west

Soil profile at 500 m west

Soil profile at 1000 m west

Figure 54. Soil profiles taken along the center of the PCI-RAS.
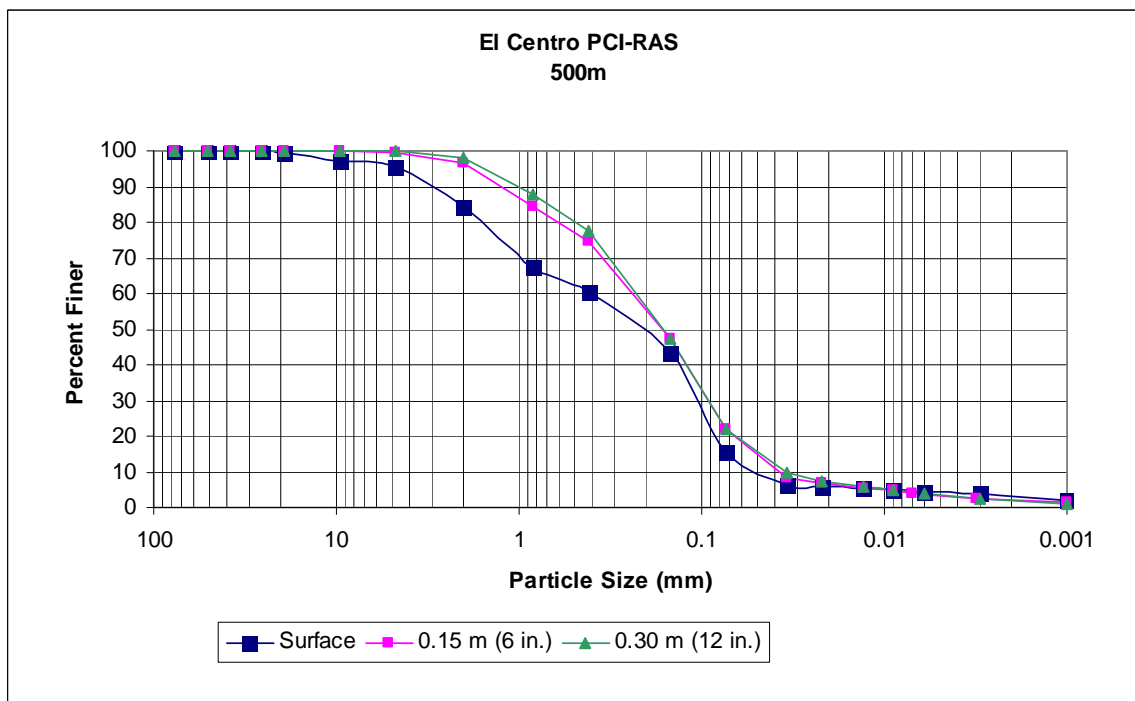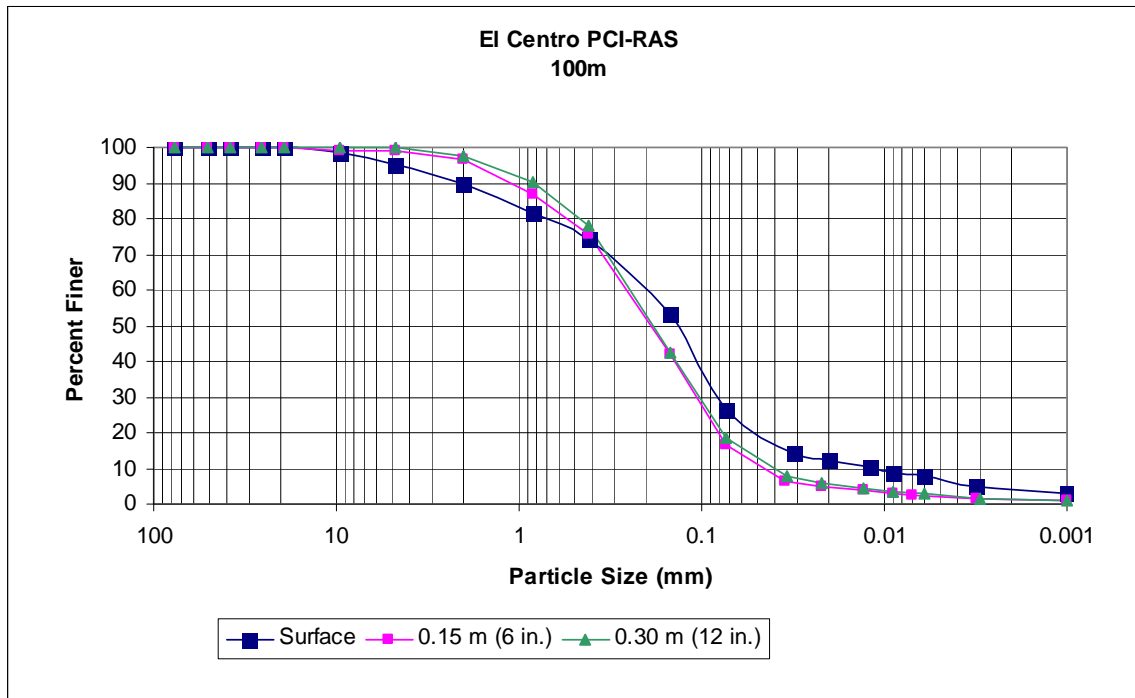
Figure 55. Gradation charts for soil samples taken at the PCI-RAS.
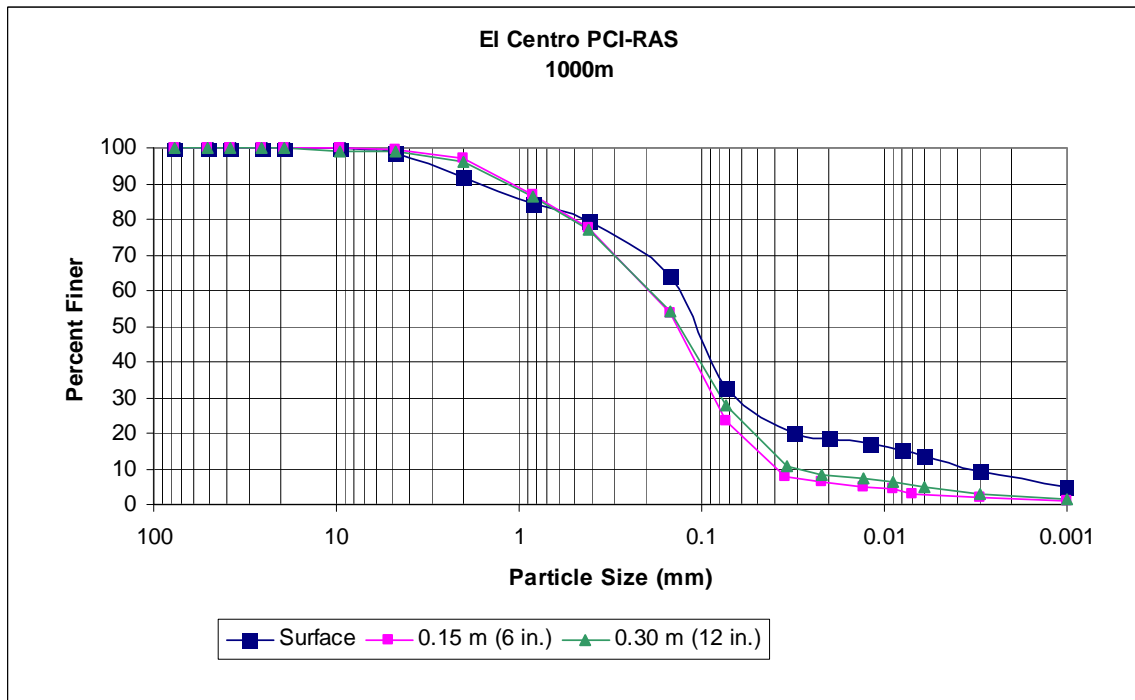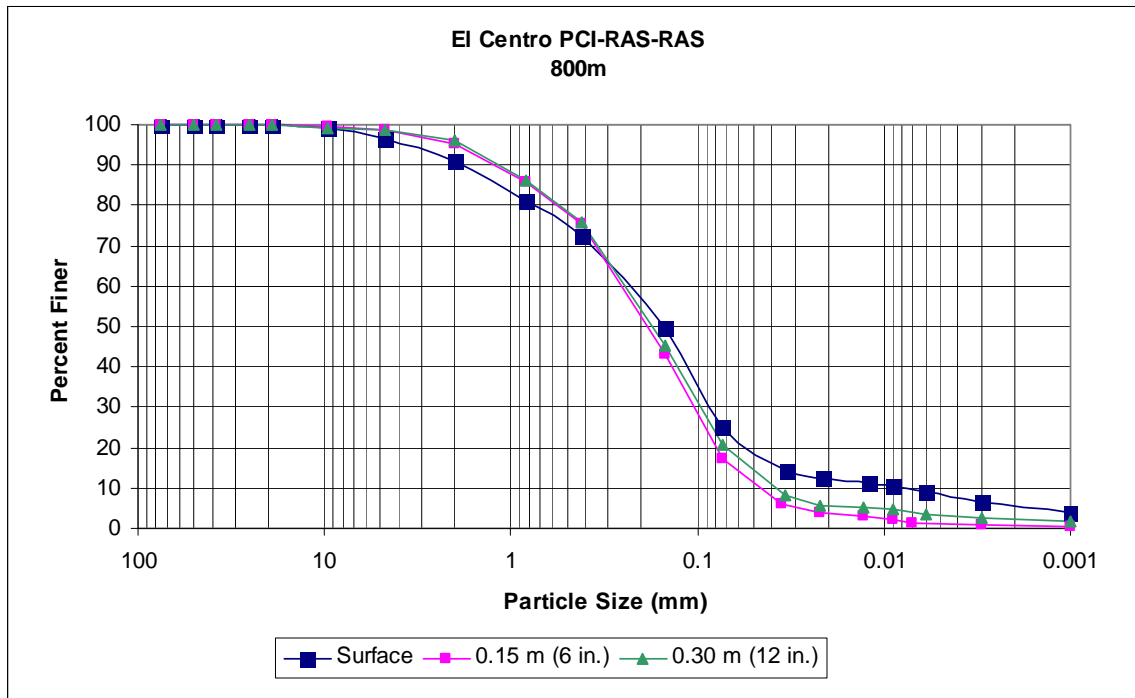
Figure 55 (cont'd).

6.3 PCI-RAS Soil Moisture

Soil moistures are measured using the Dynamax HH2 instrument at three locations. The moistures ranged from 3.7 to 5.4% volume at the surface

and 2.9 to 8.1% volume at 0.3-m (12-in.) depth (Fig. 56). This soil moisture profile is a typical measurement in the summer for the area.
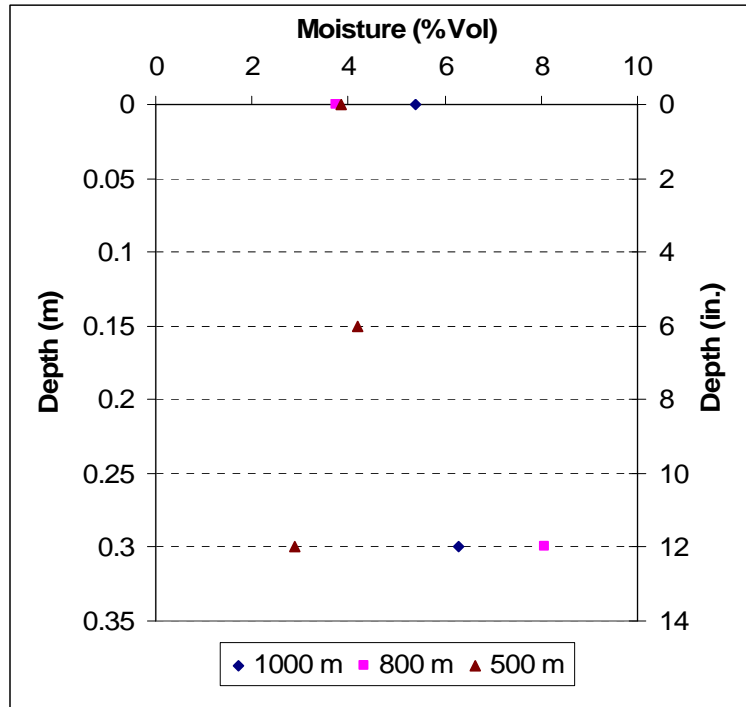
Figure 56. Soil moisture profiles at the PCI-RAS.

6.4 PCI-RAS Soil Strength

DCP is conducted at 10 locations along the PCI-RAS. The DCP are converted to CBR and are summarized in Table 15. A few of the measurements are taken in the middle of the animal burrow areas (i.e., 600, 5.5m N; 700, 8m S; 850, 6m N). The CBR profiles in the animal burrows are lower than in other areas in the RAS. Aside from having a low surface CBR value in the surface, the soil strength increased with depth in most areas of the RAS. Figure 57 represents the CBR profiles from 10 DCP measurements along the soil strength minimum and maximum layers.

Table 15. Summary of CBR values measured at the PCI-RAS.

Location along the RAS	Average CBR within 15 cm bins							Average CBR within 30 cm bins			
Distance in Meters West of 605626E											
	0-15	15-30	30-45	45-60	60-75	75-90	90-120	0-30	30-60	60-90	90-120
100	5	34	54	71	46	35		24	63	40	
300	9	37	43	35	34	23		26	40	29	
500	10	13	17	17	18	26		11	17	22	
600, 5.5m N	1	2	1	6	18	57	44	2	5	37	44
700	3	17	31	27	26	20		12	29	23	
700, 8m S	3	5	7	11	6	11		4	9	9	
800	4	31	42	19	21	25		22	29	23	
850, 6m N	0	4	8	7	14	59	44	4	7	38	44
1000	8	18	40	53	75	90	62	14	47	82	62
1100	11	26	38	48	38	29		18	43	34	
Minimum	0	2	1	6	6	11		2	5	9	44
Maximum	10	37	54	71	46	59		26	63	40	44
15th %percentile of Minimum	2	4	7	7	15	20		4	7	22	44
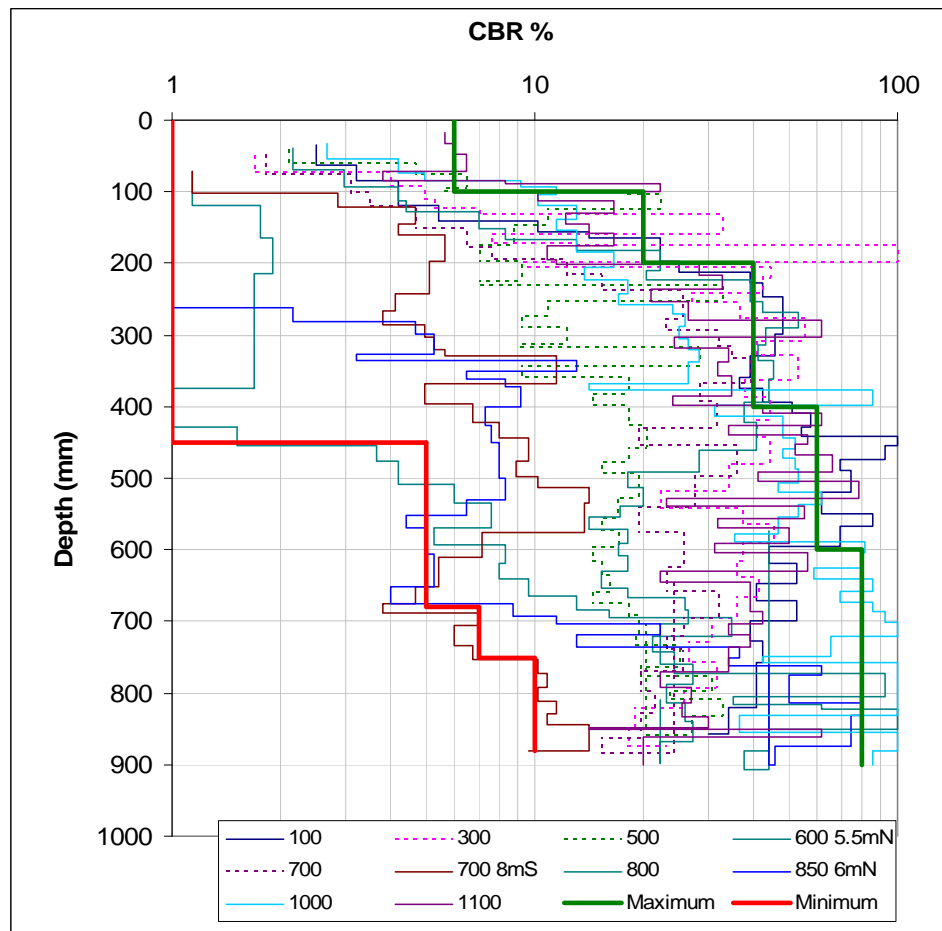
Figure 57. CBR profiles from the raw data measured along the RAS with minimum and maximum ranges.

The 0.5-kg Clegg hammer is used to measure the surface soil strength at 10 locations along the RAS. The Clegg CBR values ranged from 2 to 5% as shown in Figure 58. These are similar to typical values measured on the SI-RAS during the dry season.

0.5 kg Clegg CBR, El Centro Correct RAS Location
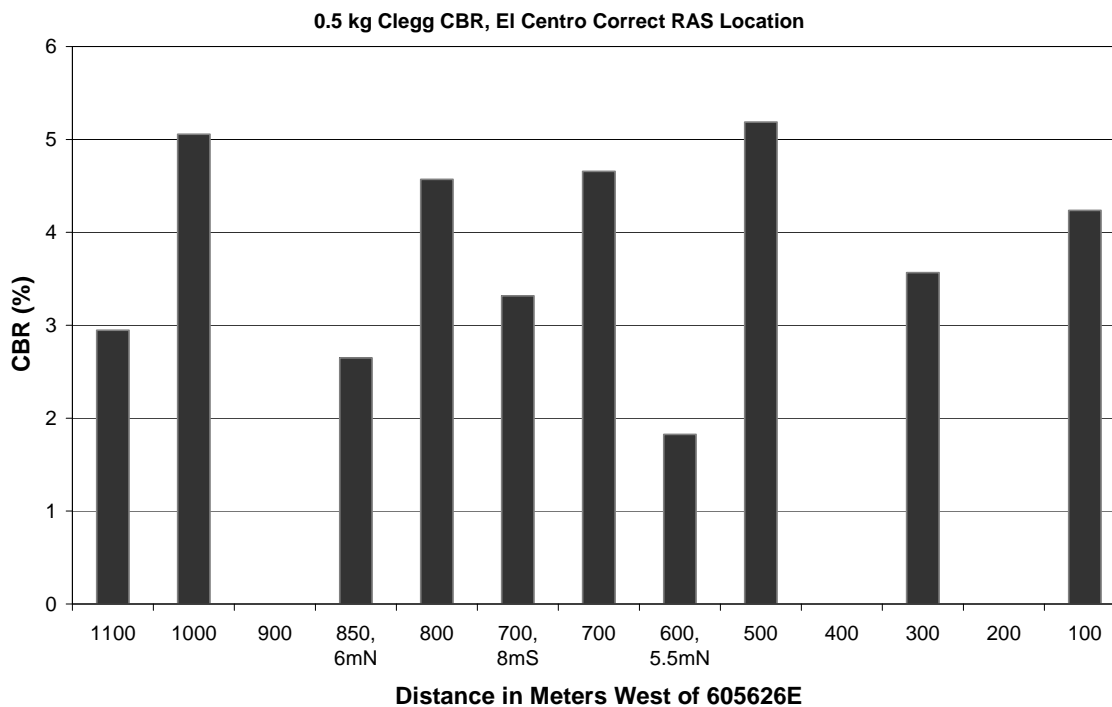
Figure 58. Clegg CBR values along the PCI-RAS.

6.5 PCI-RAS Summary

From the brief site assessment and analysis of the PCI-RAS, the OLS is considered to be smoother than the SI-RAS. The PCI-RAS is rated "Excellent" for both its geometry properties and surface characteristics.

Using the PCASE evaluation module for unsurfaced runway on subgrade material layers, the results showed allowable loads of 56 and 53 tons (125 and 118 kips) with two and one pass for both C-130 and C-17 (Table 16). This analysis uses the 15th percentile of minimum CBR profiles from the DCP measurements taken during this brief visit on 26 and 27 July 2007.

Table 16. PCASE loading capacity results for three seasons.

Aircraft	Summer Condition
C-130 AGL, metric ton (kips) Number of Passes	56 (125) 2
C-17 AGL, metric ton (kips) Number of Passes	53 (118) 1

7   OLS Software Seasonal Analysis

A goal of the OLS program was to determine the ability of the software to locate smooth, flat, and obstruction-free landing sites seasonally. There are two components of the seasonal concept. One involves identifying a season when the most OLSs are available and using that information to create a strategic OLS inventory. The second concept involves assessing the seasonal capability of the OLS software to consistently accept or reject OLS areas as acceptable.

The first concept involves using a Landsat image taken at a location during one season to locate OLSs, and then determining whether the OLSs found during that season are valid for all seasons. The OLS inventory created from such a search may be of strategic value, but the utility of such a list is dependent on the number of OLSs found at similar locations each season, and changes in land cover being minimal over time. Tactically, the validity of such a list is also dependent upon daily weather changes affecting soil moisture, and therefore soil strength.

The second seasonal concept involves evaluating the ability of the software to locate successful OLSs on images regardless of the season. That is, the capability of the software may be seasonally dependent and may be more sensitive to some factors, affecting OLS quality in some seasons.

These seasonal concepts were evaluated using only the OLS software written to locate smooth, flat, and obstruction-free locations. Soil moisture and soil strength algorithms had not yet been integrated into the software for these evaluations. Soil strength alone could cause an OLS that is acceptable one season to be rejected during another, even if other factors did not change.

7.1 OLS Software Seasonal Consistency

Strategic utility of the OLS software is dependent on its ability to consistently select high-quality OLSs each season. This is a function of the software's accuracy each season and the seasonal consistency of the region.

One measure of seasonal OLS consistency may be considered as the number of OLSs that are mapped within a Landsat image each season. A con-

sistent number of OLSs between each season may suggest that the software is locating the same OLSs each season; however, the locations of OLSs within that image may be different. It would also be useful to know the proportion of OLS that are consistently located at the same place each season (and this should be done in the future).

After techniques demonstrated by Haren (2005, personal communication, WPAFB), while assessing the seasonal accuracy of the OLS software at each RAS, ERDC tabulated the number of OLSs located per season in each Landsat image. Figure 59 shows the number of OLSs located in Landsat images in southern California covering the El Centro NAF area in path 37, row 39, during the months of May, July, and November 2005, and April 2006 (Table 17). Two versions of the Boeing OLS software were assessed: Version 7 released 28 March 2005, and Version 10 released 12 March 2007 (Almassy and Blake 2005, 2007). Version 7 of the software was used to initially locate the RAS field sites, and Version 10 of the software is the last official software release in FY07.
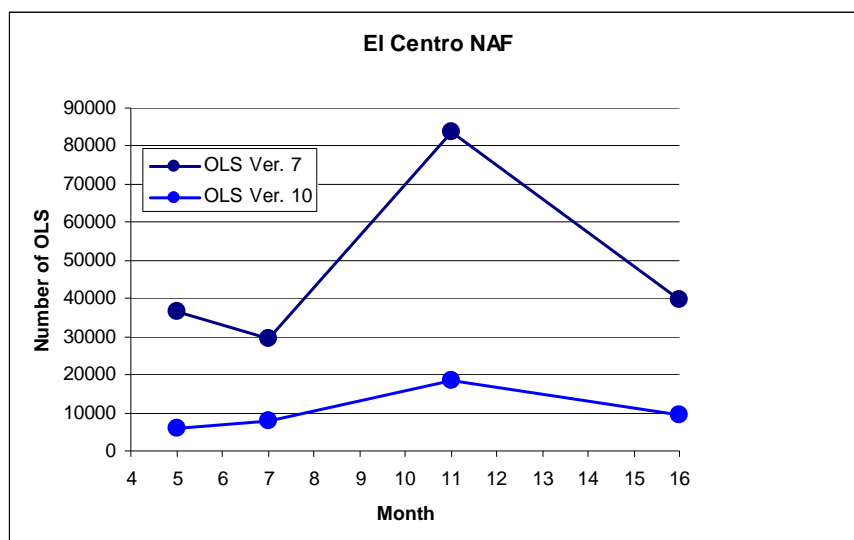
Figure 59. Number of OLSs located seasonally, by software version.

Figure 59 and Table 17 show that many more OLS are located by both versions of the software during the winter than during warmer months of the year. Though only three seasons are represented by the four points in time, they do show the general trends. Images analyzed by Haren (2005) in a preliminary analysis showed that the number of OLSs decreases as the greenness index threshold in the software is raised. That is, higher software-specified greenness index thresholds cause areas that are too green

to be omitted as candidate OLS locations. In effect, the same process is occurring seasonally. When the software is executed each season with the same greenness index threshold, areas that display a larger greenness index, especially during warmer and more moist months, will tend to be omitted as candidate OLS locations.

The variation in numbers of OLSs by season, ranging from 29,659 to 83,763 for software Version 7, and 6,030 to 18,610 for software Version 10, is an expression of seasonal variation in factors that affect the select-ability of OLSs by the software. At El Centro NAF it is not clear why these seasonal changes in OLS frequency have occurred. In an arid environment where moisture availability may drive greenness factors more than thermal and solar flux seasonal factors, reasons for larger numbers of OLSs located in November, for example, are not clear without additional analysis.

Table 17. Number of OLSs located seasonally by software.

Image	Date	V7	V10	Notes*
Row 39 Path 37	9 May 2005	36,504	6,030	No cloud
Row 39 Path 37	12 July 2005	29,659	7,872	No cloud
Row 39 Path 37	1 November 2005	83,763	18,610	No cloud
Row 39 Path 37	26 April 2006	39,824	9,352	No OLSs in cloud
* Comparisons were made only with Landsat images where OLSs were not plotted in clouds. OLSs can be plotted in clouds in OLS software V7; software V10 excludes cloudy areas for locating OLSs.				

We also assessed the frequency of OLSs plotted in the same location from season to season. The OLS software provides coordinates for the center point, and the compass orientation for each OLS. We used those coordinates and directions, and for every combination of seasons within each software version we compared OLS locations. Table 17 shows the number of OLSs compared each season.

The analysis found no occurrences of matching OLS coordinates between any season. However, this may not be a true indicator that OLSs are not located at the same location each season. Each Landsat image is unique with regard to its georegistration to the Earth's coordinate system. As a result, it is possible that any two pixels in similar relative positions in Landsat images taken in different seasons would have slightly different Earth-reference coordinates. Even the same image georeferenced to the

Earth by two different processes or individuals may produce slightly different Earth coordinates for any single pixel.

Therefore, there is still a possibility that OLSs may be located in nearly the same location for more than one season. Definitive demonstration of this will require overlaying of seasonal, georeferenced images within a geographic information system, a task not executed in this analysis.

7.2 OLS Software Seasonal Accuracy

Field work at the El Centro site was scheduled seasonally to assess the quality of OLSs with season. Field work was conducted in July 2005 (summer), November 2005 (fall), and April 2006 (spring). No winter field work was conducted. The field team assessed the quality of the selected OLS, or RAS, according to criteria listed in Table 4. Those criteria are scored as pass/fail according to measurements made in the field each season.

Version 7 and version 10 of the OLS software were used to plot the seasonal location of OLSs. Version 7 of the OLS software was used to locate the initial RAS field site. Software version 10 was the last official software version released in the OLS program, and it was assessed for that reason. The initial field site was located with a 9 May 2005 Landsat image. Figure 60 shows the location of the RAS where field work was conducted, in green. The 9 May 2005 Landsat image used to initially locate the RAS was georeferenced to the Earth's surface using only the satellite's ephemeris, called "Systematic" georeferencing by the USGS—the least accurate georeferencing method—which yielded the location shown in green. The blue OLS in Figure 60 is a more accurate location for the RAS because it was later located using a 9 May 2005 Landsat image that was "Precision" georeferenced to the Earth's surface. Subsequent discussion in this seasonal analysis refers to the blue RAS, except for the assessment of the seasonal quality of the OLS, which refers to the green RAS where all seasonal field work was conducted. The blue and green RASs are offset about 291 m north-south and 172 m east-west.
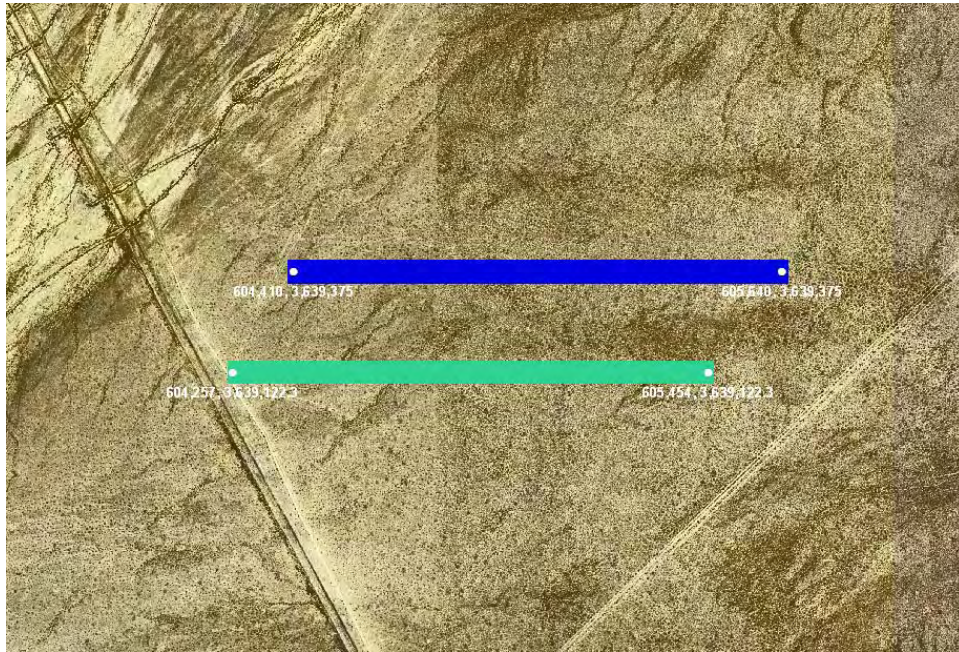
Figure 60. El Centro RAS Precision georeferenced in blue, and Systematic georeferenced in green. Field work was conducted at the green site, whereas seasonal comparisons assessing the location of other OLSs in the vicinity using OLS software Versions 7 and 10 refer to the blue OLS.

Figure 61. 9 May 2005 Landsat USGS Precision georeferenced image analyzed for OLSs with Version 7 of the OLS software. Blue OLSs are in Precision georeferenced positions. The unfilled yellow outline OLS is the RAS located site from the Systematic geoereferenced 9 May 2005 image. The filled yellow outline OLS is the field site as it should have been located from the Precision geoereferenced 9 May 2005 image.

Figure 62. 12 July 2005 Landsat USGS Precision georeferenced image with Version 7 OLS software. Blue OLSs are in Precision georeferenced positions. The unfilled yellow outline OLS is the RAS site located from the Systematic geoereferenced 9 May 2005 imageFilled yellow outline OLS is the field site as it should have been located from the Precision geoereferenced 9 May 2005 image.

Figure 63. 1 November 2005 USGS Precision georeferenced image with Version 7 OLS software. Blue OLSs are in Precision georeferenced positions. Unfilled yellow outline OLS is the RAS from the Systematic geoereferenced 9 May 2005. Filled yellow outline OLS is the field site as it should have been located from the Precision geoereferenced 9 May 2005 image.
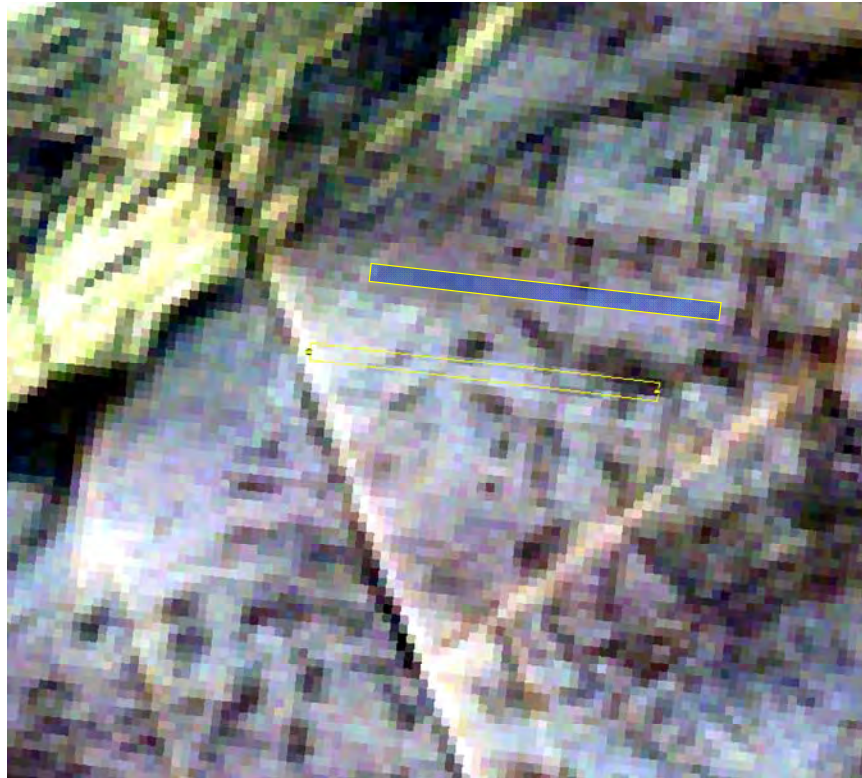
Figure 64. 26 April 2006 USGS Precision georeferenced image with Version 7 OLS software. Blue OLSs are in Precision georeferenced positions. Unfilled yellow outline OLS is the RAS site from the Systematic georeferenced 9 May 2005. Filled yellow outline OLS is the field site as it should have been located from the Precision georeferenced 9 May 2005 image.

The 9 April 2005 Landsat scene used to initially locate the El Centro OLS field site, the RAS, shows the location of the field site, and a nearby OLS west of the road and railroad running from southeast to northwest (Fig. 61). The 12 July 2005 summer image shows more OLSs plotted in the vicinity of the field site. The field site OLSs were not plotted by the software on Figure 62, but are located in Figure 62 only for reference. OLSs were located at the same location as in May, but on the west side of the railroad tracks, in addition to several more further west and immediately south. In July, a cluster of OLSs was also located east of the tracks and south of the RAS field site.

In November 2005, additional OLSs were located west of the tracks, south of the OLS RAS field site, and overlapping the field site location. Though not visible from the image, more OLSs may have been found in November because of reduced greenness during the winter. Finally, the 26 April 2007 image shows no OLSs plotted. As before, only the field RAS locations are shown for reference.

Figures 61–64 show that OLSs can appear in the same general vicinity season to season, but their absolute position and orientation may change. They may be due to changing patterns in the Landsat image, and because georectification of each image can produce different results.
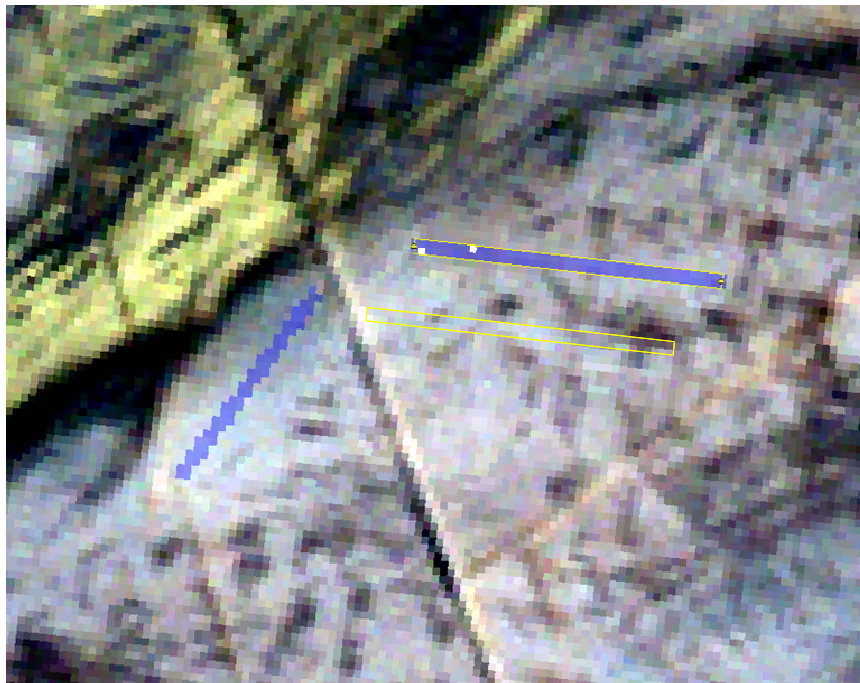

Figure 65. 1 November 2005 Landsat USGS Precision georeferenced image with Version 10 of the OLS software. Blue and red OLSs are in Precision georeferenced positions. The unfilled yellow outline OLS is the RAS field site from the Systematic georeferenced 9 May 2005 image. Filled yellow outline OLS is the field site as it should have been located from the Precision geoereferenced 9 May 2005 image.

Only the November 2005 Landsat image showed any OLSs with OLS software Version 10. The May 2005, July 2005, and April 2006 Landsat images recorded no OLSs within the immediate geographic area of the RAS field site shown in Figure 65. The November 2005 image shows several parallel OLSs oriented northeast to southwest, and crossing into the study area and possibly overlapping the Precision georeferenced RAS location. The April 2005 image used to locate the field site with software Version 7 showed no OLSs with software Version 10 within the image area of Figure 65. This suggests that Version 10 of the software is more strict, or conservative, in the selection of OLSs than was Version 7.

Table 18 shows that El Centro RAS generally passes most evaluation criteria, especially those criteria that do not vary significantly with season.

Even being an arid region where vegetation greenness typically varies with moisture content more than it does with seasonal temperature changes, OLSs still were found more frequently in the near-winter month of November than in any other season. It is not clear why this was so, but the greenness index may be a potential reason.

Table 18. Seasonal overall rating for El Centro OLS.

Surface Conditions	Summer	Fall	Spring	Comments
Potholes	Pass (Green)			Limited bowl-shape depressions caused by existing and abandoned animal burrows.
Loose aggregate	Pass with Caution (Amber)			Gravel size materials on the surface were common on the RAS that can ingest into an aircraft's engine and puncture aircraft tires.
Ruts	Pass (Green)			Limited ruts were observed on the RAS.
Rolling resistance material	Pass with Caution (Amber)			Loose materials such as granular materials along the wheel path of the OLS can increase rolling resistance on the aircraft's tire.
Dust	Pass with Caution (Amber)			Dry soil is common in semi-arid areas, partially obstructing visibility to approximately 400 m.
Animal burrows	Pass with Caution (Green to Amber)			Voids and holes created by the animals were found infrequently on the OLS. Animal burrows caused weak soil strength. The size of the holes and area are also critical.
Mounds	Fail (Red)			Mounds existed and are common on the eastern portion of the RAS.
Vegetation	Pass with Caution (Amber)			The sizes of the branches could partially obstruct the aircraft. Roots could puncture tires.
Standing water	Pass (Green)			No water ponds were observed on the OLS.
Surface drainage paths	Pass (Green)			No drainage paths.
Surface debris and organic materials	Pass (Green)			Organic materials are insignificant.
Snow depth	Pass (Green)			No snow cover.
Geometry				
Longitudinal grade	Pass (Green)			Grade along the entire OLS is within the criteria.
Transverse grade	Pass (Green)			Lateral grade is within the criteria.
Aircraft:				
C-130	Marginal	Unacceptable	Marginal	Capacity based on minimum CBR or the 15th percentile of the minimum CBR value.
C-17	Unacceptable	Unacceptable	Unacceptable	

8 Overall OLS Rating

The field work at El Centro was conducted to determine whether the OLS software identified suitable landing sites that met both the geometric and strength requirements to land an aircraft. Comprehensive ground truth data collection was conducted on the Runway Assessment Site at El Centro during three Intensive Operational Periods or field visits to assess its adequacy as a landing zone. Criteria revised from AFCESA semi-prepared airfield criteria (AFCESA 2002a, 2002b, UFC 3-260-02) were used to assess the OLSs as described in Section 3, which identified and summarized the El Centro RAS with the following:

The terrain topography of the RAS was analyzed and the overall longitudinal and transverse slopes of the RAS met the design runway criteria. Undulation or roughness of the ground was evaluated. At this RAS, mounds are present in the eastern end of the OLS with an average spacing of 2.5 m (8 ft) apart. If an aircraft is to land on this RAS, it would encounter quite a rough landing on that section of the runway. For a landing speed of 60 m/sec (120 knots), the aircraft will run over a mound approximately every 6 seconds. (This translates to an aircraft excitation of 24 hertz.)

The soil physical characteristics examined included soil type, density, color, and organic contents. The soil type found on the RAS is a non-plastic, silty sand (SM). The soil density profile had no specific trend with depth and was non-uniform, which is typical of natural soils. Soil density indirectly influences soil strength, therefore variable density will result in inconsistence soil strength. A thin (6- to 10-mm) cemented layer was found on the surface of the RAS during summer and spring season when the soil was dry. This layer was easily broken and disappeared when soil surface was wet during a rain storm event. Cemented soil layers were also observed clods in irregular thicknesses at various depths. These cemented soil clods were quite hard to break by hand but easily could be broken into pieces with a metal pick. The amount of organic content was found to be insignificant as it can be ingested into the engine and other parts of the aircraft.

Near-surface strength taken from the Clegg impact hammer indicated that a single rain storm, which significantly increased the soil moisture, also significantly reduced the soil strength.

From the DCP data, up to 30% of areas on the RAS in the fall season were found to have very low strength with a CBR of 2 or less at 0- to 0.15-m depth. Also, the soil strength at 0.15–0.30 m is also very low up to 10% of the locations. The OLS condition is summarized as moderately capable of supporting landing of a C-130 and C-17 operations for one pass at very low gross weight capacity for summer, fall, and spring seasons. Aircraft operations will cause localized soil failure such as rutting and deformation, especially on areas with animal burrows. Significant rutting of the soil resulting in sinking of aircraft wheels may destroy the aircraft landing gear, and limit clearance between the ground and engine nacelles (for C-17) or propellers (C-130).

Vegetation cover is very minimal on the RAS. The size of the vegetation, in terms of the diameter of bushes or branches, can be pushed by the force and momentum of an aircraft. Creosote bush root systems can be a problem for puncturing tires. Aircraft tires have several plys and are very rugged, so the vegetation may not be a problem at all; however, this was not part of this assessment.

Large granular materials are commonly found on this RAS, principally from loose pieces of large gravels and stones on the surface. The AFCESA criteria required that these loose materials must be removed before an aircraft operation. Rocks larger than 0.1 m (4 in.) must be removed from the operational surface (AFCESA 2002b). Loose aggregates are considered to be a potential cause of FOD, which can damage aircraft components such as engines, tires, etc. The OLS is rated as "Amber" based on loose aggregate cover between 1/10 and 1/2 of RAS. Certain amounts of loose granular materials can increase rolling resistance, especially during takeoff.

The soil is very dry most of the year. Dust is common, so visibility can be an issue. Dust also can be drawn into the engine and other parts of the aircraft.

Conditions at the Precision Corrected Imagery Runway Assessment Site (PCI-RAS) are found to be very similar to the Systematic Imagery Runway Assessment Site (SI-RAS). The PCI-RAS is rated as "Excellent" for both its

geometry properties and surface characteristics. The soil strength capacity for summer conditions is comparable to the strength measured at the SI-RAS during July 2005 visit.

The seasonal analysis shows that OLSs typically do not reappear at the same coordinate location in multiple seasons. However, OLSs may not be found in the area in other seasons, or in some cases may be located in the immediate area at different positions and orientations.

The overall rating, including the surface and subsurface characteristics at both PCI-RAS and SI-RAS for El Centro OLS based on the criteria defined in Section 3, is summarized in Tables 18 and 19. The rating is a way to quantify and define the suitability of the OLS. The OLS is rated as moderate for surface characteristics and excellent in its geometric category. The OLS is capable of landing a C-130 with ratings from marginal to unacceptable depending on the season. The OLS is rated as unacceptable for C-17 operations during three seasons because of soil strength requirements.

Table 19. Overall rating of the entire OLS.

Categories	Rating
Surface characteristics	Moderate or Caution
Geometric properties	Excellent or Pass
Aircraft loading capacity C-130 C-17	 Marginal to unacceptable Unacceptable

9 Conclusion and Recommendations

The OLS software is designed to select locations that are smooth, flat, level, and free of obstruction and woody vegetation that would harm the aircraft. It is not yet designed to consider all of the criteria desired by the Air Force. However, the main objective of the RAS is to assess the quality of the OLS selected by the Boeing software to examine the terrain characteristics and soil strength capacity to support the aircraft operations. Seasonal changes of the RAS were evaluated, including soil properties and the software's capability to select OLSs in any season.

From the assessment, the software was able to predict an OLS with regards to a piece of land that is smooth, flat, level, and relatively free of obstruction at El Centro. The OLS is acceptable in terms of its lateral and longitudinal gradients since slope measurements are below the required AFCESA design criteria. Depending on the season, the OLS is capable of landing a C-130 during summer and spring. However, because of the rain event in the fall, soil strength on the OLS was affected and changed the rating to unacceptable for C-130 operation. The OLS cannot support C-17 operations primarily because RAS sections contained low strength layers with less than the minimum CBR requirement, and this is true for all three field assessments at El Centro OLS. Soil failure in a form of rutting, depression, and irregular compaction is likely to occur as a result of aircraft dynamic loading on areas with soft soil layers. These failures can be substantial for aircraft landing and take-off, causing significant tire sinkage and soil resistance. Other features found on the OLS, such as loose materials present on the surface, also could hinder the aircraft operation. Transport aircraft could be used at the El Centro RAS, but possibly would sustain serious, if not debilitating, damage preventing a possible departure.

We conducted a thorough assessment to characterize the OLS and examine the RAS's seasonal changes. For the most part, we were able to acquire a significant amount of relevant information from the ground truth measurements. Acquiring these measurements was time-consuming and labor-intensive. For example, the most accurate way to assess the soil properties is by digging pits to collect soil specimens to determine soil type and soil density. Using an auger to collect soil samples was found to be ineffective for granular and dry soil. The nuclear gage was logistically cumbersome to transport, but is the only reliable instrument for measuring soil density in

varying soil conditions. We also encountered soil moisture accuracy or precision issues and found that some of the electronic instruments did not work well in certain soil conditions. For example, soil moisture measurements were made with multiple technologies at the same sampling locations to assess how well the different measurement methods agreed. There often was disagreement among the instruments, and in some cases instruments provided values not consistent with physical possibility. However, it was found that the mean differences were small in soil moisture between HH2 measurements and oven-dry measurements in El Centro. Oven-dried gravimetric measurements are the most direct method of measuring soil moisture and, other than sampling error, which affects all methods, has the least opportunity for error if careful laboratory methods are followed. The DCP is the standard tool for measuring soil strength (in terms of soil shear strength) by AFCESA for airfield design and evaluation and is portable for use on the OLS. The 0.5-kg Clegg hammer provides a CBR value for the upper layer of the soil based on hammer dynamic impact for soil stiffness, and can be used with the DCP data to assess the entire soil profile. Because of significant variations at the same sampling locations in CBR value between the DCP and the 0.5-kg Clegg hammer, further assessment and correlations are needed between the instruments.

Our approach was modified from AFCESA guidelines to be applicable for OLS assessments. Because the guidelines used to assess the OLS were revised from the AFCESA criteria for expedient runways, there is a need to quantify the ratings given for the unique features present on austere and natural terrain that are not normally found on runways. We need to better quantify surface roughness (mounds, undulations, swales) or perhaps use another measure of roughness index and adapt an acceptable roughness value for OLS. Also, soil resistance on aircraft landing and take-off due to surface and loose materials needs to be investigated for OLS application.

Soils on the El Centro OLS were insufficiently firm to support transport aircraft. This underscores the need to embed a soil strength calculating capability into the OLS system that will use physical properties of the soil to compute soil strength rather than relying upon the software to locate areas that are simply associated with firm soil. Though version 7 of the OLS software is certainly capable of finding locations that are promising as OLSs, the El Centro example indicates that software changes, or flatness and vegetation indices, will need some modification before fully safe OLSs can be consistently selected for transport aircraft operations.

References

Abele, G., 1990, Snow Roads and Runways, CRREL Monograph 90-3, Cold Regions Research and Engineering Laboratory, Hanover, NH 03755.

AFCESA, 2002a, "Airfield Pavement Evaluation, Standards and Procedures." Air Force Civil Engineer Support Agency, Tyndall AFB, Engineering Technical Letter 02-19.

AFCESA, 2002b, "Criteria and Guidance for C-17 Contingency and Training Operations on Semi-Prepared Airfields." Air Force Civil Engineer Support Agency, Tyndall AFB, Engineering Technical Letter 97-09.

AFCESA, 2004, "C-130 and C-17 Landing Zone (LZ) Dimensional, Marking, and Lighting Criteria." Air Force Civil Engineer Support Agency, Tyndall AFB, Engineering Technical Letter 04-7.

Affleck, R.T., C.C. Ryerson, L. Barna, and K. Claffey, 2008, Suitability Measurement and Analysis for Fort Bliss Naval Air Facility OLS. US Army Engineer Research and Development Center, Cold Regions Research and Engineering Laboratory, Hanover, New Hampshire, ERDC-CRREL Technical Report TR-08-16.

Almassy, R., and P. Blake, 2005, Opportune Landing Site Multispectral (OLS-MS) Software Operation Description, Version 7.0. Boeing Company.

Almassy, R., and P. Blake, 2007, Opportune Landing Site Multispectral (OLS-MS) Software Operation Description, Version 10.0. Boeing Company.

ASTM, 2003, American Society for Testing Materials, West Conshohocken, Pennsylvania

Barna, L.A., C.C. Ryerson, and R.T. Affleck, 2008, Opportune Landing Site Southeastern Indiana Field Data Collection and Assessment. US Army Engineer Research and Development Center, Cold Regions Research and Engineering Laboratory, Hanover, New Hampshire, ERDC-CRREL Technical Report TR-08-22.

Blake, P., 2007, Personal communication on thresholds for vegetation and gradient, Boeing Company, Technology Strategy Lead Network & Space Systems, 562-797-5996 (tel), pamela.l.blake@boeing.com.

Brown, B., Evaluation Product Manager, Lafayette Instrument Company, PO Box 5729, 3700 Sagamore Parkway North, Lafayette IN 47903, Tel: 765-423-1505, ext. 202, Fax: 765-423-4111, e-mail: bbrown@lafayetteinstrument.com, Web site www.lafayetteinstrument.com.

Clegg, B., 1980, An Impact Soil Test as Alternative to California Bearing Ratio. Proceedings, 3rd Australian-New Zealand (ANZ) Geomechanics Conference, Wellington, New Zealand, 1 225–230.

Crandell, J., Managing Director of Dr Baden Clegg Pty Ltd, Unit 2, 23 Bishop Street, Jolimont, Western Australia 6014, email: J.drclegg@iinet.net.au, Web site www.clegg.com.au.

EM 1110-2-1906, Engineering Manual, Engineering and Design, Laboratory Soils Testing, Headquarters, Department of the Army Office of the Chief of Engineers, Nov. 1970.

Godwin, R., N. Warner, D. Smith, 1991, The development of a dynamic drop-cone device for the assessment of soil strength and the effects of machinery traffic, J. agric. Engng. Res, v 48, p. 123–131.

Herrick, J., and R. Jones, 2002, A dynamics cone penetrometer for measuring soil penetration resistance, Soil Sci. Soc. Am. J. 66:1320–1324.

Manley, D., 2001, "Identifying Unprepared Landing Sites for Advanced Theater Transport Aircraft (and Terrain Trafficability for Military Vehicles)." The Boeing Company, Phantom Works, Long Beach, CA. 3 p.

Millar, L.R. (1977). An Application of the Soil Impact Tester to Road Pavement Construction, Master Thesis, University of Western Australia.

Munsell Soil Color Charts, 2000, Revised washable edition, GretagMacbeth, 617 Little Britain Road, New Windsor, NY 12553.

PCASE, Pavement Design Evaluation Software, www.pcase.com.

Rollings, M., and R. Rollings, 1996, *Geotechnical Materials in Construction*, McGraw-Hill.

Ryerson, C., and J. McDowell, 2007, Anywhere-Anytime: Enhancing Battlespace Vertical Mobility. AIAA 2007-1103, American Institute of Aeronautics and Astronautics 45th Aerospace Sciences Meeting and Exhibit, 8–11 January, Reno, 9 p.

Ryerson, C., F. Scott, and B. Tracy, in preparation, OLS Suitability Assessment, draft submitted for 2008 Transportation Systems Workshop Phoenix, AZ, 21–24 April 2008.

Stolf, R., R. Klaus, and C. Vaz, 2005, Response to "Comments on 'Simultaneous Measurement of Soil Penetration Resistance and Water Content with a Combined Penetrometer–TDR Moisture Probe' and 'A Dynamic Cone Penetrometer for Measuring Soil Penetration Resistance'" Soil Sci Soc Am J 69:927–929.

ThetaProbe Soil Moisture SensorTYPE ML2x, User Manual, ftp://ftp.dynamax.com/Manuals/ml2x.pdf, Copyright 1999 Delta-T Devices Ltd., 128 Low Road, Burwell, Cambridge, CB5 0EJ, England.

Unified Facilities Criteria Handbook "Pavement Design for Airfields, UFC 3-260-02.

USDA–Natural Resources Conservation Service, 1981, Soil Survey of Imperial County, CA, Imperial Valley Area.

User Manual for the Profile Probe type PR2, ftp://ftp.dynamax.com/Manuals/PR2.pdf, Copyright 1999 Delta-T Devices Ltd., 128 Low Road, Burwell, Cambridge, CB5 0EJ, England.

Vaz, C., and J. Hopmans, 2001, Simultaneous Measurement of Soil Penetration Resistance and Water Content with a Combined Penetrometer-TDR Moisture Prove, Soil Sci Soc Am J 65:4–12.

Vincent, R. (unpublished) Continental United States Simulacrums to Four Areas of Interest Overseas.

Vincent, R.K., and D.L. Jennings, 2004, "A Four-State Evaluation of the Boeing Landing Suitability Index (BLSI) for Automatically Mapping Candidate Aircraft Operating Sites in Natural Terrain from LANDSAT TM Data." *Journal of Terramechanics* Vol. 41, pp. 151–162.

Webster, S.L., R.H. Grau, and T.P. Williams, 1992, Description and Application of Dual Mass Dynamic Cone Penetrometer, Instruction Report GL-92-3, USACE Waterways Experiment Station, Vicksburg, MS.